

This is a repository copy of *Spin-Coupled Generalized Valence Bond Theory: New Perspectives on the Electronic Structure of Molecules and Chemical Bonds*.

White Rose Research Online URL for this paper:

<https://eprints.whiterose.ac.uk/id/eprint/171105/>

Version: Accepted Version

---

**Article:**

Dunning, Thom, Xu, Lu, Cooper, David L. et al. (1 more author) (2021) Spin-Coupled Generalized Valence Bond Theory: New Perspectives on the Electronic Structure of Molecules and Chemical Bonds. *Journal of Physical Chemistry A*. pp. 2021-2050. ISSN: 1089-5639

<https://doi.org/10.1021/acs.jpca.0c10472>

---

**Reuse**

Items deposited in White Rose Research Online are protected by copyright, with all rights reserved unless indicated otherwise. They may be downloaded and/or printed for private study, or other acts as permitted by national copyright laws. The publisher or other rights holders may allow further reproduction and re-use of the full text version. This is indicated by the licence information on the White Rose Research Online record for the item.

**Takedown**

If you consider content in White Rose Research Online to be in breach of UK law, please notify us by emailing [eprints@whiterose.ac.uk](mailto:eprints@whiterose.ac.uk) including the URL of the record and the reason for the withdrawal request.

## Spin-Coupled Generalized Valence Bond Theory: New Perspectives on the Electronic Structure of Molecules and Chemical Bonds

Thom H. Dunning,\* Jr., Lu T. Xu, David L. Cooper,\* and Peter B. Karadakov

**ABSTRACT:** Spin-Coupled Generalized Valence Bond (SCGVB) theory provides the foundation for a comprehensive theory of the electronic structure of molecules. SCGVB theory offers a compelling orbital description of the electronic structure of molecules as well as an efficient and effective zero-order wave function for calculations striving for quantitative predictions of molecular structures, energetics and other properties. The orbitals in the SCGVB wave function are usually semi-localized and, for most molecules, can be interpreted using concepts familiar to all chemists (hybrid orbitals, localized bond pair, lone pairs, etc.). SCGVB theory also provides new perspectives on the nature of the bonds in molecules such as  $C_2$ ,  $Be_2$  and  $SF_4/SF_6$ . SCGVB theory contributes unparalleled insights into the underlying cause of the first-row anomaly in inorganic chemistry as well as the electronic structure of organic molecules and the electronic mechanisms of organic reactions. The SCGVB wave function accounts for non-dynamical correlation effects and, thus, corrects the most serious deficiency in molecular orbital (RHF) wave functions. Dynamical correlation effects, which are critical for quantitative predictions, can be taken into account using the SCGVB wave function as the zero-order wave function for multireference configuration interaction or coupled cluster calculations.

### 1. INTRODUCTION

Orbital models of the electronic structure of atoms and molecules are universally used by chemists as a means of understanding and explaining a broad range of atomic and molecular phenomena. Open any textbook in physical chemistry, organic chemistry or inorganic chemistry and you will find an extensive discussion of the role of atomic and molecular orbitals in chemistry. For example, in Ian Fleming's 2010 book on *Molecular Orbitals and Organic Chemical Reactions*,<sup>1</sup> the author states:

*Organic chemists with a serious interest in understanding and explaining their work usually express their ideas in molecular orbital terms, so much so that it is now an essential component of every organic chemist's skills to have some acquaintance with molecular orbital theory.*

Although there have been arguments about orbitals and orbital theories in both the chemical education literature<sup>2-4</sup> and the chemical philosophy literature,<sup>5-8</sup> few chemists today question the utility of orbital theories. Molecular orbitals, and their quantitative realization in the restricted Hartree-Fock (RHF) wave function, are considered by most chemists to be the foundation for the orbital theory of the electronic structure of molecules. However, many molecules and molecular processes cannot be adequately described by a single configuration RHF wave function. This list includes molecules such as singlet biradicals,  $Be_2$  and  $C_2$  as well as making and breaking bonds and many chemical reactions and excited states. An accurate zero-order description of these molecules or molecular processes requires a multiconfiguration wave

function.

The most popular multiconfiguration approaches today are the Full Optimized Reaction Space<sup>9-11</sup> (FORS) and Complete Active Space Self-Consistent Field<sup>12-14</sup> (CASSCF) methods. These methods define a set of active orbitals, often the union of the valence orbitals on each of the atoms, and then construct all possible configurations that can be formed using these orbitals (full configuration interaction for “ $N$ -electrons in  $M$ -orbitals”). The orbitals and configuration coefficients are then optimized. These approaches are extremely powerful and have many advantages, but they also have disadvantages. For one, the computational cost of the associated full CI calculations increases dramatically as  $(N, M)$  increase, which limits the use of these methods in calculations on large molecules. Although this problem can be addressed by restricted FORS/CASSCF calculations, which partition the active space into subspaces thereby limiting the number of configurations generated in the full CI,<sup>15-19</sup> any partitioning of the active space is subjective. More recently, research has been reported on adaptive sampling methods as a means of efficiently reducing the number of configurations included in the CASSCF wave function.<sup>20</sup> Finally, as noted by Xu and Dunning,<sup>21</sup> FORS/CASSCF calculations must be carefully monitored because the extraordinary flexibility of these wave functions can lead to inconsistencies in the orbitals that define the active space.

In addition to their computational cost, FORS/CASSCF wave functions, with their sheer number of delocalized orbitals, configurations and configuration coefficients, are difficult to interpret. In the landmark series of papers that introduced the FORS method, Ruedenberg et al.<sup>9-11</sup> asked the question: “Are Atoms Intrinsic to Molecular Electronic Wavefunctions?,” answered the question affirmatively, and proposed ways of extracting such information from the FORS wave function. More recently they refined the concepts introduced in those papers by defining quasi-atomic orbitals (QUAOs)<sup>22</sup> and using the QUAO concept to obtain insights into the bonding in molecules<sup>23</sup> and the orbital transformations involved in chemical reactions.<sup>24</sup> For CASSCF wave functions, Robb and coworkers,<sup>25-27</sup> Thorsteinsson et al.,<sup>28,29</sup> and Hirao<sup>30</sup> have discussed the transformation of these wave functions to valence bond wave functions as a means of interpreting the results of CASSCF calculations. Despite the utility of these approaches for interpreting FORS/CASSCF wave functions, the goal of developing a comprehensive orbital theory based on FORS/CASSCF multiconfiguration wave functions is still in its infancy.

The Spin-Coupled Generalized Valence Bond (SCGVB) wave function<sup>31-34</sup> is a multiconfiguration wave function that also describes a broad range of molecules and molecular processes.\* As a wave function based on a single product of orbitals that are usually semi-localized, the SCGVB wave function can be interpreted using concepts—hybrid orbitals, bond orbitals, lone pairs, etc.—that are familiar to all chemists. In addition, applications of SCGVB theory have also led to new concepts, e.g., the recoupled pair bond<sup>35</sup>

---

\* In prior articles in the literature the Spin-Coupled Generalized Valence Bond wave function has usually been referred to as the Spin-Coupled Valence Bond (SCVB) wave function or the full Generalized Valence Bond (full GVB) wave function. These wave functions are identical; to prevent confusion, the authors have adopted the all-encompassing SCGVB name.

## Spin-Coupled Generalized Valence Bond Theory: New Perspectives on the Electronic Structure of Molecules and Chemical Bonds

and recoupled pair bond dyad.<sup>36</sup> The SCGVB wave function describes molecules in terms of orbitals that are optimized at each geometry, allowing the atomic orbitals to change as a result of molecule formation. In addition to the changes in the orbitals, optimization of the general spin function used in the SCGVB wave function allows the spin function to change from that appropriate for the separated atoms or fragments to that appropriate for the molecule. SCGVB theory addresses a major limitation of RHF theory, providing an excellent zero-order description of molecules that require multiconfiguration descriptions, the making/breaking of bonds, and many chemical reactions and excited states. For most molecules, the SCGVB wave function captures the essential features of the FORS/CASSCF wave functions, with much reduced complexity compared to these latter wave functions.

The SCGVB wave function contains the finite set of configurations that are required to describe the non-dynamical correlation effects first identified by Sinanoğlu.<sup>37</sup> Inclusion of non-dynamical correlation effects corrects the most serious deficiency in the RHF wave function and, for many molecules, dramatically improves the resulting prediction of molecular properties. However, dynamical correlation effects must be taken into account in order to make truly quantitative predictions. Dynamical correlation effects can be accounted for by using the SCGVB wave function as the zero-order wave function in a multireference configuration interaction (MRCI) or coupled cluster (MRCC) calculation. Although MRCI calculations can be performed using the non-orthogonal SCGVB orbitals, the transformation to orthonormal natural orbitals enables use of the traditional, well optimized machinery for MRCI/MRCC calculations. Because of the compact nature of the SCGVB wave function, these calculations are usually less computationally expensive than the corresponding calculations based on FORS/CASSCF wave functions.

In this Perspective Article, we focus on the orbital description of the electronic structure of molecules provided by SCGVB theory and illustrate the many ways this theory provides a compelling orbital description of a broad class of molecules and molecular processes. In addition to describing the electronic structure of molecules in terms that align well with traditional chemical concepts, SCGVB theory also provides new perspectives that aid in the resolution of a number of puzzling problems in molecular electronic structure theory such as the nature of the bonding in Be<sub>2</sub>, C<sub>2</sub>, SF<sub>4</sub>/SF<sub>6</sub>, and more. SCGVB theory also provides new insights into the well-known first-row anomaly in inorganic chemistry as well as the electronic structure of organic molecules and the electronic mechanisms of organic reactions. In a famous after-dinner speech at the Boulder Conference in 1960, Coulson critiqued the nascent field of computational chemistry, noting that it was becoming:

*“... so remote from the normal natural conventional concepts of chemistry, such as bonds, orbitals, and overlapping hybrids, as to carry the work itself out of the sphere of real quantum chemistry.”<sup>38</sup>*

This is not the case for SCGVB theory. SCGVB theory provides a direct connection between quantum mechanics and basic chemical concepts. In fact, SCGVB theory enables quantum chemists to better

“understand these concepts and show what are the essential features in chemical behavior.”<sup>38</sup>

The outline of the article is as follows. In Section 2 we provide a brief overview of the basic elements of SCGVB theory as well as the extension of SCGVB theory to  $N$ -electrons in  $M$ -orbitals, which is important for describing some classes of molecular species. We also provide a brief comparison of SCGVB theory with other orbital theories of the electronic structure of molecules. Finally, we discuss the use of the SCGVB wave function as the zero-order wave function in multireference configuration interaction (MRCI) calculations. In Section 3, we discuss the insights SCGVB theory provides into the nature of chemical bonds, the electronic structure of molecules, and the electronic mechanisms of chemical reactions. In the fourth section we provide a few examples that illustrate the use of the SCGVB wave function in MRCI calculations to provide more accurate predictions of molecular structures, energetics and other properties. Finally, in the last section, we summarize our thoughts about the role that SCGVB theory has been playing and will continue to play in our understanding of the electronic structure of molecules.

## 2. OVERVIEW OF SCGVB THEORY

In this section we provide a brief overview of SCGVB theory, including the generalization of SCGVB theory to  $N$ -electrons in  $M$ -orbitals, which enables additional classes of molecules to be properly described. We also discuss the relationship of SCGVB to other theories of the electronic structure of molecules. Finally, we discuss the use of the SCGVB wave function as the zero-order wave function in multireference configuration interaction calculations. Throughout this section, we use the  $N_2$  molecule to illustrate the application of SCGVB theory.<sup>39</sup>

**2.1. SCGVB Theory.** Although the SCGVB wave function can take a number of different forms depending on the number of singly occupied active orbitals in the wave function, the most common form of the SCGVB wave function is:

$$\Psi_{\text{SCGVB}} = \hat{A} \phi_{c1} \phi_{c1} \cdots \phi_{cn_c} \phi_{cn_c} \phi_{v1} \phi_{v1} \cdots \phi_{vn_v} \phi_{vn_v} \phi_{a1} \cdots \phi_{an_a} \alpha\beta \cdots \alpha\beta \alpha\beta \cdots \alpha\beta \Theta_{S,M_S}^{n_a} \quad (1)$$

In Eq. (1), the orbitals  $\{\phi_{ci}, i = 1-n_c\}$  are the  $n_c$  doubly occupied core orbitals, the  $\{\phi_{vi}, i = 1-n_v\}$  are the  $n_v$  doubly occupied valence orbitals, and the  $\{\phi_{ai}, i = 1-n_a\}$  are the  $n_a$  singly occupied active valence orbitals. The spin function is a product of  $\alpha\beta$ 's spin functions for each of the  $n_c + n_v$  doubly occupied orbitals and a general spin function,  $\Theta_{S,M_S}^{n_a}$ , for the  $n_a$  electrons in the active valence orbitals. All of the orbitals as well as the spin function in Eq. (1) are optimized in SCGVB calculations.

The orbitals in the SCGVB wave function are selected to describe the molecule or molecular process of interest. For example, in the formation of  $N_2$  from two ground state nitrogen atoms,  $^4S(1s^2 2s^2 2p^3)$ , the four  $N1s$  and  $N2s$  orbitals are the doubly occupied core and valence orbitals, while the six  $N2p$  orbitals are the singly occupied active valence orbitals. At  $R = \infty$ , the SCGVB orbitals are simply the RHF orbitals of

## Spin-Coupled Generalized Valence Bond Theory: New Perspectives on the Electronic Structure of Molecules and Chemical Bonds

the nitrogen atom. The active valence orbitals in Eq. (1) need not be orthogonal to one another. In  $N_2$ , the 2p orbitals on the two atoms overlap as  $R$  decreases, although the  $(\sigma, \pi_x, \pi_y)$  orbital pairs in  $N_2$  are orthogonal to each other by symmetry. The active valence orbitals can be taken to be orthogonal to all of the doubly occupied orbitals without any loss of generality—the antisymmetrizer,  $\hat{A}$ , eliminates any components of the doubly occupied orbitals from the active orbitals in the SCGVB wave function. In  $N_2$ , this means that the six active orbitals are orthogonal to the four doubly occupied orbitals. The SCGVB active orbitals are, in general, semi-localized, corresponding to bond pairs, lone pairs, etc. in line with traditional chemical concepts. The doubly occupied orbitals may be delocalized just as in RHF theory. These orbitals can be transformed to semi-localized orbitals using any of the standard localization procedures.<sup>40-44</sup>

Optimization of the SCGVB orbitals at each molecular geometry enables the SCGVB wave function to describe the changes in the atomic orbitals caused by molecule formation. Although the atomic orbitals change in a number of ways, e.g., hybridization, polarization, delocalization, and contraction, they usually retain a clear connection with the atomic orbitals from which they arose; see the plots of the valence orbitals of  $N_2$  in Figure 1 at  $R = \infty$  and  $R_e$ <sup>45</sup> (also included is the SCGVB orbital diagram used to represent the formation of  $N_2$  from two ground state nitrogen atoms). In recognition of the intimate connection between SCGVB atomic and molecular orbitals, we will use the original SCGVB atomic orbitals with a prime to designate the SCGVB molecular orbitals, e.g.,  $N2p_z'$  and  $N2p_{x,y}'$  to denote the nitrogen  $\sigma$  and  $\pi_{x,y}$  bond orbitals in  $N_2$ . This connection of the SCGVB molecular orbitals with atomic orbitals facilitates interpretation of the SCGVB wave function using concepts familiar to chemists. However, applications of SCGVB theory have also led to the development of new chemical concepts that provide insights into the nature of the chemical bonds in a variety of unusual molecules (see the following section).

The overlaps of the  $\sigma$ , ( $N2p_{zA}'$ ,  $N2p_{zB}'$ ), and  $\pi_x$ , ( $N2p_{xA}'$ ,  $N2p_{xB}'$ ), orbitals of  $N_2$  plotted as a function of  $R$  in Figure 2. The overlaps increase monotonically from zero at  $R = \infty$  to values approaching unity as  $R$  decreases. This increase in the overlap of the SCGVB orbitals is a result of two factors: (i) the decrease in  $R$ , which brings the orbitals closer together, and (ii) hybridization and delocalization of the orbitals. Although there is not a simple correlation between bond orbital overlaps and the bond energy, strong bonds tend to result from highly overlapping orbitals. At  $R_e$  the  $\sigma$  bond orbitals in  $N_2$  have an overlap of 0.89, while the  $\pi$  orbitals have an overlap of just 0.69, in line with chemists' intuition that  $\sigma$  bonds are stronger than  $\pi$  bonds. The non-bonding orbitals are also changed by molecular formation. These changes are largely a result of minimizing Pauli repulsion<sup>46</sup> between the electron pairs. Thus, in Figure 2, the  $N2s_A'$  and  $N2s_B'$  lone pair orbitals in  $N_2$  are seen to be polarized away from the newly formed ( $N2p_{zA}'$ ,  $N2p_{zB}'$ )  $\sigma$ -bond pair.

The spin function in Eq. (1),  $\Theta_{S,M_S}^{n_a}$ , ensures that the SCGVB wave function has the proper spin symmetry. It is a linear combination of all of the linearly independent ways ( $f_S^{n_a}$ ) of coupling the spins of electrons in the  $n_a$  active valence orbitals to yield a state with a given  $(S, M_S)$ <sup>47</sup>:

$$\Theta_{S,M_S}^{n_a} = \sum_{k=1}^{f_S^{n_a}} c_{S,k} \Theta_{S,M_S;k}^{n_a} \quad (2a)$$

with

$$f_S^{n_a} = \frac{(2S+1)n_a!}{(\frac{1}{2}n_a + S + 1)(\frac{1}{2}n_a - S)} \quad (2b)$$

At the separated atom limit, the SCGVB spin function is that appropriate for the collection of atoms. For example, in N<sub>2</sub> the spin function at  $R = \infty$  describes two nitrogen <sup>4</sup>S atoms with their spins coupled to yield an overall singlet state. Optimization of the spin coupling coefficients as a function of the molecular geometry,  $\{c_{S,k}\}$ , ensures that the spin function appropriate for the atoms smoothly changes to that appropriate for the molecule as the internuclear separations decrease. For most molecules near their equilibrium geometries, the perfect pairing spin coupling,  $\frac{1}{\sqrt{2}}(\alpha\beta - \beta\alpha)\frac{1}{\sqrt{2}}(\alpha\beta - \beta\alpha)\cdots$ , is the dominant spin coupling when the orbitals are ordered as sequential bond pairs. This spin coupling corresponds to the classical valence bond (VB) definition of chemical bonds.

The spin coupling coefficients,  $\{c_{S,k}\}$ , depend on the ordering of the orbitals in the SCGVB wave function. As such, identification of the essential features of the electronic structure of a molecule may require re-ordering the active orbitals. In addition, it is sometimes necessary to switch between different types of spin functions. The three main types of spin functions employed in SCGVB theory were introduced by Rumer,<sup>48</sup> Kotani,<sup>49</sup> and Serber<sup>50,51</sup>:

- The Rumer spin functions are products of  $n_{pair} = \frac{1}{2}n_a - S$  singlet pairs,  $\frac{1}{\sqrt{2}}(\alpha\beta - \beta\alpha)$ , and  $2S$   $\alpha$  spin functions, where  $S$  is the total spin. Although straightforward construction of spin functions in this way leads to more than  $f_S^{n_a}$  spin functions, the diagrammatic techniques developed by Rumer<sup>48</sup> and extended to non-singlet states by Simonetta et al.<sup>52</sup> can be used to determine a set of the linearly dependent spin functions. Another option is to use the *leading term* algorithm,<sup>52</sup> which is better suited to computer implementation.
- The Kotani spin functions are formed through successive coupling of individual electron spins according to the addition rules for angular momenta. This is illustrated by the Kotani branching diagram; see Figure 3. Each circle in this diagram corresponds to an allowed value of the total spin  $S$  for a given number of electrons  $n_a$ . The spin function is represented by the path which follows the arrows connecting the sequence of points. The number of spin couplings,  $f_S^{n_a}$ , for a given number of electrons ( $n_a$ ) and total spin,  $S$ , is shown inside the circle at  $(n_a, S)$ .
- The Serber spin functions are based on electron pairs and can be visualized by means of a Serber branching diagram, similar to the Kotani branching diagram. In this case, the spins of successive

## Spin-Coupled Generalized Valence Bond Theory: New Perspectives on the Electronic Structure of Molecules and Chemical Bonds

electron pairs, (1,2)(3,4)···, are coupled to be either singlet or triplet and these pairs are then used to construct the  $n_e$ -electron spin functions using the addition rules for angular momenta.

The three types of spin functions offer different insights into the nature of the SCGVB wave function.<sup>53</sup>

The Kotani spin functions are popular in SCGVB theory and have the advantage that the spin functions are orthonormal and the squares of the spin coupling coefficients,  $(c_{S,k}^2)$ , represent the contribution, or weight ( $w_{S,k}$ ), of that spin coupling in the total SCGVB wave function. To provide a concrete example of the use of the Kotani spin functions, we list the spin couplings in the Kotani representation for the singlet state of  $N_2$  in Table 1. For a six-electron singlet state there are five linearly independent spin couplings,  $\Theta_{0,0,k}^6$ ,  $k = 1-5$ . These couplings are represented symbolically by the paths taken in traversing the Kotani branching diagram:  $\alpha\alpha\alpha\beta\beta\beta$ ,  $\alpha\alpha\beta\alpha\beta\beta$ ,  $\alpha\beta\alpha\alpha\beta\beta$ ,  $\alpha\alpha\beta\beta\alpha\beta$ , and  $\alpha\beta\alpha\beta\alpha\beta$ . The spin coupling weights for these spin functions are plotted in Figure 4 as a function of  $R$ . The spin coupling weights are shown in Figure 4(a) for the “molecular” ordering of the orbitals, i.e., as sequential bond pairs:  $(N2p_{zA}', N2p_{zB}')$ ,  $(N2p_{xA}', N2p_{xB}')$ , and  $(N2p_{yA}', N2p_{yB}')$ . With this ordering, the perfect pairing spin function,  $\alpha\beta\alpha\beta\alpha\beta$  ( $\Theta_{0,0,5}^6$ ), is the dominant spin function at  $R_e$ , with  $w_{0,5} = 0.92$ , in line with chemists’ view that the  $N_2$  molecule has a triple bond. In Figure 4(b) the spin coupling weights for  $N_2$  with the “atomic” ordering of the orbitals:  $(N2p_{zA}', N2p_{xA}', N2p_{yA}')$  and  $(N2p_{zB}', N2p_{xB}', N2p_{yB}')$ . This plot shows that at large  $R$ , the wave function approaches that for the  $N_A(^4S) \times N_B(^4S)$  spin coupling,  $\alpha\alpha\alpha\beta\beta\beta$  ( $\Theta_{0,0,1}^6$ ). Although we do not provide a plot of the spin coupling weights for the orbitals ordered as  $(N2p_{zA}', N2p_{zB}')$  and  $(N2p_{xA}', N2p_{yA}', N2p_{xB}', N2p_{yB}')$ , see the middle row in Table 1, it is easy to understand why the largest contribution of the  $\alpha\beta\alpha\alpha\beta\beta$  spin function with this quasi-atomic ordering of the orbitals has its maximum value at intermediate  $R$ . At all  $R$  these wave functions are equivalent—the SCGVB wave function does not depend on the ordering of the orbitals—but each provides different insights into the electronic structure of the molecule: one at  $R_e$  (molecular ordering), one at  $R = \infty$  (atomic ordering), and the last at intermediate  $R$  (quasi-atomic ordering).

For molecules like benzene, use of the Rumer spin functions provides clear insights into the electronic structure of the molecule. Five spin functions are also needed to describe the  $\pi$  system of benzene in SCGVB theory. In this case, the five Rumer spin functions correspond to the two Kekulé structure and the three Dewar structures. SCGVB calculations on benzene<sup>53</sup> find that each of the Kekulé structures has a coefficient of 0.41, while each of the Dewar structures has a coefficient of just 0.06, in line with chemists’ concept of the nature of the  $\pi$  bonding in benzene. (For the non-orthogonal Rumer spin functions, the Chirgwin-Coulson<sup>54</sup> or Gallup-Norbeck<sup>55</sup> formulas must be used to calculate the contributions of each spin coupling in the SCGVB wave function.) The wave function for benzene can also be expressed in terms of the Kotani spin functions, although in this case the coefficients are not so easily interpreted:  $c_{0,1} = -0.07$ ,  $c_{0,2} = 0.43$ ,  $c_{0,3} = -0.31$ ,  $c_{0,4} = -0.31$  and  $c_{0,5} = 0.79$ . The true nature of the bonding in the  $\pi$  system of benzene is not at all clear in the Kotani representation, despite the fact that the resulting wave function is exactly the same as that in the Rumer representation.



The Serber spin functions are orthonormal, just as the Kotani spin functions are. These functions are used less often in SCGVB theory, although, in selected cases, they can provide valuable insights into the electronic structure of the molecules of interest.<sup>53</sup>

Transformations between the representations of  $n_a$ -electron spin functions in the Kotani, Rumer and Serber spin bases can be carried out in a straightforward manner with the use of a specialized code for symbolic generation and manipulation of spin functions; see the article on SPINS.<sup>56</sup> This code is also capable of calculating the changes in the spin-coupling coefficients caused by a reordering of the active valence orbitals.

**2.2. SCGVB( $N,M$ ) Theory.** There are obvious instances for which a single spatial configuration with “ $N$ -electrons in  $N$ -orbitals”, as in Eq. (1), is not the most appropriate choice for the SCGVB wave function for a given molecule. Consider, for example, the  $\pi$ -electron systems of the cyclopentadienyl anion,  $C_5H_5^-$ , and the tropylium cation,  $C_7H_7^+$ . Both of these planar ring systems involve six  $\pi$  electrons but in one case there are five carbon centers and in the other there are seven, so a conventional SCGVB calculation with six active orbitals does not lead to a straightforward description of the electronic structure of these molecules. Such considerations prompted Karadakov et al.<sup>57</sup> to develop the SCGVB( $N,M$ ) formulation in which a subset of all possible “ $N$ -electrons in  $M$ -orbitals” spatial configurations is adopted, namely, those in which as few active orbitals as possible, *i.e.*  $|N - M|$ , are doubly occupied (for  $N > M$ ) or missing (for  $N < M$ ), with all others being singly occupied. In order to retain other essential features of the original SCGVB model, each spatial configuration is combined with a flexible spin function which allows for all possible modes of coupling the spins of the electrons in the  $M$  orbitals. The inactive orbitals, active orbitals, spin coupling coefficients and the coefficients in front of each of the different orbital strings are fully optimized in the SCGVB( $N,M$ ) wave function.

Other symmetry considerations can also dictate the use of a SCGVB( $N,M$ ) wave function. For example, Xu and Dunning<sup>21</sup> showed that a SCGVB(4,5) wave function correctly describes the dissociation of the ground states ( $X^1\Sigma^+$ ) of BH and BF into atoms with the resulting boron atom wave function fully accounting for the 2s-2p near-degeneracy effect. In the SCGVB(4,4) wave function, only one of the  $2p\pi^2$  configurations is included.

**2.3. Relationship of SCGVB Theory to Other Orbital Theories.** Since the orbitals in the SCGVB wave function are variationally optimized, there is a close relationship to the RHF wave function, which is also based on variationally optimized orbitals. In fact, the RHF wave function can be derived from the SCGVB wave function by imposing three constraints: (i) restricting the spin function,  $\Theta_{S,M_S}^{n_a}$ , to be the perfect pairing spin function; (ii) requiring the orbitals in different pairs to be orthogonal (strong orthogonality); and (iii) requiring the singly occupied orbitals in each pair to be identical (double occupancy). The limitations of the RHF wave function, including its inability to properly describe some molecules and molecular processes and its tendency to break space and spin symmetry, are a direct consequence of one or more of these constraints.

## Spin-Coupled Generalized Valence Bond Theory: New Perspectives on the Electronic Structure of Molecules and Chemical Bonds

There is also a close relationship between SCGVB theory and valence bond (VB) theory.<sup>58,59</sup> In classical valence bond theory, the wave function is constructed from atomic orbitals and usually includes the covalently bonded configuration plus the singly ionic configurations. In SCGVB theory the orbitals are optimized to take into account the changes in the atomic orbitals and the singly ionic configurations are largely accounted for by orbital delocalization.<sup>60</sup> A step toward SCGVB theory was taken by van Lenthe and Balint-Kurti,<sup>61,62</sup> who developed the VBSCF method. In this method the orbitals on each atom are optimized but, unlike the fully optimized SCGVB orbitals, they are constrained to be localized on a specific atom. The resulting orbitals can be regarded as the optimum atomic hybrid orbitals for a VB wave function.<sup>63</sup> Finally, in the Breathing Orbital Valence Bond (BOVB) method<sup>64,65</sup> the orbitals on each atom are optimized using the same locality constraint as in the VBSCF method, but the orbitals are allowed to be different in each of the configurations in the VB wave function, e.g., the orbitals in the covalent and ionic configurations need not be the same. The BOVB wave function includes correlation effects beyond those included in the SCGVB wave function. In fact, it has been argued that the BOVB wave function includes the dynamical correlation required to describe molecular formation.<sup>66,67</sup>

The SCGVB method and the variational subspace valence bond method (VSVB) of Fletcher et al.<sup>68</sup> are also related, although not identical. The VSVB method optimizes the orbitals, just as in SCGVB theory, but imposes constraints in the form of partially disjoint subspaces of basis functions for the VSVB orbitals. These constraints prevent the variational collapse of the VSVB orbitals, a result which is achieved in SCGVB theory through other means depending on the specific program being used (e.g., CASVB,<sup>29,69</sup> VB2000,<sup>70</sup> and XMVB<sup>71</sup>). VSVB calculations as well as SCGVB calculations result in semi-localized orbitals. Although the VSVB method shares the same underlying concepts as the SCGVB method, the VSVB wave function with its additional constraints is not the same as the SCGVB wave functions. One advantage of VSVB theory, as implemented in the VALENCE software package,<sup>72</sup> is that the calculations are well suited for today's large heterogeneous, multiprocessor computers.

Finally, there is a close relationship between the SCGVB wave function and the corresponding Full Optimized Reaction Space (FORS) and valence Complete Active Space Self-Consistent Field (vCASSCF) wave functions. By rewriting the SCGVB wave function in its natural orbital (NO) form, see the following section, the configurations in the SCGVB(NO) wave function can be shown to be a subset of the configurations in the FORS or vCASSCF wave functions. In fact, the configurations in the SCGVB wave function are usually the dominant configurations in the latter wave functions. As a result, SCGVB wave functions capture the essential features of FORS and vCASSCF wave functions.

**2.4. Dynamical Electron Correlation.** Since the early days of quantum chemistry, it has been recognized that there are two distinct types of electron correlation<sup>37</sup>: non-dynamical correlation, which is a result of the near degeneracy of configurations, e.g., the  $2s^2$  and  $2p^2$  near degeneracy in beryllium-, boron- and carbon-like atoms as  $Z \rightarrow \infty$  and the  $\sigma_g^2$  and  $\sigma_u^2$  near degeneracy in  $H_2$  as  $R \rightarrow \infty$ , and dynamical

correlation, which is a result of the intrinsic correlation of the electrons and often expressed as the requirement that the wave function must vanish as the distance between any two electrons “ $i$ ” and “ $j$ ” vanishes, i.e., as  $r_{ij} \rightarrow 0$ . The SCGVB and SCGVB( $N,M$ ) wave functions contain the finite set of configurations needed to describe both types of near-degeneracy effects, i.e., they account for all of the non-dynamical correlation effects.

Dynamical correlation effects are missing in the SCGVB wave function and must be taken into account in order to make accurate predictions of molecular structure, energetics and other properties. Dynamical correlation can be included in SCGVB-based calculations by using the SCGVB wave function as the zero-order wave function in a multireference configuration interaction (MRCI) or coupled cluster (MRCC) calculation. As noted in Section 2.1, the active orbitals in the SCGVB wave function,  $\{\phi_{ai}\}$ , are non-orthogonal, although they are orthogonal to the doubly occupied core and valence orbitals,  $\{\phi_{ci}, \phi_{vi}\}$ . The non-orthogonal SCGVB active orbitals have been used directly in MRCI calculations coupled with excitations to sets of non-orthogonal virtual orbitals obtained as higher energy solutions of the SCGVB one-electron operators similar to Fock operators.<sup>73-75</sup> Unlike the virtual orbitals from RHF calculations, these virtual orbitals are concentrated in the region of interest and are, thus, well suited for MRCI calculations; SCGVB-based virtual orbitals have also been optimized for use in the MRCI calculations.<sup>76</sup> Although the resulting MRCI calculations were able to capture the essential feature of the electronic structure of the molecules of interest, especially in studies of multiple states of the same symmetry,<sup>77,78</sup> the use of non-orthogonal orbitals limited the number of virtual orbitals and configurations that could be included in the calculations (see, however, the advances reported by Olsen<sup>79</sup>).

To counter the non-orthogonality problem, the SCGVB wave function can be rewritten in its natural orbital (NO) form:

$$\Psi_{\text{SCGVB}}(\phi_{ci}, \phi_{vi}, \phi_{ai}) = \Psi_{\text{SCGVB}}^{\text{NO}}(\phi_{ci}, \phi_{vi}, \phi_{ai}^{\text{NO}}) = \sum_{n=1}^{N_{\text{SCGVB}}} C_n \Phi_n(\phi_{ci}, \phi_{vi}, \phi_{ai}^{\text{NO}}) \quad (5)$$

where the  $\{\phi_{ai}^{\text{NO}}\}$  are the orthonormal natural orbitals spanning the space of the non-orthogonal SCGVB active orbitals,  $\{\phi_{ai}\}$ , and the  $\{\Phi_n\}$  are the configurations that represent the SCGVB wave function in terms of the natural orbitals. As an example of such expansions, Table 2 list the fourteen configurations,  $\{\Phi_n\}$ , in the SCGVB wave function of the  $\text{N}_2$  molecule.  $\Psi_{\text{SCGVB}}^{\text{NO}}$  can now be used as the zero-order wave function in MRCI or MRCC calculations using the machinery associated with traditional MRCI/MRCC calculations. The configurations in  $\Psi_{\text{SCGVB}}^{\text{NO}}$  are a subset of the configurations in the FORS/vCASSCF wave function. Since  $N_{\text{SCGVB}}$  in Eq. (5) is, generally, smaller than the number of configurations in the corresponding vCASSCF wave function (14 versus 176 configurations for  $\text{N}_2$ ), there is usually a reduction in the associated computational cost. Furthermore, it has been found that  $\Psi_{\text{SCGVB}}^{\text{NO}}$  contains the most important configurations in the valence CASSCF wave function, and, as we show in Section 4, the loss of accuracy is minor.

## Spin-Coupled Generalized Valence Bond Theory: New Perspectives on the Electronic Structure of Molecules and Chemical Bonds

SCGVB-inspired MCSCF and CASSCF calculations are also possible. These calculations have the advantage that they do not need to explicitly calculate the SCGVB wave function. In the SCGVB-inspired MCSCF calculations, denoted by MCSCF(SCGVB), the SCGVB wave function is used to define the *configurations* to be included in the MCSCF calculations. In the first implementation of this method, each of the active electron pairs in the molecule is defined by three types of configurations, e.g., for a bond pair this includes a bonding configuration,  $\phi_b^2$ ; an antibonding configuration,  $\phi_a^2$ ; and the cross configurations,  $(\phi_b\phi_a - \phi_a\phi_b)$ . The configurations included in the MCSCF(SCGVB) wave function are then the products of these three types of configurations for each of the electron pairs. For  $N_2$  this procedure produces the set of configurations listed in Table 2. In general, the resulting MCSCF(SCGVB) wave function differs from the full SCGVB wave function because (i) the orbitals in each bond pair are orthogonal to the orbitals in other bond pairs (strong orthogonality), (ii) most modern MCSCF programs include all possible spin functions associated with a set of multiple open shell orbitals, i.e., the singlet-coupled  $(\phi_b\phi_a + \phi_a\phi_b)$  configuration is included in the product in addition to the triplet-coupled  $(\phi_b\phi_a - \phi_a\phi_b)$  configuration (in  $N_2$  this increases the number of configurations to 20), and (iii) the coefficients of configurations that are products of configurations in the SCGVB wave function may not be exactly so. However, the differences are rarely significant in the subsequent MRCI or MRCC calculations.

In the SCGVB-inspired CASSCF calculations, denoted by CASSCF(SCGVB), the SCGVB wave function is used to define the *active space* for the CASSCF calculation. This set of orbitals is usually a subset of the valence orbitals, e.g., it does not include any doubly occupied valence orbitals,  $\{\phi_{vi}\}$ , in the SCGVB wave function. This significantly reduces the number of configurations in the wave function, which, in turn, reduces the computational cost of the subsequent MRCI or MRCC calculations. In addition, Xu and Dunning<sup>21</sup> found that the CASSCF(SCGVB) wave function eliminated the problems they encountered in the full valence CASSCF calculations on the BF molecule. This problem occurs in many other molecules.

**2.5. Computational Methodology.** Multiple programs, based on a range of different approaches, are available for calculating SCGVB wave functions, with CASVB, VB2000<sup>70</sup> and XMVB<sup>71</sup> (amongst others) all being in the public domain. The current CASVB implementation of SCGVB theory<sup>28,69</sup> in MOLPRO<sup>80,81</sup> is based on the CASSCF methodology used in that program. This has significant advantages, but it results in the same computational limitations as those for CASSCF calculations. Recently, highly efficient implementations have been developed that use somewhat different algorithms to optimize the non-orthogonal orbitals and spin-coupling coefficients in the SCGVB wave function, see, e.g., Ref. 79. This latter technique can also be used for configuration interaction calculations using non-orthogonal orbitals. We expect other algorithms for SCGVB and SCGVB-CI calculations to be developed in the future.

All of the new calculations presented in this study were performed with the MOLPRO suite of quantum chemical programs (version 2010.1). The SCGVB calculations used the CASVB module referenced above.

The full valence CASSCF, vCASSCF, calculations included all of the configurations that can be formed using the valence orbitals of the atoms involved; the configurations included in the MCSCF(SCGVB) and CASSCF(SCGVB) calculations are as described herein. All of the new MRCI calculations reported here used the internally contracted methodology implemented in MOLPRO,<sup>82-84</sup> denoted *ic*-MRCI and included all single and double excitations from the zero-order wave function. All of the new calculations reported in this article used the augmented quadruple zeta basis set.<sup>85,86</sup> All other calculations used the programs, methodologies and basis sets described in the original publications.

### 3. INSIGHTS INTO THE ELECTRONIC STRUCTURE OF MOLECULES

Despite the current pre-eminence of molecular orbital (MO) theory in chemistry, valence bond theory has a long and distinguished history in chemistry. In fact, VB theory, which is the foundation for SCGVB theory, is the basis for many of the concepts used every day by chemists—hybrid orbitals, covalent bond pairs, lone pairs, resonance, and more. Although computational considerations favored the use of MO methods over VB methods in the early decades of computational quantum chemistry, this is no longer the case and, over the past couple of decades, applications of VB theory, including modern VB theories such as SCGVB theory, have blossomed (see several recent reviews<sup>33-59</sup>; see also Olsen<sup>79</sup>).

SCGVB theory provides a comprehensive orbital theory of the electronic structure of atoms and molecules. Since the SCGVB wave function is constructed to describe the making and breaking of chemical bonds, it provides a direct connection between the electronic structure of the molecule and the electronic structure of the atoms or fragments of which it is composed. SCGVB calculations enable us to understand how the atomic orbitals and spin coupling change as a molecule is formed. As a result, the SCGVB wave function provides a well-sourced description of the bonding in molecules, even in molecules with unusual bonding motifs, such as C<sub>2</sub>, Be<sub>2</sub>, and SF<sub>4</sub>/SF<sub>6</sub>. SCGVB theory also provides an explanation for the first-row anomaly, a puzzle that pervades inorganic chemistry, as well as valuable insights into many phenomena in organic chemistry, such as resonance in aromatic molecules and the electronic mechanisms of organic reactions. Finally, analysis of the SCGVB orbitals has provided new information on basic chemical concepts, such as orbital hybridization, one of the central tenants of organic chemistry.

**3.1. New Insights into the Chemical Bond.** SCGVB theory provides an appealing description of traditional chemical bonds in most molecules as well as the unusual bonding motifs found in a broad range of other molecules. As we saw in the previous section, the SCGVB wave function is based on a product of orbitals with an associated spin function. The SCGVB method places no constraints on the form of the orbitals other than those implied by the general form of the wave function, Eq. (1), allowing them to assume their optimal shape in the molecule. At large internuclear distances the SCGVB orbitals are just the atomic orbitals. As the molecule is formed, the SCGVB orbitals hybridize, polarize, delocalize, and contract. Nevertheless, as we shall see, the SCGVB orbitals tend to be semi-localized, i.e., concentrated on one atom with small “tails” on a few surrounding atoms. Although the SCGVB wave function allows for all possible

### Spin-Coupled Generalized Valence Bond Theory: New Perspectives on the Electronic Structure of Molecules and Chemical Bonds

spin couplings for the  $n_a$  electrons in the active orbitals, the perfect pairing spin function is dominant for many molecules near their equilibrium geometry. However, this is not always the case and the deviations represent potential new bonding motifs.

As examples of nearly non-polar covalent, polar covalent and ionic bonds, consider the two orbitals in the SCGVB wave functions responsible for the bond in the ground ( $X^1\Sigma^+$ ) states of the BH, HF and LiF molecules in Figure 5. In the separated atom limit,  $R = \infty$ , the SCGVB orbitals are simply the atomic  $2p_z$  orbitals of the boron and fluorine atoms and the  $1s$  and  $2s$  orbitals of the hydrogen and lithium atoms. At the equilibrium geometries ( $R_e$ ) of these molecules, there are well defined changes in the atomic SCGVB orbitals:

- In BH, the boron bond orbital,  $B2p_z'$ , has become a  $2s$ - $2p$  hybrid orbital with a minor amount of delocalization onto the hydrogen atom, while the hydrogen bond orbital,  $H1s'$ , is a slightly modified  $H1s$  atomic orbital. The relative lack of delocalization of the bond orbitals in BH is consistent with the similar electronegativities of the boron and hydrogen atoms,  $\chi(B) = 2.0$  and  $\chi(H) = 2.2$  and is indicative of the formation of a nearly non-polar covalent bond.
- In HF, the changes in the bond orbitals reflect the formation of a polar covalent bond. Since the electronegativity of fluorine,  $\chi(F) = 4.0$ , is much larger than that of hydrogen, the  $H1s'$  orbital delocalizes onto the fluorine atom acquiring substantial  $F2p_z$  character. This delocalization results in a transfer of charge from the hydrogen atom to the fluorine atom.<sup>60</sup> The fluorine bond orbital,  $F2p_z'$ , on the other hand has changed little.
- Finally, the electronegativity of the lithium atom,  $\chi(Li) = 1.0$ , is far less than that of the fluorine atom. As a result, the LiF bond is essentially ionic,  $Li^+F^-$ , and both of the orbitals in the bond pair are centered on the fluorine atom, with one of the  $F2p_z'$  orbitals being more diffuse than the other  $F2p_z'$  orbital, as would be expected for an  $F^-$  anion.<sup>87</sup>

The changes in the SCGVB bond orbitals in BH, HF and LiF are consistent with chemists' descriptions of the nature of the bonding in these three molecules but provide the basis for a more quantitative characterization of the bonding. For example, at  $R_e$  the overlap of the bond orbitals in the three bond pairs is 0.83 (BH), 0.82 (HF) and 0.87 (LiF), respectively, all of which are indicative of strong bonds. Analysis of the SCGVB orbitals can further quantify the nature of the bond pairs. Using the projection technique developed by Xu and Dunning,<sup>88</sup> the boron bond orbital at  $R_e$  in BH is found to be a  $sp^{1.76}$  hybrid orbital at  $R_e$  with the  $B2s$  and  $B2p$  atomic orbitals accounting for 94.8% of the SCGVB orbital. This is in distinct contrast to the fluorine bond orbital in HF at  $R_e$ , which is essentially a  $F2p_z$  orbital with a very small contribution from the  $F2s$  orbital,  $s^{0.07}p$ . These and other analyses help refine our understanding of covalent and ionic bonds.

The SCGVB(2,2) wave functions for HF and LiF correspond to simple two configuration wave

functions in MO theory. The SCGVB(4,5) wave function for BH is slightly more complicated with the extra configurations arising from the need to fully describe the 2s-2p near degeneracy effect in the boron atom. Despite the simplicity of these SCGVB wave functions, they offer significantly improved predictions over those from the RHF wave functions, see Table 3, which also includes the relevant experimental data.<sup>89-92</sup> The calculated SCGVB dissociation energies are improved by 9.6 kcal/mol (LiF) to 14.5 kcal/mol (HF) over those predicted by the RHF method. There are also improvements in the calculated values of the equilibrium bond distances ( $R_e$ ) and fundamental frequencies ( $\omega_e$ ), especially for the HF molecule. The errors in the SCGVB predictions relative to the experimental results in Table 3 are largely a result of the neglect of dynamical electron correlation (see Section 4).

Consider now a diatomic molecule with multiple bonds: the nitrogen molecule,  $N_2$ , which we used as an illustrative example of the application SCGVB theory in Section 2. The calculated and experimental spectroscopic constants for  $N_2$  are given in Table 4. For  $N_2$ , the SCGVB wave function is a major improvement over the RHF wave function. The predicted dissociation energy ( $D_e$ ) for  $N_2$  increases by 49.4 kcal/mol to 171.4 kcal/mol. There is also a significant improvement in the predicted  $R_e$  and  $\omega_e$  from the SCGVB calculations:  $R_e$  increases by 0.030 Å and is only 0.002 Å shorter than the experimental value, while  $\omega_e$  decreases by 359  $\text{cm}^{-1}$  and is just 11  $\text{cm}^{-1}$  larger than the experimental value. The more dramatic improvements in  $N_2$  are related to the low overlaps associated with the  $\pi$  bonds, 0.69; RHF theory assumes these overlaps are exactly 1.0. The remaining error in the value of  $D_e$  from the SCGVB calculations is substantial, ~57 kcal/mol, although as we will show in Section 4, almost all of this error can be recovered in an *ic*-MRCI calculation based on the SCGVB wave function.

There is another interesting phenomenon in  $N_2$  that the SCGVB calculations can shed light on. In a classic paper in 1967, Bader et al.<sup>93</sup> calculated the difference in the electron density for the  $N_2$  molecule at  $R_e$  relative to that of two nitrogen atoms at the same distance (see Figure 3 in Ref. 93). As expected, they found an increase in the electron density around the midpoint of the bond. However, there was also a depletion of density near the nuclei in the bonding region along with an increase in the density on the back side of each nucleus. As noted in Section 2, as the  $N_2$  molecule is formed, the  $N2s$  orbitals, which contain electron pairs, polarize away from the  $N2p_{zA}'-N2p_{zB}'$  bond pair as a result of Pauli repulsion<sup>46</sup> (see Figure 1). The polarization of the  $N2s'$  orbitals out of the bonding region depletes the density near the nuclei in the bonding region and increases the density on the back side of each of the nitrogen nuclei, leading to the changes in the density reported by Bader et al.<sup>93</sup>

There are also chemical phenomena for which SCGVB calculations provide new insights. As noted by Bodner et al.,<sup>94</sup> chemists sometimes use conflicting rationales to explain these phenomena. One of the inconsistencies they noted was the rationale used to explain the stability of  $N_2$  and the reactivity of  $C_2H_2$ . In general chemistry the stability of the  $N_2$  molecule is attributed to the presence of a strong triple bond, while students in organic chemistry are taught that the relative reactivity of acetylene is a result of the presence of a triple bond. These statements are made despite the fact that the triple bond in  $HC\equiv CH$  (273

### Spin-Coupled Generalized Valence Bond Theory: New Perspectives on the Electronic Structure of Molecules and Chemical Bonds

kcal/mol) is stronger than that in  $\text{N}\equiv\text{N}$  (228 kcal/mol). In an attempt to understand the root cause of this inconsistency, Xu and Dunning<sup>95</sup> examined the sequence of molecules:  $\text{N}_2$ ,  $\text{HCN}$  and  $\text{HCCH}$ . Although the triple bonds in these three molecules had many similar characteristics, there was one significant difference—the weight of the perfect pairing spin coupling mode, which systematically decreased from 92% in  $\text{N}_2$ , to 88% in  $\text{HCN}$  and to just 82% in  $\text{HCCH}$ . This clearly indicates that the nature of the triple bond in  $\text{C}_2\text{H}_2$  is not the same as that in  $\text{N}_2$ —the bonds in  $\text{C}_2\text{H}_2$  are not as strongly coupled together as singlet bond pairs as in  $\text{N}_2$ . Although further studies will be required to understand how this change in spin coupling impacts the relative reactivity of  $\text{HC}_2\text{H}$  and  $\text{N}_2$ , the SCGVB calculations provide a promising first step in identifying a potential cause of this difference.

Let us now consider another simple, but very unusual, homonuclear diatomic molecule:  $\text{C}_2$ . Unlike  $\text{N}_2$ , the  $\text{C}_2$  molecule has a very complicated SCGVB wave function. Actually, the nature of the bonding in  $\text{C}_2$  has a long and controversial history. In 1939, Mulliken<sup>96</sup> noted that the valence molecular orbital configuration of  $\text{C}_2$ ,  $2\sigma_g^2 2\sigma_u^2 1\pi_{ux}^2 1\pi_{uy}^2$ , indicated that it only has  $\pi$  bonds, since the doubly occupied bonding and antibonding  $\sigma$  orbitals would approximately nullify one another. However, this prediction has to be taken with a grain of salt since the molecular orbital (RHF) wave function does not provide a proper description of the electronic structure of  $\text{C}_2$ ,<sup>97</sup> e.g., RHF calculations predict that  $\text{C}_2$  is only bound by 18.3 kcal/mol.<sup>98</sup> More recently, the VB calculations of Su et al.<sup>99</sup> and of Shaik et al.<sup>100</sup> were interpreted to indicate that  $\text{C}_2$  had a triple bond<sup>99</sup> or a quadruple bond.<sup>100,101</sup> The SCGVB calculations on  $\text{C}_2$  by Xu and Dunning,<sup>98</sup> followed by further SCGVB studies by Cooper et al.,<sup>102</sup> suggest a very different interpretation of the bonding in  $\text{C}_2$ .

To understand the electronic structure of  $\text{C}_2$ , it is critical to understand how the SCGVB wave function for the carbon atom differs from the RHF wave function. In the RHF wave function the  $\text{C}2s$  orbital is doubly occupied and the valence configuration is  $2s^2 2p_x^1 2p_y^1$ . In the SCGVB wave function there are two  $\text{C}2s$  lobe orbitals, one concentrated on the left side of the nucleus ( $\text{C}2s_-$ ) and the other concentrated on the right side of the nucleus ( $\text{C}2s_+$ ), i.e., the SCGVB configuration is  $[2s_-^1, 2s_+^1] 2p_x^1 2p_y^1$ ,<sup>35,103</sup> where the brackets indicate that the spins of the electrons in the two orbitals are singlet coupled. The splitting of the  $\text{C}2s$  orbital into  $\text{C}2s_{\pm}$  lobe orbitals is a direct result of the atomic  $2s$ - $2p$  near-degeneracy effect noted by Sinanoğlu.<sup>37</sup> The overlap of the ( $\text{C}2s_-$ ,  $\text{C}2s_+$ ) orbitals is just 0.74 and, as a result, the SCGVB energy for the carbon atom is 12.0 kcal/mol lower than the RHF energy. More important than the energy lowering, however, is the presence of the two singly occupied, weakly overlapping  $\text{C}2s_{\pm}$  lobe orbitals, which implies that the carbon atom is tetravalent (more on this later). The SCGVB orbital diagram illustrating the formation of  $\text{C}_2$  from two carbon atoms is given in Figure 6, along with the orbitals for  $\text{C}_2$  at  $R = \infty$  and  $R_e$ . The changes observed in the  $\text{C}_2$  orbitals are reminiscent of those in the  $\text{N}_2$  molecule, although there are certainly quantitative differences. As expected, the SCGVB wave function smoothly connects the  $\text{C}_2$  molecule to two carbon atoms at  $R = \infty$ .



The calculated spectroscopic constants for  $C_2$  are given in Table 4. The SCGVB predictions are a marked improvement over those from the RHF calculations with the predicted  $D_e$  increasing by 94.3 kcal/mol. The results from the SCGVB calculations on  $C_2$  also provide a measure of consistency that is missing in those from the RHF calculations. For example, the difference between the experimental and SCGVB  $D_e$ 's for  $C_2$  is 30.2 kcal/mol compared to 57.0 kcal/mol for  $N_2$ , a ratio that is consistent with the difference in the number of electrons in these two molecules. Xu and Dunning<sup>98</sup> also found that the SCGVB calculations predict a bond length (1.244 Å) intermediate between a double bond (1.345 Å) and a triple bond (1.209 Å) and a bond energy (112.6 kcal/mol) between that for a single bond (80.9 kcal/mol) and a double bond (150.5 kcal/mol), just as found experimentally. In fact, the calculated  $C_2$  bond length is 74% of the way from a double bond to a triple bond, compared to 69% for experiment, and the calculated bond energy is 46% of the way from a single bond to a double bond, compared to 55% for experiment. All told, the SCGVB description of  $C_2$  is a major improvement over the RHF description, which is not too surprising as a proper description of  $C_2$  has long been known to require a multiconfiguration zero-order wave function.<sup>104</sup>

Xu and Dunning<sup>98</sup> found that the  $C_2$  molecule was very poorly described in the full SCGVB wave function by four singlet-coupled electron pairs, i.e., by four traditional bond pairs. The perfect pairing spin coupling had a weight of only 67% in the SCGVB wave function and restricting the spin function to only this spin coupling increases the energy of  $C_2$  by 20.4 kcal/mol. This is a clear indication that  $C_2$  does not have a traditional quadruple bond. Xu and Dunning found that the best single SCGVB configuration, i.e., combination of orbitals and given spin function, was one that had a traditional  $\sigma$  bond with the spins of the remaining electrons on each of the carbon atoms, i.e., those in the ( $2s_{A-}'$ ,  $2p_{Ax}'$ ,  $2p_{Ay}'$ ) and ( $2s_{B+}'$ ,  $2p_{Bx}'$ ,  $2p_{By}'$ ) orbitals, high-spin coupled with the two high-spin sets coupled overall to yield a singlet state (a “quasi-atomic” configuration<sup>98</sup>). This configuration, which is illustrated in the orbital diagram in Figure 6, has a weight of 82% in the SCGVB wave function. Although this weight is significantly larger than the perfect pairing weight, it still indicates that the “quasi-atomic” configuration does not provide an adequate description of  $C_2$ .

Cooper et al.<sup>102</sup> carried the study by Xu and Dunning one step further. They reported results for a two-configuration wave function for  $C_2$ , a wave function that combined the perfect pairing and quasi-atomic configurations. This wave function yielded an energy just 5.7 kcal/mol above the full SCGVB energy if the orbitals from the full SCGVB wave function were used unchanged. Re-optimization of the orbitals for this two-configuration wave function decreased the error to just 0.06 kcal/mol. These results suggest that  $C_2$  requires two SCGVB configurations to provide a satisfactory zero-order description of the molecule.  $C_2$  truly has an unusual bonding motif.

In spite of the obvious elegance of the SCGVB-based description of  $C_2$ , it is fair to say that the nature of the bonding in this molecule remains controversial. For example, whereas magnetic shielding analysis suggests that  $C_2$  possesses a bulky but relatively weak quadruple bond,<sup>105</sup> there are other modes of analysis

### Spin-Coupled Generalized Valence Bond Theory: New Perspectives on the Electronic Structure of Molecules and Chemical Bonds

that appear to suggest a  $\pi$  double bond that is accompanied by weaker  $\sigma$  bonding.<sup>106,107</sup> There is no doubt that  $C_2$  will be revisited in due course with many other types of analyses in an attempt to better understand the very unusual nature of the bonding in this molecule.

Another molecule with an unusual bonding motif is the  $Be_2$  molecule.<sup>108,109</sup> As in the carbon atom, the doubly occupied 2s orbital in the RHF wave function of the beryllium atom is described in the SCGVB wave function by two lobe orbitals, ( $Be2s_-$ ,  $Be2s_+$ ); see the top row in Figure 7. This figure includes the SCGVB orbital diagram for the formation of  $Be_2$  as well as the orbitals at  $R = \infty$  and  $R_e$ . Although the beryllium dimer is only weakly bound,  $D_e = 2.66$  kcal/mol and  $R_e = 2.545$  Å, the bond is much stronger than expected from a van der Waals interaction. Xu and Dunning<sup>110</sup> found that the SCGVB wave function for  $Be_2$  was dominated by the perfect pairing spin function (88%) with an “inner” pair that resembles a traditional  $\sigma$  bond with a bond orbital overlap of  $S(Be2s_{A+}, Be2s_{B-}) = 0.83$ , and an “outer” pair that is only weakly overlapping,  $S(Be2s_{A-}, Be2s_{B+}) = 0.27$ . Thus, there are two electron pairs in overlapping orbitals that occupy the same region of space in  $Be_2$ . Pauli repulsion between the two pairs weakens what would otherwise be a strong “inner” traditional  $\sigma$  bond and results in a very weakly bound  $Be_2$  molecule.<sup>111,112</sup> In an attempt to estimate the intrinsic strength and length of the traditional  $\sigma$  bond in  $Be_2$ , i.e., a  $\sigma$  bond uncompromised by the “outer” pair, Xu and Dunning reported CCSD(T) calculations on the  $HBe_{n-1}Be-BeBe_{n-1}H$  series. Extrapolating the results to  $n = \infty$ , they concluded that the strength of the traditional  $\sigma$  bond in  $Be_2$  was approximately 62–63 kcal/mol with a length of approximately 2.13–2.14 Å. This estimate indicates that Pauli repulsion decreases the bond energy by ~60 kcal/mol and increases the bond length by ~0.4 Å. It has long been known that Pauli repulsion was substantial in  $Be_2$ , e.g., from an energy decomposition analysis (EDA), Frenking and Bickelhaupt<sup>113</sup> calculated the contribution of Pauli repulsion to the bond energy to be 41.6 kcal/mol. Although the current value for the Pauli repulsion in  $Be_2$  is significantly larger than the EDA value, the two numbers may not be strictly comparable.

The dangling orbitals on each end of the  $Be_2$  molecule in Figure 7, ( $Be2s_{A-}$ ,  $Be2s_{B+}$ ), only weakly overlap, which indicates that two ligands can be readily added to this molecule, forming a stable  $XBeBeY$  species. The impact of the ligands on the strength and length of the  $Be-Be$  bond in  $XBeBeY$  is expected to be largest when the ligands are very electronegative, as this will draw the ( $Be2s_{A-}$ ,  $Be2s_{B+}$ ) orbitals out of the  $BeBe$  bonding region, decreasing Pauli repulsion with the electrons in the  $BeBe$   $\sigma$  bond. In CCSD(T) calculations on  $FBeBeF$ , Cui et al.<sup>114</sup> found that  $D_e = 76.9$  kcal/mol and  $R_e = 2.048$  Å, in line with this expectation.

Many complexes have now been studied experimentally and computationally that feature strong  $BeBe$  bonding and/or particularly short  $BeBe$  distances, with some authors suggesting unusual and surprising bonding patterns. It has been claimed, for example, that the bonding motif in various  $Be_2X_4Y_2$  clusters, in which (X,Y) are alkali metal atoms, involves  $Be\equiv Be$  triple bonds<sup>115-117</sup> whereas that in the octahedral  $Be_2(\mu_2-Li)_4$  cluster features a  $Be=Be$  double  $\pi$  bond with no associated  $\sigma$  component.<sup>118</sup> A related example

in the ongoing computational pursuit of potentially-stable beryllium complexes that feature ultra-short BeBe distances arises from a suggestion that bridging H atoms can simulate the effect of a Be≡Be triple bond.<sup>119</sup> The resulting [NgBeH<sub>3</sub>BeNg]<sup>+</sup> cations of *D*<sub>3h</sub> symmetry, in which Ng denotes a noble gas atom used as a proxy for an inert gas matrix, have indeed been predicted to have remarkably short BeBe distances.

SCGVB theory offers a straightforward way to reveal the actual nature of the bonding patterns in systems such as those above. In the particular case of the [NgBeH<sub>3</sub>BeNg]<sup>+</sup> cations,<sup>120</sup> CCSD(T)/cc-pVQZ geometry optimizations together with SCGVB calculations using the same basis set indicate, as is to be expected, that there are only relatively weak interactions with the Ng atoms. It is found that the bonding in the central moiety is devoid of any significant direct BeBe bonding and the same turns out to be true if one or both of the Be atoms are replaced by Mg. For all of these systems, with or without the capping Ng atoms, the short metal-metal separations are found to arise instead from the positively-charged metal centers being held closely together by the three negatively-charged hydrogens, with a stabilizing contribution from three equivalent sets of highly polar 3-center, 2-electron M–H–M bonds (M = Be, Mg).

As can be seen from the brief survey above, SCGVB theory provides compelling descriptions of the bonding in molecules with standard bonding motifs (BH, HF, LiF and N<sub>2</sub>) and those with non-standard bonding motifs (C<sub>2</sub>, Be<sub>2</sub>, and Be<sub>2</sub> clusters). The descriptions of the chemical bond in molecules with standard bonding motifs are consistent with traditional chemical concepts, while those with non-standard bonding motifs provide new ways of thinking about the bonding in these molecules. In the next section we will show how new bonding motifs also provide an explanation for the first-row anomaly.

**3.2. Impact in Inorganic Chemistry.** It is well-known in inorganic chemistry that the first-row main group elements, lithium through neon, behave differently than the corresponding elements in subsequent rows of the Periodic Table. As noted in Miessler and Tarr:

*“The main group elements show the “first-row anomaly” (counting the elements Li through Ne as the first row). Properties of elements in this row are frequently significantly different from properties of the other elements in the same group. ... No single explanation accounts for all the differences between elements in this row and other elements.”<sup>121</sup>*

One of the most dramatic, but certainly not the only manifestation of this difference is the formation of “hypervalent” or “hypercoordinate” molecules by elements beyond the first row, e.g., PCl<sub>5</sub>, SF<sub>6</sub>, and ClF<sub>3</sub>. Pauling first invoked *sp<sup>n</sup>d<sup>m</sup>* orbital hybridization as the underlying reason for the ability of the second and third row elements to form additional bonds.<sup>122</sup> Pauling later noted that the bonds involving fluorine and chlorine would be very ionic and that resonance between the various ionic isomers, i.e., Cl<sub>4</sub>P<sup>+</sup>–Cl<sup>–</sup>, would stabilize the molecule.<sup>123</sup> The first rationale was ruled out by detailed molecular calculations in the late 1980s and early 1990s.<sup>124–126</sup> We will comment on the second rationale later. Another rationale—the (3-center, 4-electron) bond—was put forward by Pimentel,<sup>127</sup> Rundle<sup>128</sup> and Pitzer<sup>129</sup> in the 1950s–1960s (see also Coulson<sup>130</sup>). Rundle<sup>131</sup> noted that combining the three atomic σ orbitals involved in a molecule like

## Spin-Coupled Generalized Valence Bond Theory: New Perspectives on the Electronic Structure of Molecules and Chemical Bonds

XeF<sub>2</sub>, namely, the doubly occupied Xe5p<sub>z</sub> and two singly occupied F2p<sub>z</sub> orbitals, would give rise to bonding, non-bonding and antibonding molecular orbitals. Since there are four electrons in these orbitals, the bonding and non-bonding orbitals would each have two electrons with none in the antibonding orbital, resulting in a stable (3-center, 4-electron) bond. We will show that the latter rationale as well as the revised rationale by Pauling are consistent with our current understanding of the nature of the bonding in hypervalent molecules, although both offer incomplete and somewhat misleading descriptions of the bonding in these molecules.

The first step forward in gaining a modern understanding of the bonding in hypervalent molecules was made by Cooper et al.,<sup>132</sup> who reported SCGVB calculations on a number of hypervalent molecules in 1994. Based on the findings of that study, they argued that the bonding in hypervalent molecules could be understood if the longstanding “octet rule” was replaced by the “democracy principle.” This principle states that any electron can participate in the formation of a bond provided that the energetic incentive to do so is sufficiently large. That paper was followed by a series of papers<sup>133–136</sup> that further explored the use of this principle to describe the electronic structure of hypervalent molecules. In 2009, Woon and Dunning<sup>137</sup> used the CASSCF and CASSCF+1+2 methods as well as the CCSD(T) method to characterize the molecules in the SF<sub>n</sub> ( $n = 1–6$ ) series, considering the successive formation of these molecules from their fragments, i.e., SF<sub>*n*–1</sub> + F → SF<sub>*n*</sub>. By recasting the CASSCF orbitals as SCGVB orbitals and examining how these orbitals changed as a function of  $R(F_{n-1}S-F)$ , they showed that the stability of the first excited states of SF and SF<sub>2</sub> as well as the ground states of SF<sub>*n*</sub> ( $n \geq 3$ ) was due to two new types of bonds—the recoupled pair bond and/or the recoupled pair bond dyad. An exemplar model for the recoupled pair bond is the SF bond in the  $a^4\Sigma^-$  state of the SF molecule<sup>35,137</sup> and that for the recoupled pair bond dyad is the  $\tilde{a}^3B_1$  state of the SF<sub>2</sub> molecule.<sup>36,137</sup> Although the names for these two bonds are new, recoupled pair bonds were observed decades earlier in, e.g., the  $a^3\Pi$  state of BH and the  $a^4\Sigma^-$  state of CH by Goddard and coworkers<sup>103,138</sup> and in the ground state,  $X^2\Sigma^+$ , of BeH by Gerratt and Raimondi.<sup>74</sup>

When a recoupled pair bond is formed, the spin coupling changes from a configuration that singlet couples the spins of the two electrons in a lone pair to a configuration that singlet couples the spins of the two electrons in the bond. For example, in the  $X^2\Sigma^+$  state of BeH, the spins of the electrons in the 2s lobe orbitals, (Be2s<sub>–</sub>, Be2s<sub>+</sub>), of the beryllium atom are singlet coupled at large  $R$  and the spin of the electron in the H1s orbital is free, giving rise to a  $^2\Sigma^+$  state. We will denote this configuration as [Be2s<sub>–</sub>,Be2s<sub>+</sub>]H1s, since the spins of the electrons in the Be2s<sub>±</sub> orbitals are singlet coupled. At  $R_e$ , the configuration changes to [H1s',Be2s<sub>+</sub>']Be2s<sub>–</sub>', i.e., the singlet coupled pair has changed from the Be2s<sub>±</sub> lobe orbitals to the BeH bond orbitals—a *recoupling* of the singlet pair. The overlap of the (Be2s<sub>+</sub>', H1s') orbitals at  $R_e$  is 0.81, which is indicative of a strong bond, although the strength of the bond is weakened by Pauli repulsion between the electron in the Be2s<sub>–</sub>' orbital and the bond pair. Thus, formation of the recoupled pair bond is a three-electron process resulting in a two-center bond plus an electron in the remaining lone pair lobe orbital, in this case, Be2s<sub>–</sub>'. That there are three electrons in three orbitals involved in the formation of a recoupled

pair bond has important consequences, especially for hypervalent molecules (see below).

A similar situation is found for the carbon atom. Bringing a hydrogen atom up to the  $C2s_{\pm}$  lobe orbitals results in the formation of a  $[C2s_{+}', H1s']$  bond pair in the  $CH(a^4\Sigma^-)$  state. Although the  $C2s_{-}'$  orbital overlaps the  $C2s_{+}'$  and  $H1s'$  bond orbitals, which leads to Pauli repulsion, the overlap of the  $(C2s_{-}', C2s_{+}')$  orbitals has decreased from 0.74 at  $R = \infty$  to 0.51 at  $R_e$ , while the overlap of the  $(C2s_{-}', H1s')$  orbitals is just 0.27. As a result, the strength of the recoupled pair bond in the  $CH(a^4\Sigma^-)$  state is 67 kcal/mol, only 17 kcal/mol weaker than the strength of the covalent bond in the ground state  $X^2\Pi$  of the CH molecule, 84 kcal/mol. However, this is not the case for hypervalent molecules like  $SF_n$ .

The sulfur atom has the configuration,  $3s^23p_x^23p_y^2$ , in its ground state, so all of the 3p orbitals are occupied and the formation of a  $S3s_{\pm}$  lobe pair is not possible, i.e., the  $S3s$  orbital is doubly occupied. Woon and Dunning<sup>137</sup> found, as expected, that the ground state of SF was a  $^2\Pi$  state, with a polar covalent  $S3p_z-F2p_z'$  bond; the calculated  $D_e$  was 83.3 kcal/mol (experimental value:  $82.5 \pm 1.6$  kcal/mol<sup>139</sup>). However, they also found a low-lying excited state, the  $SF(a^4\Sigma^-)$  state, which was bound by 36.2 kcal/mol (see also Yang and Boggs<sup>140</sup>). As they increased  $R$  for this state, they found that, in the CASSCF wave function, the pair of electrons in the  $S3p_z$  orbital of the sulfur atom was described by a pair of 3p lobe orbitals,  $(S3p_{z-}, S3p_{z+})$ . These lobe orbitals are linear combinations of  $S3p_z$  and  $S3d_{z^2}$  orbitals, although the  $S3d_{z^2}$  orbital is very different from the  $3d_{z^2}$  orbital in the excited states of the sulfur atom. The  $S3d_{z^2}$  orbital makes an important, but not particularly large contribution to the  $(S3p_{z-}, S3p_{z+})$  orbitals, consistent with the calculations in the late 1980s and early 1990s. The addition of a small amount of  $3d_{z^2}$  character to the  $S3p_z$  orbital is important because it results in the formation of  $3p_{\pm}$  lobe orbitals that are concentrated on the left and right sides of the sulfur atom, just as in the carbon atom (see Figure 8 in Ref. 35). However, the overlap between the two  $3p_{\pm}$  orbitals is high, 0.86.<sup>35</sup> Because of this, it is difficult for a ligand to form a bond with the electron in the  $S3p_{z+}'$  orbital without the bond pair having an unacceptably large overlap, and hence substantial Pauli repulsion, with the electron in the  $S3p_{z-}'$  orbital. As a result, formation of a recoupled pair bond with the electron in the  $S3p_{z+}$  orbital is *conditional*, i.e., its formation depends on the nature of the ligand. A key characteristic for the ligand is its electronegativity.<sup>141</sup> If the ligand is very electronegative, as are the fluorine and chlorine atoms or the hydroxyl radical, the sulfur-ligand bond will be very polar with the  $S3p_{z+}'$  orbital significantly delocalized onto the fluorine ligand, just as we saw for the  $H1s'$  orbital in HF. This reduces the overlap with the  $S3p_{z-}'$  orbital, and hence the Pauli repulsion, between the sulfur-ligand bond pair and the electron in the  $S3p_{z-}'$  orbital. As an example, the overlap between the  $S3p_{z-}'$  and  $S3p_{z+}'$  orbitals decreases from 0.86 in the sulfur atom to 0.60 at  $R_e$  in the  $SF(a^4\Sigma^-)$  molecule and the overlap between the  $S3p_{z-}'$  and  $F2p_z'$  orbitals is just 0.19.<sup>34</sup>

A recoupled pair bond dyad is formed when a second bond is formed using the electron in the lobe orbital left over from forming a recoupled pair bond, e.g., the  $S3p_{z-}'$  orbital in the  $SF(a^4\Sigma^-)$  state. If the ligand is, again, a very electronegative element like the fluorine atom, delocalization of the  $S3p_{z-}'$  orbital in the  $SF(a^4\Sigma^-)$  state onto the incoming fluorine atom will minimize the Pauli repulsion between the two

## Spin-Coupled Generalized Valence Bond Theory: New Perspectives on the Electronic Structure of Molecules and Chemical Bonds

bond pairs. As a result of this reduction, the F–SF bond in the  $\text{SF}_2(\tilde{a}^3\text{B}_1)$  state relative to the  $\text{F} + \text{SF}(a^4\Sigma^-)$  limit is calculated to be unusually strong, 106.6 kcal/mol.<sup>137</sup> For comparison, the energy of the second bond in the ground state of  $\text{SF}_2$  is calculated to be 91.0 kcal/mol relative to  $\text{F} + \text{SF}(X^2\Pi)$ . The net effect is that the resulting  $\text{SF}_2(\tilde{a}^3\text{B}_1)$  state is calculated to lie just 31.8 kcal/mol above the ground state ( $\tilde{X}^1\text{A}_1$ ) of  $\text{SF}_2$ , with the bonds in the recoupled pair bond dyad being, on average, only 16 kcal/mol weaker than the polar covalent bonds in the ground state. The unusual strength of the recoupled pair bond dyad is the underlying reason that hypervalent molecules are so stable.

In the ground states of SF and  $\text{SF}_2$ , the strengths of the bonds are similar, 83.3 kcal/mol (S–F) versus 91.0 kcal/mol (FS–F), as are their lengths, 1.601 Å versus 1.592 Å.<sup>137</sup> Thus, the formation of the second bond in the  $\text{SF}_2(\tilde{X}^1\text{A}_1)$  state has a minor effect on the first bond [the difference in bond strengths is partly due to the loss of the exchange coupling between the electrons in the 2p orbitals in the  $\text{S}(^3\text{P})$  state when the first bond is formed<sup>142</sup>]. However, in the excited states of SF and  $\text{SF}_2$  the two bonds are very different. The S–F bond in the  $\text{SF}(a^4\Sigma^-)$  state is very weak, 36.2 kcal/mol, while the FS–F bond in the  $\text{SF}_2(\tilde{a}^3\text{B}_1)$  state formed from  $\text{F} + \text{SF}(a^4\Sigma^-)$  is very strong, 106.6 kcal/mol. Furthermore, the calculated lengths of the bonds in the  $\text{SF}_2(\tilde{a}^3\text{B}_1)$  state, 1.666 Å, are much shorter than that in the  $\text{SF}(a^4\Sigma^-)$  state, 1.882 Å. Thus, unlike the bonds in the  $\text{SF}_2(\tilde{X}^1\text{A}_1)$  state, the two SF bonds in the  $\text{SF}_2(\tilde{a}^3\text{B}_1)$  state are strongly coupled.

Let us now consider the formation of  $\text{SF}_3$  and  $\text{SF}_4$ . Normally, one would consider the formation of  $\text{SF}_3$  from  $\text{SF}_2(\tilde{X}^1\text{A}_1) + \text{F}$ , but the structure of the ground state of  $\text{SF}_3$  is very different than that of the ground state of  $\text{SF}_2$  (see Figure 8). Consider instead the formation of  $\text{SF}_3$  from  $\text{SF}_2(\tilde{a}^3\text{B}_1) + \text{F}$ . The SCGVB wave function for the  $\text{SF}_2(\tilde{a}^3\text{B}_1)$  state has two singly occupied orbitals, one in the  $\text{SF}_2$  plane ( $\varphi_{a_1}$ ) and one in the perpendicular plane ( $\varphi_{b_1}$ ). Formation of  $\text{SF}_3(\tilde{X}^2\text{A}')$  from  $\text{F} + \text{SF}_2(\tilde{a}^3\text{B}_1)$  results in the formation of a traditional polar covalent bond with the electron in the  $\varphi_{b_1}$  orbital with the calculated strength of the resulting  $\text{F}_2\text{S–F}$  bond being 87.8 kcal/mol,<sup>137</sup> intermediate between the strengths of the polar covalent bonds in the  $\text{SF}(X^2\Pi)$  and  $\text{SF}_2(\tilde{X}^1\text{A}_1)$  states. The SCGVB wave function for  $\text{SF}_3$  still has one free, singly occupied orbital and formation of a second polar covalent bond leads to the ground state ( $\tilde{X}^1\text{A}_1$ ) of  $\text{SF}_4$ . The evolution of  $\text{SF}_n$  from SF to  $\text{SF}_4$  is illustrated in Figure 8. As can be seen, the ground state geometries as well as the bond energies of  $\text{SF}_3$  and  $\text{SF}_4$  can best be understood by focusing on the pathway from the ( $\tilde{a}^3\text{B}_1$ ) state of  $\text{SF}_2$  to the  $\tilde{X}^2\text{A}'$  state of  $\text{SF}_3$  and the  $\tilde{X}^1\text{A}_1$  state of  $\text{SF}_4$ <sup>137</sup>:

- In  $\text{SF}_2$ , the calculated bond angle is 162.7°; in  $\text{SF}_3$  the corresponding (axial) bond angle is 163.4°. In  $\text{SF}_2$  the SF bond length is 1.666 Å; in  $\text{SF}_3$  the axial bond length is 1.657 Å. Finally, the equatorial (polar covalent) bond in  $\text{SF}_3$  is, as expected, nearly perpendicular to the  $\text{SF}_2$  plane (87.6°) with a bond length of 1.566 Å, compared to 1.592 Å in the ground state of  $\text{SF}_2$ .
- In  $\text{SF}_4$ , the axial bond angle has opened slightly to 172.1° and the bond length has decreased slightly to 1.645 Å. The equatorial bond lengths are 1.548 Å, slightly shorter than in  $\text{SF}_3$ , and the equatorial bond

angle is  $101.4^\circ$ , compared to  $97.9^\circ$  in  $\text{SF}_2(\tilde{X}^1A_1)$ . Finally, the angle between the equatorial fluorine atoms and the axial fluorine atoms is  $87.5^\circ$ , essentially the same as in  $\text{SF}_3$ .

In  $\text{SF}_4$ , there is a recoupled pair bond dyad, two polar covalent bonds and a lone pair that arises from the doubly occupied  $S3s$  orbital. The lone pair orbital is polarized away from the two equatorial SF bonds as a result of Pauli repulsion. Formation of  $\text{SF}_5$  from  $\text{F} + \text{SF}_4(\tilde{X}^1A_1)$  requires formation of a recoupled pair bond. As a result, the calculated strength of the  $\text{F}_4\text{S}-\text{F}$  bond, 41.1 kcal/mol, is much weaker than a SF polar covalent bond and comparable to that of the recoupled pair bond in the  $\text{SF}(a^4\Sigma^-)$  state. The calculations also reveal a substantial change in geometry for  $\text{SF}_5$ .<sup>137</sup> Because of the remarkable stability of the recoupled pair bond dyad and the relative weakness of the recoupled pair bond, it is energetically better to form two recoupled pair bond dyads and a polar covalent bond in  $\text{SF}_5$  than a recoupled pair bond dyad, two polar covalent bonds, and a recoupled pair bond.<sup>137</sup> Similar tradeoffs occur in other hypervalent molecules.  $\text{SF}_6$  results from forming a polar covalent bond with the electron in the remaining singly occupied orbital in  $\text{SF}_5$  that is nearly perpendicular to the two recoupled pair bond dyads. The geometry of  $\text{SF}_6$  is an octahedron with a bond length of 1.561 Å. At 109.2 kcal/mol, the  $\text{F}_5\text{S}-\text{F}$  bond is the strongest bond in the series.

As has been shown by Dunning and coworkers, the structures and energetics of all of the hypervalent molecules that they studied— $\text{SF}_n$ ,<sup>137</sup>  $\text{SF}_{n-1}\text{Cl}$ ,<sup>143</sup>  $\text{SCl}_n$ ,<sup>144</sup>  $\text{PF}_n$ ,<sup>145</sup>  $\text{PF}_{n-1}\text{Cl}$ ,<sup>146</sup>  $\text{H}(\text{SO})$ ,<sup>147</sup>  $\text{S}_2\text{F}_4$ ,<sup>148,149</sup>  $\text{SO}_2$ ,<sup>150,151</sup>  $\text{Cl}_n\text{SO}$ ,<sup>152</sup>  $\text{ClF}_n$ ,<sup>153</sup>  $\text{ClF}_n^+$ ,<sup>154</sup> and  $\text{ClF}_n^{-155}$ —follow the pattern observed above for  $\text{SF}_n$  (see also Refs. 156, 157, and 158). In all of these molecules there are polar covalent bonds, recoupled pair bonds and recoupled pair bond dyads with the most stable structures and the bond energies being determined by the interplay of these three types of bonding. Dunning and coworkers<sup>147</sup> have also shown that the formation of a recoupled pair  $\pi$  bond dyad is responsible for: (1) the HSO isomer being of lower energy than the SOH isomer, despite the fact that an OH bond is inherently stronger than an SH bond by tens of kcal/mol; (2) the greater strength and shorter length of the bonds in  $\text{SO}_2$  as compared to the corresponding bonds in  $\text{O}_3$ ,<sup>150</sup> and (3) the NSF isomer being of lower energy than the FNS isomer despite the fact that the reverse is true in the analogous oxygen compounds.<sup>159,160</sup> A recoupled pair bond dyad is also responsible for the unusual T-shaped transition states for inversion found for  $\text{F}_2\text{PH}$  and  $\text{PF}_3$  as compared to the  $D_{3h}$ -like transition states in  $\text{FPH}_2$  and  $\text{PH}_3$ .<sup>161,162</sup> *From these studies, it is clear that recoupled pair bonds and recoupled pair bond dyads involving  $np$  lone pairs ( $n > 2$ ) are not a rarity in chemistry: they are ubiquitous in compounds of the second and third row elements and probably beyond.*

So, how does the SCGVB description of the bonds in hypervalent molecules compare with the traditional VB description of Pauling<sup>123</sup> and the MO descriptions of Pimentel, Rundle and Pitzer<sup>127-129</sup>? Consider the  $\tilde{a}^3B_1$  state of  $\text{SF}_2$ , one of the simplest molecules with a recoupled pair bond dyad. It is certainly possible to envision the stability of this state as arising from resonance between the  $\text{F}_l^--\text{S}^+\text{F}_r$  and  $\text{F}_r\text{S}^+-\text{F}_l^-$  structures as argued by Pauling. On the other hand, in SCGVB theory the bonds in the recoupled pair bond dyad are simply two very polar SF bonds. In regard to the (3-center, 4-electron) bond postulated by Pimentel-Rundle-Pitzer, SCGVB theory provides a very different interpretation of the orbitals involved.

## Spin-Coupled Generalized Valence Bond Theory: New Perspectives on the Electronic Structure of Molecules and Chemical Bonds

The natural orbitals from the SCGVB wave function describing the two bonds in the recoupled pair bond dyad for the  $\text{SF}_2(\tilde{a}^3\text{B}_1)$  state are plotted in the top row of Figure 9. As can be seen, the orbitals are localized in the two SF bond regions ( $\text{F}_l\text{--SF}_r$ ,  $\text{F}_r\text{S--F}_l$ ) and the occupation numbers of the natural orbitals are each 1.98. If we form symmetry orbitals,  $(\varphi_{a_1}, \varphi_{b_2})$ , from these two bond orbitals, the resulting delocalized molecular orbitals are simply the plus and minus combinations of the natural bond orbitals shown in the middle row in Figure 9. The bottom row of this figure contains the orbital diagrams for both the SCGVB description (left) and the Pimentel-Rundle-Pitzer description<sup>131</sup> (right). The SCGVB diagram shows the  $a_1$  and  $b_2$  orbitals arising from the two SCGVB natural bond orbitals are doubly occupied, while the Pimentel-Rundle-Pitzer diagram has the  $a_1$  and  $b_2$  orbitals arising from the bonding and non-bonding combinations of the three ( $\text{S}3p_z$ ,  $\text{F}2p_z$ ,  $\text{F}2p_x$ ) orbitals doubly occupied. These are two, very different views of the origins of the two doubly occupied orbitals in  $\text{SF}_2$ —one based on rigorous theoretical calculations, the other based on informed, although speculative reasoning.

In summary, the SCGVB description of the recoupled pair bonds and recoupled pair bond dyads accounts in a simple and straightforward manner for the origin of the bonding as well as the properties of the  $\text{SF}_n$  series, including the dramatic variations in the  $\text{F}_{n-1}\text{S--F}$  bond strengths, the dramatic shortening of the SF bonds in recoupled pair bond dyads in  $\text{SF}_2\text{--SF}_6$  (axial bonds), the presence of low-lying excited states in SF and  $\text{SF}_2$ , and the structures of  $\text{SF}_3\text{--SF}_6$  as well as the excited states of  $\text{SF}_2$ .

The interplay between covalent bonds and recoupled pair bonds also plays a significant role in Group 14 compounds. Even in the simple  $\text{XH}_n$  series ( $\text{X} = \text{C}, \text{Si}, \text{Ge}; n = 1\text{--}4$ ), significant variations can be attributed to this interplay. Xu et al.<sup>163</sup> showed that the change in the spatial and spin symmetry of the ground state from  $\text{CH}_2$ , which is a  $^3\text{B}_1$  state, to  $\text{SiH}_2$  and  $\text{GeH}_2$ , which are  $^1\text{A}_1$  states, is a direct result of the weakness of the recoupled pair bonds in the excited  $a^4\Sigma^-$  states of SiH and GeH. Although the recoupled pair bond in the  $\text{CH}(a^4\Sigma^-)$  state is calculated to be quite strong, 66.6 kcal/mol, the recoupled pair bonds in the  $\text{SiH}(a^4\Sigma^-)$  and  $\text{GeH}(a^4\Sigma^-)$  states are far weaker: 34.6 kcal/mol and 25.6 kcal/mol, respectively. As a result, the ground states of  $\text{SiH}_2$  and  $\text{GeH}_2$  have two covalent bonds, while the ground state of  $\text{CH}_2$  has a recoupled pair bond dyad, further stabilized by 2s-2p hybridization. The difference in the spatial and spin symmetry of the  $\text{XH}_2$  ground states then affects the spatial symmetry of the  $\text{XH}_3$  molecules. Formation of a covalent bond with the electron in the singly occupied  $\varphi_{a_1}$  orbital in the  $\text{CH}_2(\tilde{X}^3\text{B}_1)$  state leads to planar  $\text{CH}_3$  with three equivalent bonds. In the ground ( $\tilde{X}^1\text{A}_1$ ) states of  $\text{SiH}_2$  and  $\text{GeH}_2$  there are two singly occupied lone pair orbitals with electrons with singlet coupled spins in addition to the two covalent bonds. One of the lone pair orbitals points below the molecular plane ( $\varphi_{lp_-}$ ), the other orbital points above the plane ( $\varphi_{lp_+}$ ). When an electron in one of these orbitals is used to form a bond with a hydrogen atom, the resulting  $\text{SiH}_3$  and  $\text{GeH}_3$  molecules are pyramidal. Because the  $\text{H}_2\text{X--H}$  bonds in  $\text{SiH}_3$  and  $\text{GeH}_3$  are recoupled pair bonds, the bond energies are calculated to be 42.3 kcal/mol ( $\text{X} = \text{Si}$ ) or 52.2 kcal/mol ( $\text{X} = \text{Ge}$ ) weaker than the  $\text{H}_2\text{C--H}$  bond.



Although the underlying reason for the relative weakness of the recoupled pair bond in the  $a^4\Sigma^-$  states of SiH and GeH could not be definitively established, Xu et al.<sup>163</sup> offered two possible explanations: (i) the decrease in the overlap of the orbitals in the recoupled pair bond (CH: 0.83, SiH: 0.78, GeH: 0.77), which directly weakens the bond, and/or (ii) the increasing overlap between the ( $ns_-'$ ,  $ns_+'$ ) orbitals at  $R_e$  (CH: 0.51, SiH: 0.56, GeH: 0.60), which leads to increased Pauli repulsion between the electron in the  $ns_-'$  orbital and the bond pair.

**3.3. Impact in Organic Chemistry.** SCGVB also theory provides a compelling description of molecules and molecular processes in organic chemistry. As an example, consider the benzene molecule, the prototype aromatic molecule. In traditional VB theory the wave function for the electrons in the  $\pi$  system of the benzene molecule is taken to be a combination of the two Kekulé structures involving the atomic  $C2p_z$  orbitals on each atom. Later, three additional configurations—the para-bonded (so-called Dewar) structures—were added. In SCGVB theory the  $\pi$  system of benzene is described by an antisymmetrized product of six optimized, semi-localized orbitals, one for each electron, with a linear combination of the five spin functions that describe the six-electron singlet state. If the Rumer spin functions are used, these five spin functions represent the two Kekulé configurations and the three para-bonded configurations, i.e., the SCGVB description of benzene automatically includes all of the configurations of importance in the VB description of the  $\pi$  system of benzene.

The first SCGVB calculations on benzene were reported by Cooper et al. in 1986.<sup>164</sup> They found that each of the six  $\pi$  orbitals was localized on one of the carbon atoms with slight polarization toward the neighboring atoms. They also found that the sum of the configuration weights for the Kekulé structures was 0.81 and that for the para-bonded structures was 0.19, in line with chemists' expectations. Several follow-up studies of benzene and related molecules were reported,<sup>165-170</sup> including one that focused on the vertically excited states of benzene,<sup>77</sup> which showed that many of the low-lying excited states also had simple descriptions in SCGVB theory, e.g., the first singlet excited state ( $S_1$ ,  $^1B_{2u}$ ) was simply the difference of the two Kekulé configurations. As discussed below, this is an indicator of anti-aromaticity.

More recently, Xu et al.<sup>171</sup> addressed the puzzling SCGVB prediction of a planar, but non- $D_{6h}$  structure for the ground state of benzene (Small and Head-Gordon<sup>172</sup>). This study, like the other studies referenced above, focused on the  $\pi$ -electron system and found that the SCGVB energy was 39.4 kcal/mol below the RHF energy and only 4.8 kcal/mol above that of the corresponding CASSCF energy. Thus, the SCGVB wave function accounts for 89% of the correlation energy accounted for in the full CI CASSCF wave function with six electrons in six  $\pi$ -orbitals. Top and side views of one of the six  $\pi$  orbitals are pictured in Figure 10. In agreement with the work of Cooper et al.,<sup>164</sup> the  $C2p_z'$   $\pi$  orbitals are each centered on one of the carbon atoms but polarized toward the two neighboring carbon atoms. The shape of the orbital is consistent with the dominance of the Kekulé configurations in the SCGVB wave function. Xu et al.<sup>171</sup> found that the SCGVB prediction of a planar, but (slightly) non-hexagonal geometry was likely due to an interaction between the Kekulé and para-bonded (Dewar) configurations and could be eliminated by adding

### Spin-Coupled Generalized Valence Bond Theory: New Perspectives on the Electronic Structure of Molecules and Chemical Bonds

doubly ionic configurations ( $ion=2$ ) to the SCGVB wave function (singly ionic configurations are included through optimization of the orbitals). However, they found it was critical to re-optimize the orbitals in the SCGVB + ( $ion=2$ ) wave function. The energy of the latter wave function was essentially the same as the CASSCF energy, so higher orders of ionicity are clearly unimportant at this level of theory.

SCGVB calculations have also provided insights into a key difference between aromatic, anti-aromatic and non-aromatic molecules. The singlet ground state of square planar ( $D_{4h}$ ) cyclobutadiene,  $C_4H_4$ , is an exemplar for anti-aromatic molecules, even though the square planar geometry is not the optimum geometry for the ground state of the molecule. It was initially thought that the SCGVB hallmark of anti-aromaticity was the observation of so-called anti-pairs which, in the case of the ground ( $^1B_{1g}$ ) state of  $C_4H_4$ , take the form of in- and out-of-phase combinations of the  $C2p_z'$  orbitals across each diagonal, with the spins of the electrons in each pair overwhelmingly triplet coupled with the two triplet pairs coupled overall into a singlet state.<sup>173</sup> There is, however, an alternate SCGVB wave function with semi-localized active orbitals, similar to those in benzene, with an energy that is less than 0.03 kcal/mol above the anti-pair solution.<sup>174</sup> This alternate solution features  $C2p_z'$  orbitals across each diagonal with the spins of the electrons in these orbitals being *exclusively* triplet coupled. As a consequence, the spin function reduces to just the first Kotani/Serber spin coupling which, when transformed to the Rumer basis, corresponds to the difference rather than the sum of the two Kekulé configurations. The idea that anti-pairs could be linked to anti-aromaticity was completely abandoned when an SCGVB wave function with anti-pairs was observed in benzene while investigating the mechanism of a particular hydrogen shift.<sup>175</sup> *It is now clear that the out-of-phase combination of the two Kekulé configurations is the true signature of “anti-resonance.”*

As noted in the previous section, the SCGVB( $N,M$ ) method was motivated by the need to be able to properly describe the SCGVB wave functions for molecules such as the cyclopentadienyl anion ( $C_5H_5^-$ ) and tropylium cation ( $C_7H_7^+$ ). In the case of  $C_5H_5^-$ , for example, the SCGVB(6,5) wave function provides an accurate representation of the molecule as well as a remarkably clear model for the electronic structure of this aromatic anion that closely resembles that of benzene; see Figure 11. The SCGVB wave function for  $C_5H_5^-$  is dominated by the five Kekulé-type structures with the corresponding total weight being very similar to that in benzene; the same is true for the para-bonded structures. Each of the symmetry-unique SCGVB orbitals is localized on one of the carbon atoms, although, in this case, the orbital “tails” extend to more distant atoms than in benzene, as expected for an orbital with partial anionic character. The SCGVB(6,5) wave function accounts for 97% of the correlation energy predicted by a CASSCF(6,5) wave function. Similar results were obtained using an SCGVB(6,7) wave function for  $C_7H_7^+$  and, subsequently, in analogous SCGVB( $N,M$ ) calculations for a range of aromatic annulene ions,<sup>176</sup> with high levels of resonance being observed for all of the species with  $4n+2$   $\pi$  electrons, clearly demonstrating their aromaticity.

Karadakov and Cooper<sup>177</sup> also studied the local minima and transition-state geometries of species that

have been considered to exhibit homoconjugation and homoaromaticity, providing new insights into the electronic structure of these molecules and consistently recovering 95%–98% of the correlation energy provided by the corresponding CASSCF wave function. In each case, analysis of the forms of the SCGVB or SCGVB( $N,M$ ) orbitals, the magnitudes of the overlaps between them, and the compositions of the associated resonance patterns provided compelling descriptions of the various bonding motifs. Much the same was true for the SCGVB(8,9) wave function used to describe the  $\pi$ -electron system in the monocyclic cyclononatetraenyl cation,  $C_9H_9^+$ , with the results confirming in detail Heilbronner's ideas about the electronic structure of such Möbius annulenes.<sup>178</sup> As in benzene, many  $\pi$ -electron ring systems that are aromatic in their ground ( $S_0$ ) state become anti-aromatic upon vertical excitation to the first singlet excited ( $S_1$ ) electronic state, with the monocyclic cyclononatetraenyl cation being no exception.<sup>179</sup> Such a reversal in behavior is easily detected in SCGVB theory by the observation of anti-resonance in the  $S_1$  state, which is characterized by the out-of-phase combination of Kekulé configurations as mentioned earlier. Analogous behavior has been observed in various polycyclic fused aromatic compounds involving cyclopropenyl rings.<sup>180</sup>

Alongside the use of the full spin space, which proves so useful, for example, in distinguishing clearly between aromatic, anti-aromatic and non-aromatic  $\pi$ -electron systems, a key feature of SCGVB theory is the variational flexibility of the orbitals, given that they are expanded in the full molecular basis set without any constraints. It has been shown (see Ref. 181 and references therein) that the relative energetic importance of the different numbers of spin and orbital degrees of freedom leads, in some instances but not in others, to a preference for bent bond descriptions over the corresponding  $\sigma$ - $\pi$  separated solutions. Bent bonds have also been observed in a somewhat different context, namely for the in-plane  $\sigma$  bonding in strained ring systems. In studies of various such species, ranging from cyclobutane and cyclopropane to aziridine and thiirane, Karadakov et al.<sup>182,183</sup> found there was little to distinguish the bonding in these species from that in alkane chains except that, due to the geometry of the nuclear frameworks, the participating orbitals in these small rings bend in order to reduce the strain, while minimizing the loss of bond orbital overlaps.

SCGVB theory has also provided important insights into the electronic mechanisms of a broad range of organic chemical reactions (see Ref. 184 and references therein). In these studies, appropriate sets of calculations were first carried out to locate the transition state ( $TS$ ) and then SCGVB calculations were carried out at a sequence of geometries along the intrinsic reaction coordinate ( $IRC$ ) connecting reactants to products and passing through the transition state ( $TS$ ). The resulting SCGVB wave functions were analyzed, with the analysis involving an examination of the changes in the SCGVB orbitals and their overlaps as well as in the mode of spin coupling along the  $IRC$ . As an example, consider the SCGVB description of the electronic mechanism of the Diels–Alder reaction between *cis*-butadiene and ethylene.<sup>185</sup> The SCGVB wave function for this reaction consisted of six active valence orbitals, chosen so as to accommodate the six electrons in the  $\pi$  orbitals of butadiene and ethylene involved in the bond-breaking and bond-formation processes, and a singlet spin function,  $\Theta_{00}^6$ , consisting of five spin couplings expressed

## Spin-Coupled Generalized Valence Bond Theory: New Perspectives on the Electronic Structure of Molecules and Chemical Bonds

in the Rumer spin basis.

Throughout the reaction, each valence orbital remains well-localized around one of the carbon atoms and  $\Theta_{00}^6$  is dominated by the two Kekulé-type Rumer spin functions: (1–2,3–4,5–6) and (1–6,2–3,4–5). However, the valence orbital shapes, overlaps and spin-coupling pattern vary considerably along the reaction path. Initially, the  $\pi$  bonds in *cis*-butadiene are formed by the symmetry-related pairs of orbitals ( $\varphi_1, \varphi_2$ ) and ( $\varphi_3, \varphi_4$ ), while the pair ( $\varphi_5, \varphi_6$ ) is responsible for the ethylene  $\pi$  bond (see the leftmost orbital column,  $IRC = -0.6 \text{ amu}^{1/2}\text{bohr}$ , in Figure 12, which shows the symmetry-unique  $\varphi_1, \varphi_2$  and  $\varphi_6$  orbitals before the *TS*). At this point the reactant-like spin coupling (1–2,3–4,5–6) has a very large weight. At the *TS* (see the middle orbital column,  $IRC = 0$ , in Figure 12), the  $\varphi_1$  and  $\varphi_6$  orbitals are now distorted more towards one another, while the  $\varphi_2$  orbital distorts towards its partner by symmetry, the  $\varphi_3$  orbital. In parallel, there is a decrease in the distortions (and overlap) linking the  $\varphi_1$  and  $\varphi_2$  orbitals. The overlaps between all valence orbitals participating in breaking and forming bonds become very much the same as do the weights of the (1–2,3–4,5–6) and (1–6,2–3,4–5) Rumer spin couplings, indicating benzene-like resonance and aromaticity. After the *TS* (see the rightmost orbital column,  $IRC = +0.6 \text{ amu}^{1/2}\text{bohr}$ , in Figure 12), orbitals  $\varphi_1$  and  $\varphi_6$  appear to be much more  $sp^3$ -like and become engaged in one of the two new  $\sigma$  bonds formed during the reaction. Similarly, the pair of orbitals ( $\varphi_2, \varphi_3$ ) becomes responsible for the newly formed  $\pi$  bond. At this point the product-like spin coupling (1–6,2–3,4–5) becomes the most important spin function. The changes in the SCGVB wave function during the course of the Diels–Alder reaction between *cis*-butadiene and ethylene strongly suggest that this reaction follows a homolytic mechanism that could reasonably be described using six half curly arrows (‘harpoons’) to indicate the simultaneous breaking of the three  $\pi$  bonds in the reactants and the formation of the three new bonds, two  $\sigma$  and one  $\pi$ , in the product, instead of the traditional heterolytic mechanisms that are usually found in organic chemistry textbooks with three full curly arrows for the supposed shifts of three electron pairs.

Analogous SCGVB descriptions are found for various other organic reactions, such as the markedly asynchronous hetero-Diels–Alder reaction of acrolein ( $\text{H}_2\text{C}=\text{CH}-\text{CH}=\text{O}$ ) and ethylene<sup>186</sup> and the synchronous “aromatic” gas-phase retro-Diels–Alder reaction of bicyclo[2.2.1]hept-2-ene (norbornene) to cyclopentadiene and ethylene.<sup>187</sup> Similarly, the gas-phase concerted 1,3-dipolar cycloaddition reaction between methyl azide ( $\text{CH}_3\text{N}_3$ ) and ethylene is found to follow a homolytic mechanism. It is characterized by an almost simultaneous breaking of the two coplanar  $\pi$  bonds in methyl azide and of the  $\pi$  bond in ethylene, and the subsequent reengagement of the orbitals initially involved in these bonds into two new bonds, closing the triazole ring, and a lone pair on the central nitrogen in the product.<sup>188</sup> On the other hand, heterolytic mechanisms, realized through the movement of electron pairs, are observed for 1,3-dipolar cycloaddition reactions that involve 1,3-dipoles with more polar coplanar  $\pi$  bonds, such as fulminic acid ( $\text{HCNO}$ ) and diazomethane ( $\text{CH}_2\text{N}_2$ ).<sup>189, 190</sup> The insights provided by this powerful SCGVB-based methodology are also well demonstrated by a study of the “suprafacial with inversion” lowest-energy pathway of a [1,3] sigmatropic rearrangement linking bicyclo[3.2.0]hept-2-ene and norbornene, for which

the SCGVB approach reveals in a particularly clear cut way the singlet diradical character of the structure along the plateau in the energy profile.<sup>191</sup>

We will close this subsection on organic chemistry by discussing the concept of orbital hybridization, a concept that is considered one of the “ground truths” in organic chemistry (see, e.g., Refs. 192 and 193). Hybrid orbitals were introduced by Pauling<sup>194</sup> and Slater<sup>195</sup> in the early years of quantum chemistry, arguing that these orbitals maximize the overlap of the orbitals involved in a bond, leading to stronger bonds. In addition, the use of  $sp^3$  hybrid orbitals for the carbon atom in methane accounted for the tetravalence of the carbon atom and the tetrahedral structure of the molecule. Despite the ubiquitous use of hybrid orbitals in chemical thinking, there were early concerns about the use of hybrid orbitals<sup>196</sup> and more recently there has been a spirited discussion in the chemistry education literature about the role of hybrid orbitals in the chemistry curriculum<sup>197-203</sup> (see also Refs. 204 and 205).

In both the VBSCF and SCGVB wave functions, the orbitals are optimized, so these wave functions offer an unbiased opportunity to assess the nature of the bond orbitals in these wave functions. Shaik et al.<sup>63</sup> reported VBSCF calculations on methane and acetylene as well as a number of other molecules and used the overlaps of the orbitals on the carbon atoms to compute the hybridization ratios ( $h_{2p/2s}$ ). They reported that the overlap of the carbon hybrid orbitals is 0.674 in methane and 0.415 in acetylene, which corresponds to a hybridization ratio,  $h_{2p/2s}$ , of 1.76 in methane and of 0.41 in acetylene. Although the trend is correct, these values clearly differ significantly from the traditional hybridization ratios for these two molecules: 3.0 ( $\text{CH}_4$ ) and 1.0 ( $\text{C}_2\text{H}_2$ ). The deviations are sufficiently large that this analysis calls into question the traditional VB concept of hybrid orbitals.

Xu and Dunning<sup>88</sup> developed a projection technique to determine  $h_{2p/2s}$  for SCGVB orbitals and reported results for methane, ethylene and acetylene—the traditional models for  $sp^3$ ,  $sp^2$  and  $sp$  hybrid orbitals. This technique has the advantage that it provides  $h_{2p/2s}$  for each of the orbitals in the molecule, which means that  $h_{2p/2s}$  for the carbon-centered CC  $\sigma$  bond orbitals in ethylene and acetylene can be different than those for the CH bond orbitals in those molecules. The projection technique also has the advantage that it provides a measure of the total contribution of the atomic 2s and 2p orbitals to the SCGVB orbital ( $P_{2s+2p}^2$ ) with values close to unity indicating that the orbitals are predominately 2s-2p hybrid orbitals. Xu and Dunning investigated three versions of the SCGVB wave function: the SCGVB(PP/SO) wave function in which the spin function is constrained to be the perfect pairing spin function and the orbitals in different pairs are required to be orthogonal, the SCGVB(PP) wave function in which the orbitals are permitted to be non-orthogonal but the perfect pairing spin function is retained, and the SCGVB wave function which includes the full set of spin functions and non-orthogonal orbitals. The VBSCF wave function used by Shaik et al.<sup>63</sup> is similar to, but not exactly the same as the SCGVB(PP) wave function.

The results of the analysis of Xu and Dunning are summarized in Table 5. They found that the carbon-centered orbitals of the CH bonds from the SCGVB(PP/SO) wave functions were close to those from traditional VB theory: 2.97 ( $\text{CH}_4$ ), 2.16 ( $\text{C}_2\text{H}_4$ ), and 1.22 ( $\text{C}_2\text{H}_2$ ). For the CC  $\sigma$  bonds, the hybridization

### Spin-Coupled Generalized Valence Bond Theory: New Perspectives on the Electronic Structure of Molecules and Chemical Bonds

ratios for the SCGVB(PP/SO) wave functions were indeed different than those for the CH orbitals, being 1.49 ( $\text{C}_2\text{H}_4$ ) and 0.77 ( $\text{C}_2\text{H}_2$ ). However, once the strong orthogonality restriction was lifted, these ratios changed significantly. The hybridization ratio for the carbon-centered orbitals in the CH bonds in the SCGVB(PP) wave function is 1.58 ( $\text{CH}_4$ ), 1.03 ( $\text{C}_2\text{H}_4$ ), and 0.29 ( $\text{C}_2\text{H}_2$ ). These ratios are close to, if somewhat smaller than, those obtained by Shaik et al.<sup>63</sup> for  $\text{CH}_4$  (1.76) and  $\text{C}_2\text{H}_2$  (0.41). Eliminating the restriction on the mode of spin coupling results in an even more dramatic change in  $h_{2p/2s}$ : 0.57 ( $\text{CH}_4$ ), 0.57 ( $\text{C}_2\text{H}_4$ ) and 0.76 ( $\text{C}_2\text{H}_2$ ) for the carbon-centered CH bond orbitals and 0.39 ( $\text{C}_2\text{H}_4$ ) and 0.37 ( $\text{C}_2\text{H}_2$ ) for the carbon-centered CC  $\sigma$  bond orbitals. Despite the fact that the optimized SCGVB orbitals do not correspond to the hybrid orbitals of traditional VB theory, they are still hybrid orbitals as can be seen from the large values of  $P_{2s+2p}^2$ . The carbon-centered orbitals in the CH bond are all well described as a combination of carbon atom 2s and 2p orbitals with values of  $P_{2s+2p}^2$  greater than 0.98. The carbon-centered orbitals in the CC bond show somewhat larger differences from unity, 0.90 ( $\text{C}_2\text{H}_4$ ) and 0.93 ( $\text{C}_2\text{H}_2$ ), although the values are still very close.

So, what are we to conclude from the studies by Shaik et al.<sup>63</sup> and by Xu and Dunning<sup>88</sup>? First, the VBSCF and SCGVB orbitals are indeed hybrid orbitals—Xu and Dunning explicitly demonstrated that these orbitals are dominated by the carbon atom 2s and 2p orbitals in all of the molecules they considered. However, the VBSCF and SCGVB orbitals are not the  $sp^3$ ,  $sp^2$  and  $sp$  hybrid orbitals of traditional VB theory. In nearly all cases the decrease in the energy resulting from relaxation of the constraints on the wave function is associated with an increase in the 2s component of the hybrid orbitals. The observed increases in the C2s contribution indicates inclusion of more of the carbon  $^3\text{P}(2s^22p^2)$  state and less of the  $^4\text{S}(2s^12p^3)$  state in the SCGVB wave function, a result that is consistent with the fact that the  $^4\text{S}$  excited state of the carbon atom lies 96 kcal/mol<sup>206</sup> above the  $^3\text{P}$  ground state. (When Pauling and Slater proposed the use of  $sp^3$  hybrid orbitals in methane, the  $^4\text{S}$  state was thought to lie only 35-40 kcal/mol above the  $^3\text{P}$  state.<sup>196</sup>) However, inclusion of additional C2s character in the hybrid orbitals decreases the overlap of the carbon-centered hybrid orbitals and the hydrogen bond orbital, which would be expected to weaken the CH bonds. Thus, the optimum hybrid orbital appears to be the result of a compromise between the energy of the carbon atom, which favors more C2s ( $^3\text{P}$ ) character, and the strength of the CH bond, which favors more C2p ( $^4\text{S}$ ) character.

But, what about the use of  $sp^3$  orbitals to define the tetravalence of carbon and the tetrahedral geometry of methane? As we saw earlier, the SCGVB description of the ground state of the carbon atom involves four singly occupied orbitals ( $\text{C}2s_-$ ,  $\text{C}2s_+$ ,  $\text{C}2p_z$ ,  $\text{C}2p_x$ ). Although the ( $\text{C}2s_-$ ,  $\text{C}2s_+$ ) orbitals overlap, that overlap is sufficiently small that each of these orbitals can form strong bonds to a hydrogen atom as in, e.g., the  $\text{CH}(a^4\Sigma^-)$  state. On the surface, the SCGVB configuration of the carbon atom would be expected to lead to two different types of bonds in  $\text{CH}_4$ : two  $\text{C}2s_{\pm}\text{-H}1s$  bonds and two  $\text{C}2p\text{-H}1s$  bonds. However, the energy lowering associated with 2s-2p hybridization combined with Pauli repulsion between the resulting bond pairs leads, instead, to the observed tetrahedral structure of methane with four equivalent bonds. Similar

arguments apply to other organic molecules. Although SCGVB theory does not lead to the hybridization ratios of traditional VB theory, which are often invoked to rationalize the structure of organic molecules, the structures of these molecules do still follow from a straightforward application of quantum chemical principles.

#### 4. DYNAMICAL ELECTRON CORRELATION

Although the SCGVB wave function includes the finite set of configurations required to describe non-dynamical correlation effects, it cannot describe dynamical correlation effects. The latter effects are required for quantitative predictions of the structures, energetics and other properties of molecules. Fortunately, they can be taken into account using either multireference configuration interaction (MRCI) or multireference coupled cluster (MRCC) calculations based on the SCGVB wave function. To facilitate calculations that include dynamical correlation, the SCGVB wave function, in which the active orbitals ( $\phi_{ai}$ ) are non-orthogonal, can be recast, as noted in Section 2.3, as a multiconfiguration wave function, SCGVB(NO), in terms of orthogonal natural orbitals,  $\{\phi_{ci}, \phi_{vi}, \phi_{ai}^{\text{NO}}\}$ , and used in standard MRCI/MRCC calculations. As also noted in the Section 2.3, SCGVB-inspired wave functions can also be used as zero-order wave functions in subsequent MRCI/MRCC calculations.

The SCGVB-inspired approaches are based on using the SCGVB wave function, Eq. (1), to define either (i) the configurations to be used in an MCSCF calculation, denoted as MCSCF(SCGVB), or (ii) the active orbitals to be used in a CASSCF calculation, denoted as CASSCF(SCGVB). In this section we will report calculations on a few diatomic molecules using both of these latter approaches, given that these alternatives to the SCGVB(NO) wave function, especially in the case of the MCSCF(SCGVB) method, are less computationally expensive than the SCGVB(NO)-based approach. The results of the *ic*-MRCI calculations with the SCGVB-inspired zero-order wave functions will then be compared to the results obtained from *ic*-MRCI calculations using the full vCASSCF wave function as the zero-order wave function.

There are significant variations in the number of configurations in the zero-order wave function for the three types of *ic*-MRCI calculations. There are only two configuration state functions (CSFs) in the MCSCF(SCGVB) wave functions for the bonds in HF, HCl, F<sub>2</sub>, Cl<sub>2</sub> and ClF molecules versus three CSFs in the CASSCF(SCGVB) wave function. The full vCASSCF wave functions, on the other hand, contain 8 CSFs for HF and HCl, 10 CSFs for F<sub>2</sub> and Cl<sub>2</sub> (D<sub>2h</sub>), and 16 CSFs for ClF (C<sub>2v</sub>). The MCSCF(SCGVB) wave functions for the N<sub>2</sub>, P<sub>2</sub> and PN molecules are obtained by multiplying together the three configurations describing each of the  $\sigma$  and two  $\pi$  bonds. This generates 27 spatial configurations for N<sub>2</sub> and P<sub>2</sub>, but only 14 spatial configurations have the correct D<sub>2h</sub> symmetry. As noted earlier, these fourteen configurations are essentially equivalent to the SCGVB(NO) wave function if only one of the spin functions is used for the configurations with four open shells (see Table 2).<sup>207</sup> However, most modern computational chemistry codes include all of the spin functions associated with a given open shell configuration, which

## Spin-Coupled Generalized Valence Bond Theory: New Perspectives on the Electronic Structure of Molecules and Chemical Bonds

increases the number of CSFs in the MCSCF(SCGVB) wave function to 20. The CASSCF(SCGVB) wave functions have 55 CSFs for  $N_2$  and  $P_2$  ( $D_{2h}$ ) and PN ( $C_{2v}$ ), while the full vCASSCF wave function has 176 CSFs for  $N_2$  and  $P_2$  ( $D_{2h}$ ) and 328 CSFs for PN ( $C_{2v}$ ). The increase in the number of CSFs in the zero-order wave functions can be expected to result in increased computational costs for the corresponding *ic*-MRCI calculations.

Table 6 lists the major spectroscopic constants ( $R_e$ ,  $\omega_e$ ,  $D_e$ ) for HF, HCl,  $F_2$ ,  $Cl_2$ , ClF,  $N_2$ ,  $P_2$ , and PN from *ic*-MRCI calculations using the MCSCF(SCGVB), CASSCF(SCGVB) and full valence CASSCF (vCASSCF) wave functions as the zero-order wave functions for an *ic*-MRCI calculation including all single and double excitations from the zero-order wave functions. The potential energy curve for  $N_2$  obtained from *ic*-MCSCF(SCGVB)+1+2 and full *ic*-vCASSCF+1+2 calculations is shown in Figure 13.

The first conclusion to be drawn from Table 6 is the close agreement between the full *ic*-vCASSCF+1+2 and *ic*-MCSCF(SCGVB)+1+2 and *ic*-CASSCF(SCGVB)+1+2 predictions for both  $R_e$  and  $\omega_e$ . The values of the  $R_e$ 's are, in general, the same to 0.001 Å or better and the values of the  $\omega_e$ 's are the same to a few wavenumbers (we will discuss the differences in the results for HF in the following paragraph). The differences in the calculated values of the  $D_e$ 's are more significant, ranging from 0.7 kcal/mol (HCl) to 2.4 kcal/mol ( $P_2$ ). Although the predictions of  $D_e$  from the *ic*-MRCI calculations do not reach the level of chemical accuracy, they are a substantial improvement over the SCGVB predictions, with the *ic*-MCSCF(SCGVB)+1+2 calculations being less computationally expensive than the full *ic*-vCASSCF+1+2 calculations. It would be interesting to see if MRCC calculations would significantly reduce the errors in the  $D_e$  predictions. The second conclusion to be drawn from the data in Table 6 is that there is little reason to use the *ic*-CASSCF(SCGVB)-based method. The differences between the values of the  $R_e$ 's and  $\omega_e$ 's predicted by the *ic*-CASSCF(SCGVB)+1+2 calculations and the *ic*-MCSCF(SCGVB)+1+2 calculations are negligible and the corresponding differences in the values of  $D_e$ 's are just a few tenths of a kcal/mol. A more comprehensive investigation of these two methods is currently underway by two of the authors (LTX and THDJr).

One interesting aside to note in Table 6 is the difference in the dissociation energies predicted by the *ic*-MCSCF(SCGVB)+1+2 and full *ic*-vCASSCF+1+2 calculations for HF—the former is 1.0 kcal/mol larger than the latter; it is the only negative number in the last column of Table 4. This is surprising since the configurations in the MCSCF(SCGVB) wave function are a small subset of the configurations in the full vCASSCF wave function. This difference is a direct result of the problems that can arise in full vCASSCF calculations, as discussed in detail by Xu and Dunning.<sup>21</sup> At small  $R$ , the  $F1s'$  orbital, a closed orbital, mixes with the  $F2s'$  orbital, an active orbital, in the full vCASSCF wave function. Although this mixing lowers the vCASSCF energy, it increases the energy of the *ic*-vCASSCF+1+2 wave function by 1.0 kcal/mol, resulting in the observed decrease in the calculated dissociation energy. The MCSCF(SCGVB) and *ic*-MCSCF(SCGVB)+1+2 calculations, which include the  $F2s'$  orbital in the closed space, do not have



this problem. The mixing of the  $F1s'$  and  $F2s'$  orbitals also affect  $R_e$  and  $\omega_e$ , where the differences are larger than in the other molecules, 0.005 Å ( $R_e$ ) and 8 cm<sup>-1</sup> ( $\omega_e$ ).

The potential energy curves of  $N_2$  plotted in Figure 13 illustrate the close agreement between the *ic*-MCSCF(SCGVB)+1+2 and full *ic*-vCASSCF+1+2 calculations for all internuclear distances,  $R$ . The differences in the potential energy curves are barely discernible, so the difference ( $\Delta$ ) between the two curves has also been plotted. The small difference between the two potential energy curves is fully consistent with the difference in  $D_e$ 's given in Table 6.

## 5. CONCLUSIONS

From the results described herein and in many other studies in the literature, it is clear that SCGVB theory is the foundation for a comprehensive theory of the electronic structure of molecules. SCGVB theory is an orbital theory that explicitly includes the effects of non-dynamical correlation and, as a result, is able to describe a broad range of molecules and molecular phenomena. SCGVB theory provides a wealth of information on the nature of the chemical bond and the electronic structure of molecules, filling the gap first noted by Charles Coulson in 1960.<sup>38</sup> Coulson voiced the concern that the connection between computational chemistry and basic chemical concepts was being lost. This is not true for SCGVB theory, where computational studies show that, for many molecules, traditional chemical concepts are well founded, although, even for these molecules, SCGVB theory provides new avenues to explore, e.g., the role of spin coupling as the cause for the difference in the reactivity of the triple bonds in  $N_2$  and  $C_2H_2$  and the nature of hybrid orbitals. For molecules, such as  $C_2$ ,  $Be_2$ ,  $SF_n$ , anti-aromatic organic molecules, and the excited states of both inorganic and organic molecules, SCGVB theory provides new concepts that extend our basic understanding of the chemical bond and the electronic structure of molecules.

Because SCGVB theory can model the making and breaking of bonds, it explicitly describes the changes in the electronic structure of a molecule as it is formed from its constituent atoms. As the molecule is formed, the atomic orbitals smoothly transform into the molecular orbitals of the molecule and the spin function smoothly changes from that appropriate for the collection of atoms to that appropriate for the molecule. For most molecules, the SCGVB orbitals are semi-localized and resemble modified versions of their atomic counterparts. The changes in the orbitals are largely consistent with traditional chemical thinking—the bond orbitals polarize, hybridize, delocalize and contract. Hybridization of the bond orbitals increases their overlap, which, in turn, increases the strength of the bond, and delocalization of the bond orbitals implicitly builds ionic character into the wave function, the magnitude of which depends on the relative electronegativities of the two atoms involved. Orbitals containing electron pairs that are not involved in bonding also change as new bonds are formed, polarizing away from the new bond pairs to reduce Pauli repulsion among the electron pairs. This polarization results in shifts in the charge density which, at first sight, may seem puzzling, as was the case in  $N_2$ ,<sup>93</sup> although these shifts are simply a manifestation of the Pauli Principle.

### Spin-Coupled Generalized Valence Bond Theory: New Perspectives on the Electronic Structure of Molecules and Chemical Bonds

There is a clear distinction in SCGVB theory between the electronic structure of molecules containing elements in the first row of the Periodic Table (Li–Ne) and those in subsequent rows (Na–Ar, K–Kr). This difference is a result of the ability of the late main group elements in the second and third rows to form new types of bonds—recoupled pair bonds and recoupled pair bond dyads—using the electrons in their  $np$  lone pairs (see Ref. 137 and subsequent papers). (The difficulty of forming bonds with 2p lone pairs was discussed by Takeshita and Dunning.<sup>208</sup>) However, the bonds formed with the electrons in the ( $np_-$ ,  $np_+$ ) lone pairs are *conditional*, the bonds can only be formed if the element is very electronegative. This is a direct result of Pauli repulsion. Recoupled pair bonds have been referred to as 2-center, 3-electron bonds<sup>209</sup> and recoupled pair bond dyads have been referred to as 3-center, 4-electron bonds<sup>130</sup> in the past. SCGVB theory provides a simple, straightforward description of the bonds. A recoupled pair bond tends to be much weaker than the corresponding covalent bond, while the second bond in the recoupled pair bond dyad tends to be strong, at times even stronger than the corresponding covalent bond. The interplay between polar covalent bonds and these two new types of bonds explains many of the differences in the structures and energetics of compounds containing second- and third-row elements versus the first-row elements—the so-called first-row anomaly. From the studies reported to date, it is clear that recoupled pair bonds and recoupled pair bond dyads are not a rarity in chemistry—they are, in fact, ubiquitous.

SCGVB theory has also contributed to our understanding of the electronic structure of organic molecules and the electronic mechanisms of organic reactions. Resonance in aromatic molecules such as benzene are naturally described by the SCGVB wave function, with the five spin couplings associated with the six electrons in the  $\pi$  system of benzene corresponding to the two Kekulé and three para-bonded (Dewar) structures. SCGVB theory also provides succinct representations of many of the excited states of organic molecules, e.g., the first valence state of benzene ( $S_1$ ) is described by an antisymmetric combination of the two Kekulé structures. As shown by subsequent studies on square planar cyclobutadiene, the antisymmetric combination of Kekulé structures is the hallmark of anti-aromaticity. SCGVB theory also shows that small ring alkanes such as cyclopropane and cyclobutane have bent bonds, which are a result of balancing the strain energy against the bond energy (orbital overlap). SCGVB theory has also provided important insights into the electronic mechanisms of a broad range of organic chemical reactions. For example, SCGVB theory shows that the Diels-Alder reaction of *cis*-butadiene and ethylene follows a homolytic mechanism that should be described using six half curly arrows ('harpoons') to indicate the simultaneous breaking of the three  $\pi$  bonds in the reactants and the formation of the three new bonds in the product, instead of the traditional heterolytic mechanisms that are usually found in organic chemistry textbooks with three full curly arrows for the supposed shifts of three electron pairs.

SCGVB theory has also found, in the molecules studied thus far, that the carbon-centered bond orbitals in organic molecules are 2s-2p hybrid orbitals. However, they are far from the hybrid orbitals of traditional VB theory, e.g., in methane the bond orbital semi-localized on the carbon atom is an  $sp^{0.57}$  hybrid orbital. Nonetheless, the C2s and C2p atomic orbitals comprise 98.5% of the hybrid orbital. The optimum hybrid

orbitals appear to be the result of a compromise between the energy of the carbon atom, which favors more 2s ( $^3P$ ) character, and the strength of the CH bond, which favors more 2p ( $^4S$ ) character. Furthermore, SCGVB theory finds that the tetravalence of the carbon atom is a simple result of the fact that there are four singly occupied orbitals, ( $C2s_-$ ,  $C2s_+$ ,  $C2p_x$ ,  $C2p_z$ ), in the atom. Although the spins of the electrons in the ( $C2s_-$ ,  $C2s_+$ ) orbitals are singlet coupled, the overlap of these orbitals is sufficiently small that the electrons in these orbitals can form bonds with hydrogen and other elements. The tetrahedral structure of methane is a result of two factors: an energetic imperative associated with 2s-2p hybridization and Pauli repulsion. Although SCGVB theory does not lead to the traditional hybridization ratios, which are often invoked to rationalize the structure of organic molecules, the structures of these molecules still follow from a straightforward application of quantum chemical principles.

Since the early days of quantum chemistry, two distinct types of electron correlation have been recognized: non-dynamical and dynamical correlation. The SCGVB( $N,N$ ) and SCGVB( $N,M$ ) wave functions contain the finite set of configurations that describe non-dynamical correlation effects. By including these effects, SCGVB theory corrects the major deficiency in molecular orbital (RHF) theory and, as a result, SCGVB theory provides an excellent zero-order description of a broad range of molecules and molecular processes. To account for the effects of dynamical correlation, the SCGVB wave function can be used as the zero-order wave function in multiconfiguration configuration interaction (MRCI) and coupled cluster (MRCC) calculations. Although the SCGVB active orbitals are non-orthogonal, which complicates these calculations, this problem can be overcome by re-expressing the SCGVB wave function in terms of its orthonormal natural orbitals. With this transformation, the existing machinery for MRCI or MRCC calculations can be fully utilized. It is also possible to perform SCGVB-inspired MCSCF and CASSCF calculations, which have the advantage that they avoid the need for a prior SCGVB calculation.

In summary, Spin-Coupled Generalized Valence Bond (SCGVB) theory provides an appealing orbital description of the electronic structure of molecules as well as a means, through MRCI/MRCC calculations, for making quantitative predictions of molecular structures, energetics and other properties. Over the past fifty years, applications of SCGVB theory, and its earlier incarnations as GVB and SCVB theory, have shown that it is indeed possible, as Goddard and Palke first stated in 1969, to deduce

*“concepts concerning molecular bonding based entirely on ab initio calculations starting with the Schrödinger equation and independent of chemical prejudices.”<sup>210</sup>*

In addition, SCGVB theory addresses the concern first raised by Coulson in 1969 about the disconnect between computational chemistry and traditional chemical concepts. As we have shown, SCGVB theory provides support for many traditional chemical concepts as well as new concepts about the electronic structure of molecules and the nature of the chemical bond that transcend these concepts.

## Spin-Coupled Generalized Valence Bond Theory: New Perspectives on the Electronic Structure of Molecules and Chemical Bonds

### ■ AUTHOR INFORMATION

#### Corresponding Authors

Thom H. Dunning, Jr. – *Department of Chemistry, University of Washington, Seattle, Washington 98195-1700, United States*; orcid.org/0000-0002-3290-6507; Email: [thdj@uw.edu](mailto:thdj@uw.edu)

David L. Cooper – *Department of Chemistry, University of Liverpool, Liverpool, L69 7ZD, United Kingdom*; orcid.org/0000-0003-0639-0794; Email: [dlc@liverpool.ac.uk](mailto:dlc@liverpool.ac.uk)

#### Authors

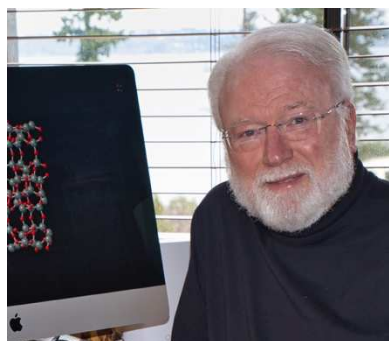
Lu T. Xu – *Department of Chemistry, University of Washington, Seattle, Washington 98195-1700, United States*; orcid.org/0000-0001-8206-4902; Email: [ltxu@uw.edu](mailto:ltxu@uw.edu)

Peter B. Karadakov – *Department of Chemistry, University of York, York, YO10 5DD, United Kingdom*; orcid.org/0000-0003-0639-0794; Email: [peter.karadakov@york.ac.uk](mailto:peter.karadakov@york.ac.uk)

#### Notes

The authors declare no competing financial interest.

#### Biographies



**Thom H. Dunning, Jr.** is a professor emeritus in the Department of Chemistry at the University of Illinois Urbana-Champaign, a research professor in the Department of Chemistry at the University of Washington and a Battelle Fellow at the Pacific Northwest National Laboratory. Professor Dunning received his B.S. in Chemistry from the Missouri University of Science and Technology in 1965 and his Ph.D. in Chemistry from the California Institute of Technology in 1970. Professor Dunning was a postdoctoral fellow with Professor Russel M. Pitzer at the Battelle Memorial Institute and Professor William A. Goddard III at the California Institute of Technology before joining the Los Alamos National Laboratory in 1973. Professor Dunning spent nearly 30 years at the national laboratories of the U.S. Department of Energy (LANL, Argonne National Laboratory, and Pacific Northwest National Laboratory) before accepting an appointment in the Department of Chemistry at the University of North Carolina, Chapel Hill, where he was also responsible for supercomputing and networking for the UNC system. After leaving UNC-Chapel Hill, Professor Dunning spent a couple of years at the University of Tennessee, Knoxville and Oak Ridge National Laboratory before joining the University of Illinois at Urbana-Champaign in 2004 as Director of the National Center for Supercomputing Applications and Distinguished Professor in the Department of Chemistry. Dr. Dunning retired from the University of Illinois in 2013 and rejoined the Pacific Northwest National Laboratory and the University of Washington. Professor Dunning is a Fellow of the American Chemical Society, the American Physical Society, and the Association for the Advancement of Science. He is also a member of the International

**T. H. Dunning, Jr., L. T. Xu, D. L. Cooper, and P. B. Karadakov**

Academy of Quantum Molecular Science. He received the E. O. Lawrence Award in Chemistry from the U.S. Department of Energy in 1997 and the ACS' Computers in Chemical and Pharmaceutical Research Award in 2011. Professor Dunning's research focuses on the development of GVB/SCGVB-based orbital theories of the electronic structure of molecules and the development of computational techniques for the quantitative prediction of molecular structures, energetics and other properties.



**Lu T. Xu** is a research scientist in the Department of Chemistry at the University of Washington. Dr. Xu received her B.S. in Chemistry from Tsinghua University in Beijing, China in 2009 and her Ph.D. in Chemistry from the University of Illinois at Urbana-Champaign in 2015, under the supervision of Prof. Thom H. Dunning, Jr. In 2016 She became a joint postdoctoral scholar in the Aerothermodynamics branch at NASA Ames Research Center and Department of Aerospace Engineering at the University of Illinois at Urbana-Champaign where she worked on first principles simulation of the Martian atmosphere for Mars entry vehicles. In 2018 she became a joint postdoctoral scholar in the Computational Research division at the Lawrence Berkeley

National Laboratory and the Department of Chemistry at the University of Washington where she worked on understanding the fundamentals of chemical bonding using SCGVB and other highly accurate electronic structure methods, as well as developing SCGVB-based electronic structure theories and computational techniques. Her current research is a continuation of her work in SCGVB and SCGVB-based electronic structure development.



David L. Cooper is a reader in Physical Chemistry in the Department of Chemistry at the University of Liverpool. He received his B.A. in Chemistry from Oxford University in 1979 and his D.Phil. in Chemistry from the same University in 1981, under the supervision of W. Graham Richards. From 1981 to 1983 he held a Smithsonian Fellowship at the Harvard-Smithsonian Center for Astrophysics, mostly working with Kate Kirby. Dr. Cooper returned to Oxford University for a further two years as a Junior Research Fellow and then Royal Society University Lecturer. It was around this time that he joined Joe Gerratt and Mario Raimondi to form 'the gang of three' to work on the development and applications of SCGVB theory. Dr. Cooper moved to the

University of Liverpool in 1985 and has been a Science and Technology Media Fellow with BBC Radio in London (1987) and a BP Venture Research Fellow (1989-93). In addition to his computational chemistry research, Dr. Cooper was heavily involved in the establishment of the award-winning Central Teaching Laboratories at the University of Liverpool and he also continues to take an active interest in the development of new schools' outreach activities. Dr. Cooper's current research focuses on studies of the electronic structures of small molecules and molecular processes, especially using SCGVB theory, but also on the use of auxiliary tools, such as domain-averaged Fermi hole analysis and multicenter bond indices, which aim to extract useful chemical information from contemporary high-accuracy density matrices.

## Spin-Coupled Generalized Valence Bond Theory: New Perspectives on the Electronic Structure of Molecules and Chemical Bonds



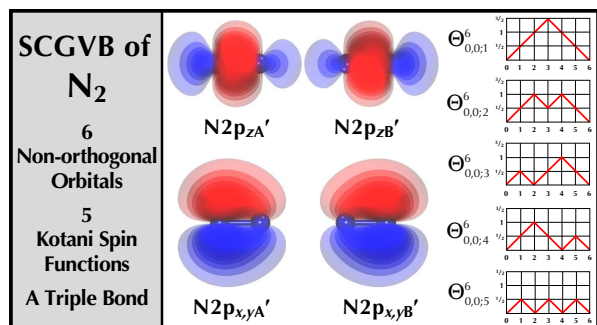
Peter B. Karadakov is a reader in Theoretical Chemistry in the Department of Chemistry at the University of York. He received his M.Sc. in Chemistry from Sofia University, Bulgaria, in 1981 and his Ph.D. in Quantum Chemistry from the Bulgarian Higher Degrees Commission in 1983. After a lectureship at the Faculty of Chemistry of Sofia University and a research position at the Institute of Organic Chemistry of the Bulgarian Academy of Sciences, during which he was doing independent research on HF instabilities in extended systems and the spin-projected HF method, including the formulation of the “extended” pairing theorem, some of which was in collaboration with Jean-Louis Calais at the University of Uppsala, in 1990 he joined the research group of Joseph Gerratt

to work on the development and applications of SCGVB theory and many-electron spin functions. In 1995 Dr. Karadakov accepted a lectureship in Physical Chemistry at University of Surrey where, through his collaboration with Graham A. Webb he became interested in theoretical NMR, which led to a collaboration with Keiji Morokuma on the calculation of NMR shieldings with the ONIOM method. In 2000 Dr. Karadakov moved to his current position at the University of York. His research is equally shared between the development and applications of SCGVB theory and the use of off-nucleus NMR shielding to describe bonding, aromaticity and antiaromaticity in the ground and excited states of molecular systems.

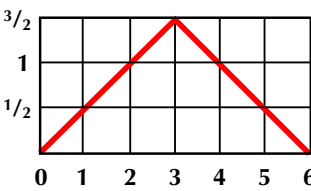
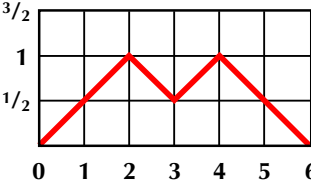
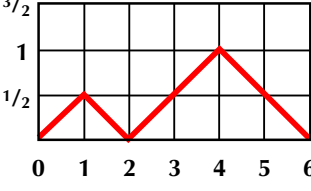
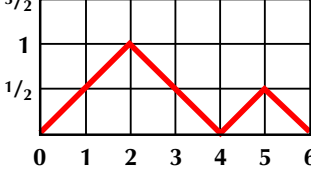
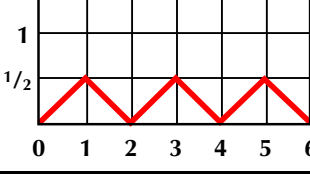
### ■ ACKNOWLEDGEMENTS

This research was supported in part by the Center for Scalable Predictive Methods for Excitations and Correlated phenomena (SPEC), which is funded by the U.S. Department of Energy, Office of Science, Basic Energy Sciences, Chemical Sciences, Geosciences and Biosciences Division, as part of the Computational Chemical Sciences Program at Pacific Northwest National Laboratory. We wish to thank all of our students and colleagues who have contributed to the development of SCGVB theory. In particular, we wish to acknowledge and thank Professors William A. Goddard III, the late Joseph Gerratt, and also Mario Raimondi for laying the foundation for the studies reported in this article.

### ■ TABLE OF CONTENTS (TOC) FIGURE



**Table 1.** The complete set of Kotani spin functions for a six-electron singlet state. There are five linearly independent spin functions for  $n_a = 6$  and  $S = M_S = 0$ . Note that each step in the path corresponds to adding one additional spin at a time, according to the usual angular momentum coupling rules.

Symbol	Symbol	Path in Branching Diagram	Relevance for N <sub>2</sub>
${}^K\Theta_{0,0;1}^6$	$\alpha\alpha\alpha\beta\beta\beta$		If the orbitals are arranged sequentially on each atom, (N2p <sub>zA</sub> ', N2p <sub>xA</sub> ', N2p <sub>yA</sub> ') and (N2p <sub>zB</sub> ', N2p <sub>xB</sub> ', N2p <sub>yB</sub> '), this spin coupling describes two <sup>4</sup> S nitrogen atoms with their spins coupled to an overall singlet state.
${}^K\Theta_{0,0;2}^6$	$\alpha\alpha\beta\alpha\beta\beta$		
${}^K\Theta_{0,0;3}^6$	$\alpha\beta\alpha\alpha\beta\beta$		If the orbitals are sequenced as (N2p <sub>zA</sub> ', N2p <sub>zB</sub> ') and (N2p <sub>xA</sub> ', N2p <sub>yA</sub> ', N2p <sub>xB</sub> ', N2p <sub>yB</sub> '), this spin coupling couples the spins of the first two electrons into a singlet, i.e., a traditional $\sigma$ bond, and the spins of the last four electrons as in the nitrogen atom.
${}^K\Theta_{0,0;4}^6$	$\alpha\alpha\beta\beta\alpha\beta$		
${}^K\Theta_{0,0;5}^6$	$\alpha\beta\alpha\beta\alpha\beta$		If the orbitals are sequenced as bonding pairs, (N2p <sub>zA</sub> ', N2p <sub>zB</sub> '), (N2p <sub>xA</sub> ', N2p <sub>xB</sub> '), and (N2p <sub>yA</sub> ', N2p <sub>yB</sub> '), this spin coupling is the perfect pairing spin coupling.

**Spin-Coupled Generalized Valence Bond Theory:  
New Perspectives on the Electronic Structure of Molecules and Chemical Bonds**

**Table 2.** List of the configurations in the SCGVB wave function for the N<sub>2</sub> molecule in terms of the orthonormal SCGVB natural orbitals:

$$\begin{aligned}
 3\sigma_g &= N_{\sigma_g} (\varphi_{2p_{zA}}, -\varphi_{2p_{zB}}) & 3\sigma_u &= N_{\sigma_u} (\varphi_{2p_{zA}}, +\varphi_{2p_{zB}}) \\
 1\pi_{xu} &= N_{\pi_u} (\varphi_{2p_{xA}}, +\varphi_{2p_{xB}}) & 1\pi_{xg} &= N_{\pi_g} (\varphi_{2p_{xA}}, -\varphi_{2p_{xB}}) \\
 1\pi_{yu} &= N_{\pi_u} (\varphi_{2p_{yA}}, +\varphi_{2p_{yB}}) & 1\pi_{yg} &= N_{\pi_g} (\varphi_{2p_{yA}}, -\varphi_{2p_{yB}})
 \end{aligned}$$

The doubly occupied NIs core orbitals are represented by [...] in the configuration list. The superscript “3” in the second column indicates that the electron spins are triplet coupled.

[...]2 $\sigma_g^2$ 2 $\sigma_u^2$ 1 $\pi_{xu}^2$ 1 $\pi_{yu}^2$ 3 $\sigma_g^2$	[...]2 $\sigma_g^2$ 2 $\sigma_u^2$ (1 $\pi_{xu}^1$ 1 $\pi_{xg}^1$ ) <sup>3</sup> (1 $\pi_{yu}^1$ 1 $\pi_{yg}^1$ ) <sup>3</sup> 3 $\sigma_g^2$
[...]2 $\sigma_g^2$ 2 $\sigma_u^2$ 1 $\pi_{xu}^2$ 1 $\pi_{yu}^2$ 3 $\sigma_u^2$	[...]2 $\sigma_g^2$ 2 $\sigma_u^2$ (1 $\pi_{xu}^1$ 1 $\pi_{xg}^1$ ) <sup>3</sup> (1 $\pi_{yu}^1$ 1 $\pi_{yg}^1$ ) <sup>3</sup> 3 $\sigma_u^2$
[...]2 $\sigma_g^2$ 2 $\sigma_u^2$ 1 $\pi_{xu}^2$ 1 $\pi_{yg}^2$ 3 $\sigma_g^2$	[...]2 $\sigma_g^2$ 2 $\sigma_u^2$ (1 $\pi_{xu}^1$ 1 $\pi_{xg}^1$ ) <sup>3</sup> 1 $\pi_{yu}^2$ (3 $\sigma_g^1$ 3 $\sigma_u^1$ ) <sup>3</sup>
[...]2 $\sigma_g^2$ 2 $\sigma_u^2$ 1 $\pi_{xg}^2$ 1 $\pi_{yu}^2$ 3 $\sigma_g^2$	[...]2 $\sigma_g^2$ 2 $\sigma_u^2$ 1 $\pi_{xu}^2$ (1 $\pi_{yu}^1$ 1 $\pi_{yg}^1$ ) <sup>3</sup> (3 $\sigma_g^1$ 3 $\sigma_u^1$ ) <sup>3</sup>
[...]2 $\sigma_g^2$ 2 $\sigma_u^2$ 1 $\pi_{xu}^2$ 1 $\pi_{yg}^2$ 3 $\sigma_u^2$	[...]2 $\sigma_g^2$ 2 $\sigma_u^2$ (1 $\pi_{xu}^1$ 1 $\pi_{xg}^1$ ) <sup>3</sup> 1 $\pi_{yg}^2$ (3 $\sigma_g^1$ 3 $\sigma_u^1$ ) <sup>3</sup>
[...]2 $\sigma_g^2$ 2 $\sigma_u^2$ 1 $\pi_{xg}^2$ 1 $\pi_{yu}^2$ 3 $\sigma_u^2$	[...]2 $\sigma_g^2$ 2 $\sigma_u^2$ 1 $\pi_{xg}^2$ (1 $\pi_{yu}^1$ 1 $\pi_{yg}^1$ ) <sup>3</sup> (3 $\sigma_g^1$ 3 $\sigma_u^1$ ) <sup>3</sup>
[...]2 $\sigma_g^2$ 2 $\sigma_u^2$ 1 $\pi_{xg}^2$ 1 $\pi_{yg}^2$ 3 $\sigma_g^2$	
[...]2 $\sigma_g^2$ 2 $\sigma_u^2$ 1 $\pi_{xg}^2$ 1 $\pi_{yg}^2$ 3 $\sigma_u^2$	



**Table 3.** Spectroscopic constants for the ground states ( $X^1\Sigma^+$ ) of the BH, HF and LiF molecules from HF and SCGVb with an aug-cc-pVQZ basis set.

Molecule	Method	$E_e(\text{a.u.})$	$R_e (\text{\AA})$	$\omega_e (\text{cm}^{-1})$	$D_e (\text{kcal/mol})$
BH	HF	-25.131428	1.2201	2487	64.32
	SCGVb <sup>a</sup>	-25.187009	1.2490	2287	77.40
	Expt'l <sup>b,c</sup>	—	1.2324	2367	85.0
HF	HF	-100.069039	0.8973	4470	100.3
	SCGVb	-100.092107	0.9149	4129	114.8
	Expt'l <sup>b,d</sup>	—	0.9168	4138	141.2
LiF	HF	-106.991162	1.5545	942	93.66
	SCGVb	-107.006472	1.5683	931	103.3
	Expt'l <sup>b,e</sup>	—	1.5639	910.3	138.8

<sup>a</sup> To ensure that the SCGVb wave function describes the 2s-2p near-degeneracy effect in the boron atom in full, an SCGVb(4,5) wave function was used; see Ref. 21.

<sup>b</sup> Ref. 89.

<sup>c</sup> Ref. 90.

<sup>d</sup> Ref. 91.

<sup>e</sup> Ref. 92.

**Spin-Coupled Generalized Valence Bond Theory:  
New Perspectives on the Electronic Structure of Molecules and Chemical Bonds**

**Table 4.** Spectroscopic constants for the ground states ( $X^1\Sigma_g^+$ ) of the  $N_2$  and  $C_2$  molecules from HF and SCGVB calculations with an aug-cc-pVQZ basis set.

Molecule	Method	$R_e$ (Å)	$\omega_e$ (cm <sup>-1</sup> )	$D_e$ (kcal/mol)
$N_2^a$	HF	1.066	2729	122.0
	SCGVB	1.096	2370	171.4
	Expt'l	1.0977	2359	228.4
$C_2^b$	HF	1.239	1904	18.3
	SCGVB	1.244	1845	112.6
	Expt'l	1.2425	1854.7	142.8

<sup>a</sup> Ref. 39.

<sup>b</sup> Ref. 98.

**Table 5.** Hybridization ratios ( $h_{2p/2s}$ ) and total atomic ( $2s+2p$ ) compositions ( $P_{2s+2p}^2$ ) of the carbon-centered bond orbitals from SCGVB calculations on methane, ethylene and acetylene with the aug-cc-pVQZ basis set (Ref. 88).

Molecule	Bond	SCGVB(PP/SO)		SCGVB(PP)		SCGVB
		$h_{2p/2s}(VB)$	$h_{2p/2s}$	$h_{2p/2s}$	$h_{2p/2s}$	$P_{2s+2p}^2$
CH <sub>4</sub>	CH	3.0	2.97	1.58	0.57	0.985
C <sub>2</sub> H <sub>4</sub>	CH	2.0	2.16	1.03	0.57	0.982
	CC	2.0	1.49	0.82	0.39	0.904
C <sub>2</sub> H <sub>2</sub>	CH	1.0	1.22	0.29	0.76	0.983
	CC	1.0	0.77	0.29	0.37	0.934

**Table 6.** Spectroscopic constants for a selection of diatomic molecules from MCSCF(SCGVb)+1+2, CASSCF(SCGVb)+1+2, and full vCASSCF+1+2 calculations with an aug-cc-pVQZ basis set. For HF, HCl, F<sub>2</sub>, Cl<sub>2</sub>, and ClF, the MCSCF(SCGVb) and CASSCF(SCGVb) wave functions are the same.  $\Delta$  is the difference between the vCASSCF+1+2 and MCSCF(SCGVb)+1+2 results.

Molecule	Method	$R_e$ (Å)	$\omega_e$ (cm <sup>-1</sup> )	$D_e$ (kcal/mol)
HF	MCSCF(SCGVb)+1+2	0.916	4165	138.1
	vCASSCF+1+2	0.921	4173	137.1
	$\Delta$	0.005	8	-1.0
HCl	MCSCF(SCGVb)+1+2	1.276	2994	104.7
	vCASSCF+1+2	1.276	2992	105.4
	$\Delta$	0.000	-2	0.7
F <sub>2</sub>	MCSCF(SCGVb)+1+2	1.415	890	33.7
	vCASSCF+1+2	1.416	895	34.5
	$\Delta$	0.001	5	0.8
Cl <sub>2</sub>	MCSCF(SCGVb)+1+2	2.000	550	53.5
	vCASSCF+1+2	2.000	550	55.0
	$\Delta$	0.000	0	1.5
ClF	MCSCF(SCGVb)+1+2	1.629	782	56.6
	vCASSCF+1+2	1.631	782	57.5
	$\Delta$	0.002	0	0.9
N <sub>2</sub>	MCSCF(SCGVb)+1+2	1.100	2355	223.4
	CASSCF(SCGVb)+1+2	1.100	2353	223.6
	vCASSCF+1+2	1.101	2348	224.9
	$\Delta$	0.001	-7	1.5
P <sub>2</sub>	MCSCF(SCGVb)+1+2	1.906	774	109.4
	CASSCF(SCGVb)+1+2	1.907	773	109.8
	vCASSCF+1+2	1.906	775	111.8
	$\Delta$	0.000	1	2.4
PN	MCSCF(SCGVb)+1+2	1.497	1330	140.7
	CASSCF(SCGVb)+1+2	1.497	1329	141.0
	vCASSCF+1+2	1.498	1329	142.7
	$\Delta$	0.001	-1	2.0

**Spin-Coupled Generalized Valence Bond Theory:  
New Perspectives on the Electronic Structure of Molecules and Chemical Bonds**

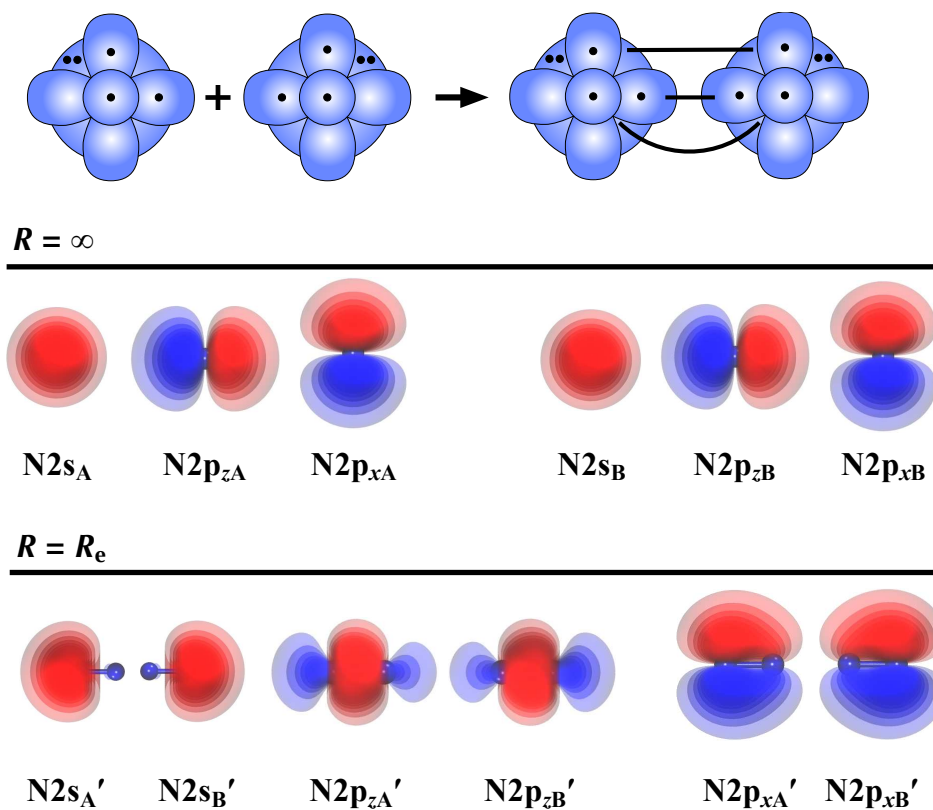


**Figure 1.** Orbital diagram representing the formation of  $N_2$  along with contour plots of the valence SCGVB orbitals for the ground ( $X^1\Sigma_g^+$ ) state of the  $N_2$  molecule at  $R = \infty$  (separated atoms) and  $R = R_e$ . Contours are shown from 0.025 to 0.25 in increments of 0.025.

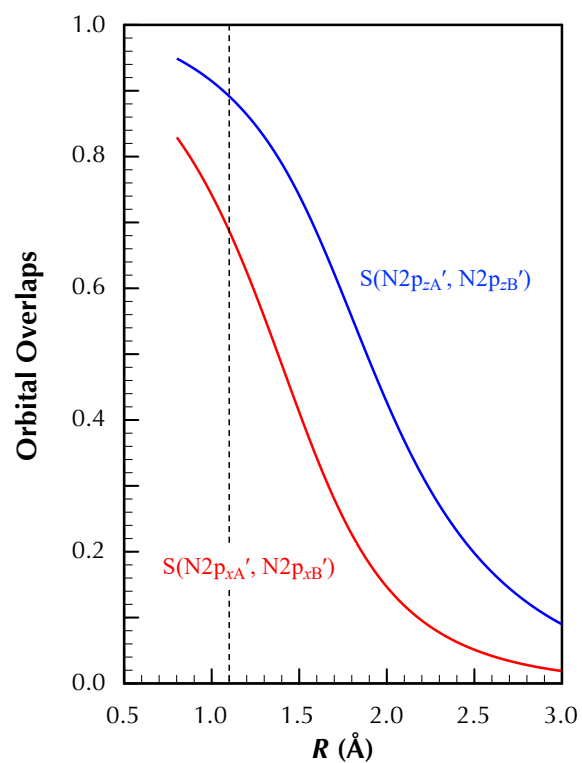


**Figure 2.** Overlaps of the  $(N2p_{zA'}, N2p_{zB'})$  and  $(N2p_{xA'}, N2p_{xB'})$  bond orbitals as a function of the internuclear distance  $R$ . A vertical line is drawn at  $R_e = 1.101$  Å.

**Spin-Coupled Generalized Valence Bond Theory:  
New Perspectives on the Electronic Structure of Molecules and Chemical Bonds**

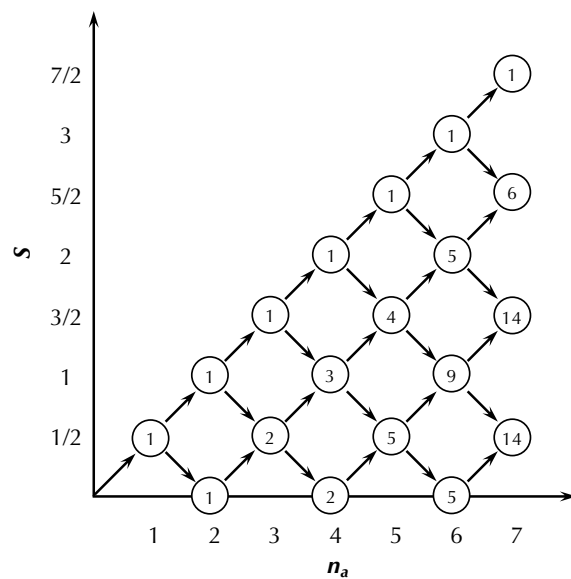


**Figure 3.** Branching diagram for the Kotani spin functions. The path to any  $(n_a, S)$  combination is defined by the arrows. The number in the circle is the number of linearly independent spin function for the given  $(n_a, S)$  combination.

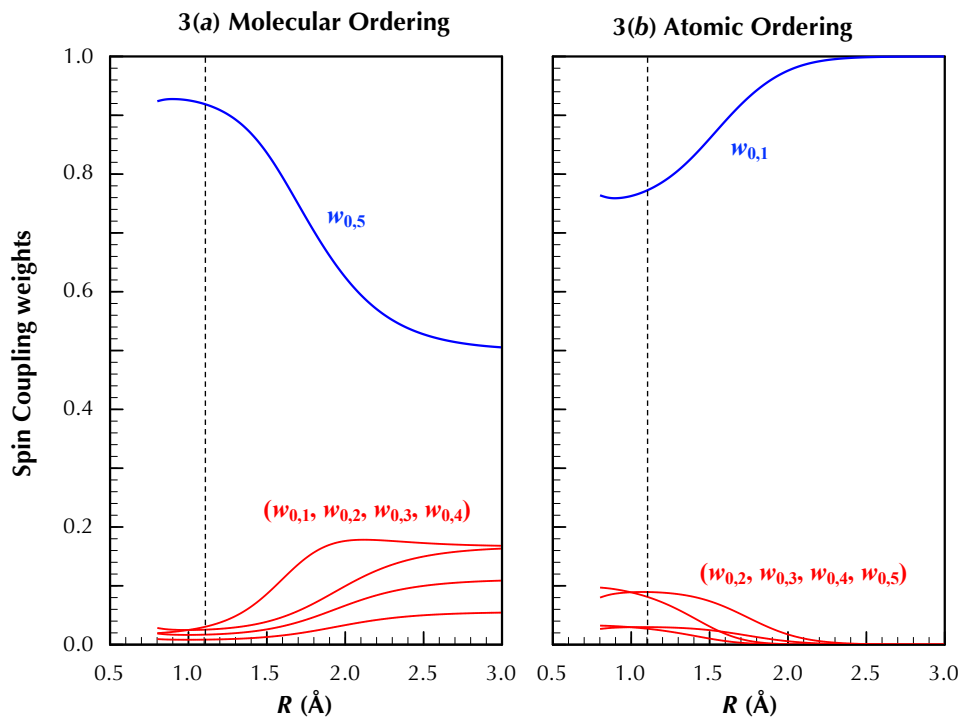


**Figure 4.** The spin coupling weights,  $w_{0,k} = c_{0,k}^2$ , for the Kotani spin functions of the SCGVb wave function for  $N_2$  as a function of  $R$ . The weight of the dominant spin coupling is plotted in blue; those of the minor spin couplings are plotted in red. The spin coupling coefficients are plotted for two different orderings: molecular and atomic; see the text. A vertical line is drawn at  $R_e = 1.101$  Å.

**Spin-Coupled Generalized Valence Bond Theory:  
New Perspectives on the Electronic Structure of Molecules and Chemical Bonds**

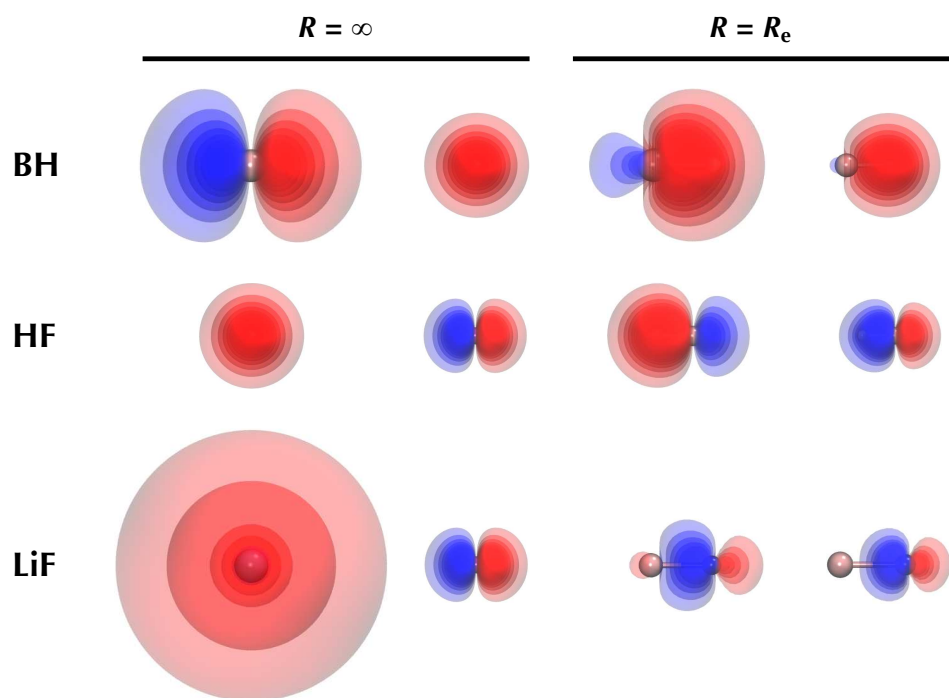


**Figure 5.** Contour plots of the bond orbitals for the ground ( $X^1\Sigma^+$ ) states of the BH, FH and LiF molecules. Contours are shown from 0.025 to 0.25 in increments of 0.025.



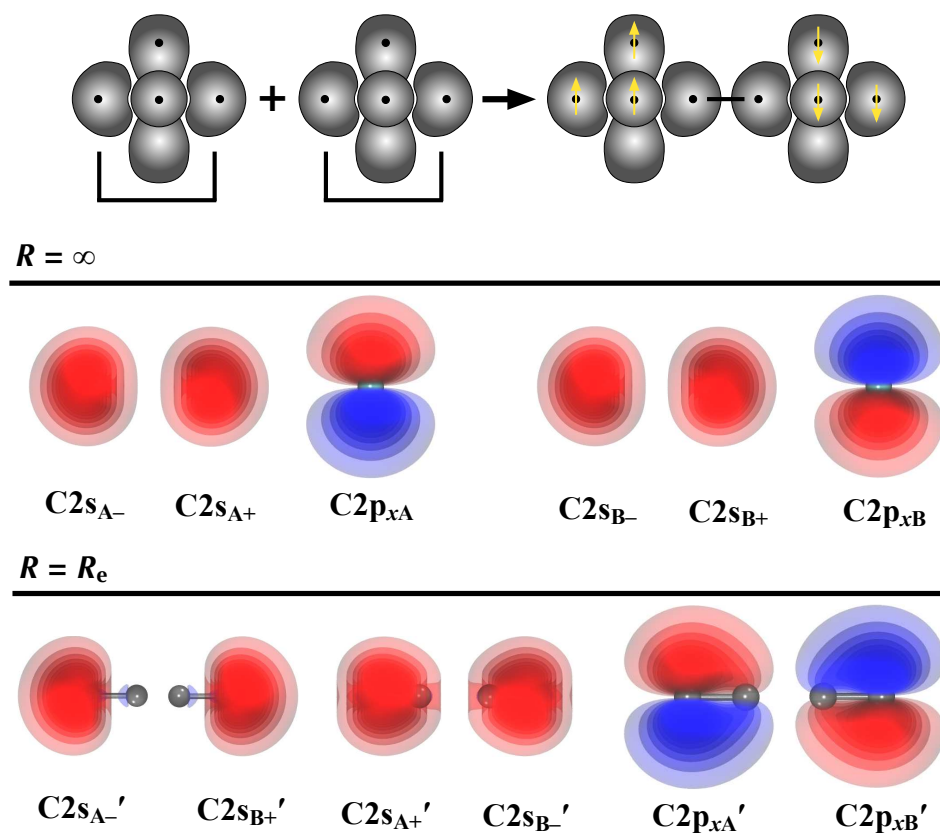


**Figure 6.** Orbital diagram representing the formation of  $C_2$  along with contour plots of the valence SCGV orbitals for the ground ( $X^1\Sigma_g^+$ ) state of the  $C_2$  molecule at  $R = \infty$  and  $R = R_e$ . Contours are shown from 0.025 to 0.25 in increments of 0.025.

**Spin-Coupled Generalized Valence Bond Theory:  
New Perspectives on the Electronic Structure of Molecules and Chemical Bonds**

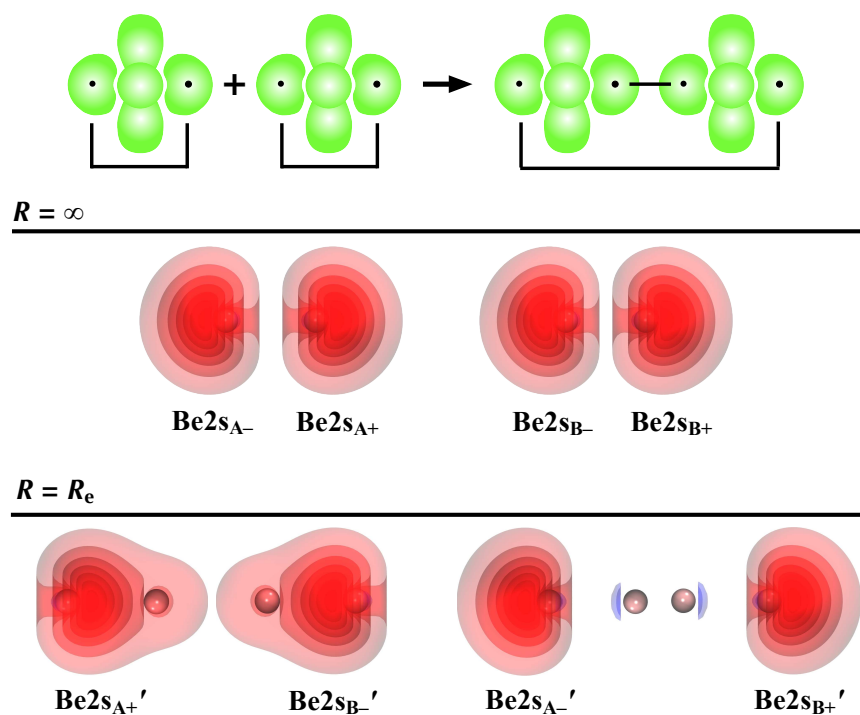


**Figure 7.** Orbital diagram representing the formation of  $\text{Be}_2$  along with contour plots of the valence SCGVB orbitals for the ground ( $X^1\Sigma_g^+$ ) state of the  $\text{Be}_2$  molecule at  $R = \infty$  and  $R = R_e$ . Contours are shown from 0.025 to 0.25 in increments of 0.025.

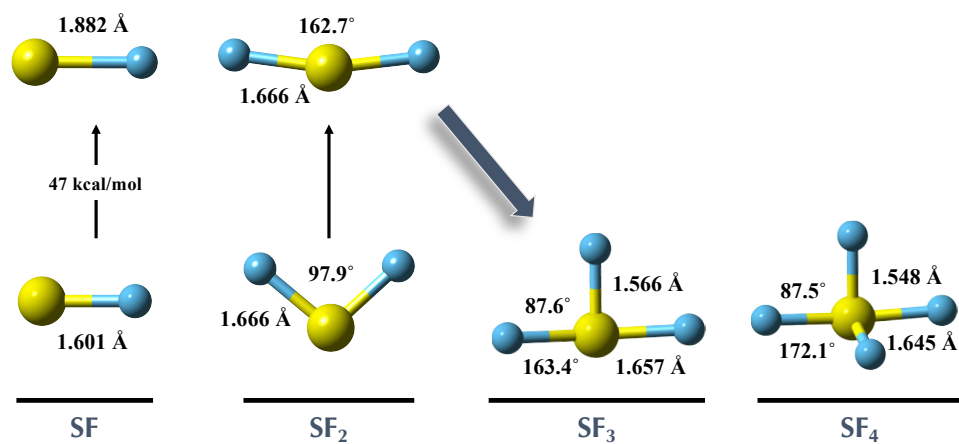


**Figure 8.** The SF<sub>n</sub> sequence from SF to SF<sub>4</sub>. Geometrical parameters from CCSD(T)/RCCSD(T) calculations with the aug-cc-pVQZ basis set.

1  
2  
3

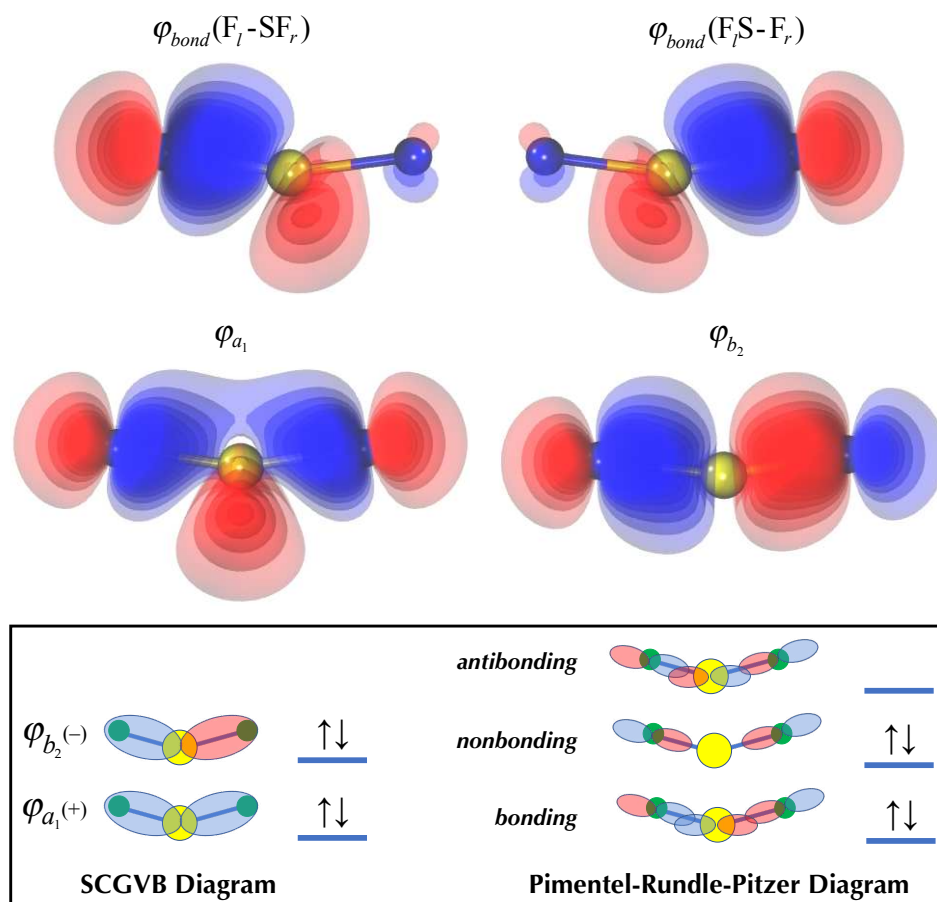


**Figure 9.** The SCGVb natural orbitals ( $n_{\text{occ}} = 1.98$ ) describing the left ( $l$ ) and right ( $r$ ) bonds in the  $\text{SF}_2(\tilde{a}^3B_1)$  state (top row) The corresponding delocalized orbitals are plotted in the middle row. The SCGVb MO diagram describing these two bonds is pictured in the bottom row where it is contrasted with the Rundle-Pimentel-Pitzer diagram.

4  
5  
6

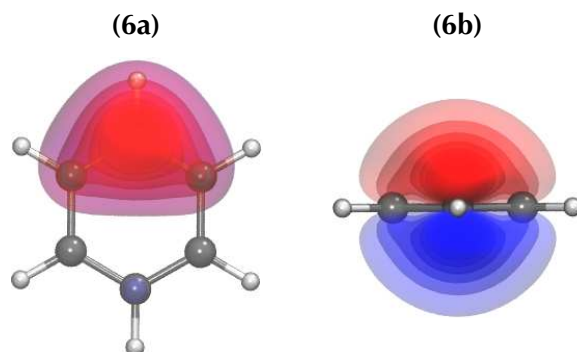


**Figure 10.** Contour plots of one of the six SCGVb  $\pi$  orbitals for benzene: (6a) top view of the orbital and (6b) side view of the orbital. Contours are shown from 0.025 to 0.25 in increments of 0.025.

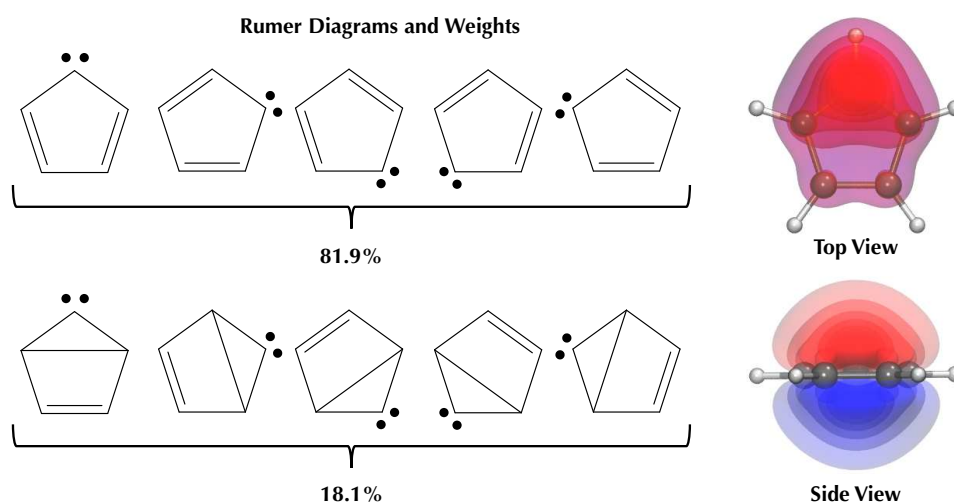


**Figure 11.** Rumer diagrams and percentage weights for the cyclopentadienyl anion ( $C_5H_5^-$ ) molecule along with contour plots of one of the five SCGVb  $\pi$  orbitals. Contours are shown from 0.025 to 0.25 in increments of 0.025.

# Spin-Coupled Generalized Valence Bond Theory: New Perspectives on the Electronic Structure of Molecules and Chemical Bonds

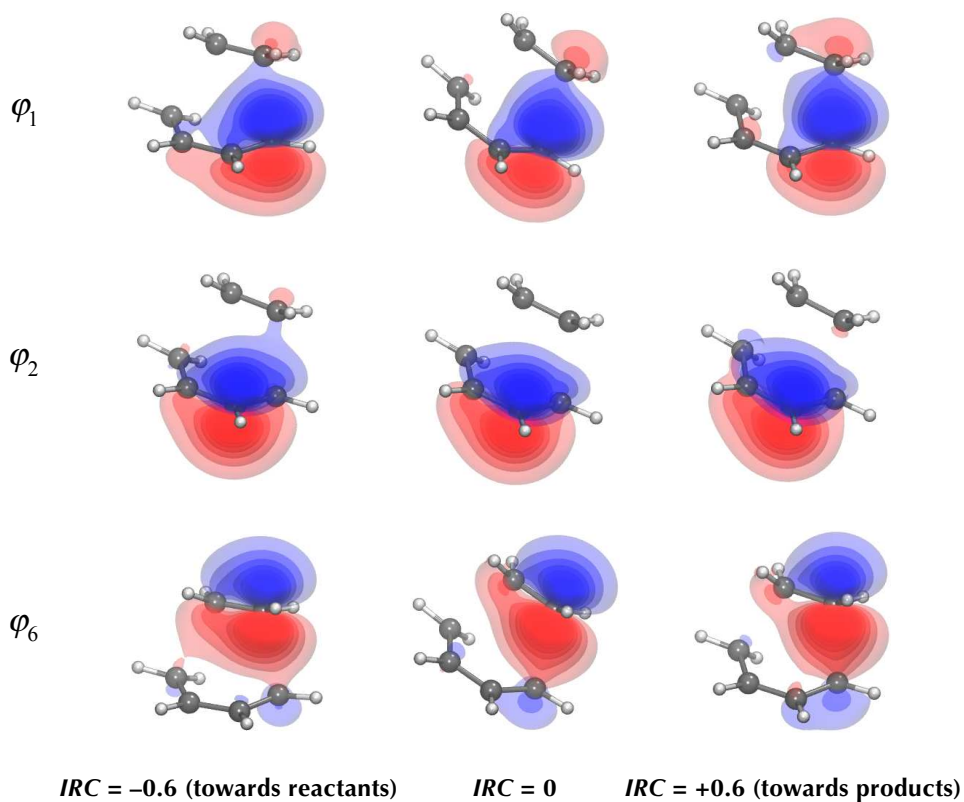


**Figure 12.** Contour plots of the symmetry-unique valence orbitals along the reaction path (intrinsic reaction coordinate, *IRC*) for the Diels–Alder reaction between *cis*-butadiene and ethene. Orbitals  $\varphi_3$ ,  $\varphi_4$  and  $\varphi_5$  can be obtained from  $\varphi_2$ ,  $\varphi_1$  and  $\varphi_6$  through reflections in the  $\sigma_h$  plane passing through the midpoints of the ethylene and central butadiene C–C bonds. Distances along the *IRC* in  $\text{amu}^{1/2} \text{ bohr}$ . Contours are shown from 0.025 to 0.25 in increments of 0.025.

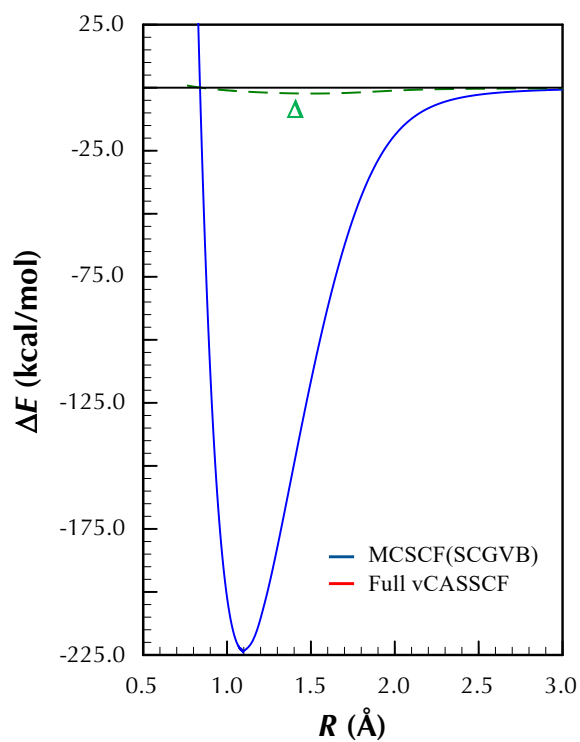


**Figure 13.** Potential energy curves for the ground state of the  $N_2$  molecules from MCSCF(SCGVb)+1+2 (blue) and full vCASSCF+1+2 (red) calculations with the aug-cc-pVQZ basis set. The green curve ( $\Delta$ ) at the top of the plot is the difference between the two curves.

**Spin-Coupled Generalized Valence Bond Theory:  
New Perspectives on the Electronic Structure of Molecules and Chemical Bonds**

23 ■ REFERENCES

24

- (1) Fleming, I. *Molecular Orbitals and Organic Chemical Reactions*; John Wiley & Sons, Ltd.: Chichester, West Sussex, United Kingdom, 2010.
- (2) Bent, H. A. Should Orbitals Be X-Rated in Beginning Chemistry Courses? *J. Chem. Educ.* **1984**, *61*, 421-423.
- (3) Autschbach, J. Orbitals: Some Fiction and Some Facts. *J. Chem. Educ.* **2012**, *89*, 1032-1040.
- (4) Clauss, A. D.; Nelsen, S. F.; Ayoub, M.; Moore, J. W.; Landis, C. R.; Weinhold, F. Rabitt-Ears Hybrids, VSEPR Sterics, and Other Orbital Anachronisms. *Chem. Educ. Res. Pract.* **2014**, *15*, 417.
- (5) Scerri, E. R. Philosophy of Chemistry—A New Interdisciplinary Field? *J. Chem. Educ.* **2000**, *77*, 522-525.
- (6) Woody, A. I. Putting Quantum Mechanics to Work in Chemistry: The Power of Diagrammatic Representation. *Phil. Sci.* **2000**, *67*, S612-SS627.
- (7) Jenkins, Z. Do You Need to Believe in Orbitals to Use Them?: Realism and the Autonomy of Chemistry. *Phil. Sci.* **2003**, *70*, 1052-1062.
- (8) Labarca, M.; Lombardi, O. Why Orbitals Do Not Exist? *Found. Chem.* **2010**, *12*, 149-157.
- (9) Ruedenberg, K.; Schmidt, M. W.; Gilbert, M. M.; Elbert, S. T. Are Atoms Intrinsic to Molecular Wave Functions? I. The FORS Model. *Chem. Phys.* **1982**, *71*, 41-49.
- (10) Ruedenberg, K.; Schmidt, M. W.; Gilbert, M. M. Are Atoms Intrinsic to Molecular Wave Functions? II. Analysis of FORS Orbitals. *Chem. Phys.* **1982**, *71*, 51-64.
- (11) Ruedenberg, K.; Schmidt, M. W.; Gilbert, M.; Elbert, S. T. Are Atoms Intrinsic to Molecular Wave Functions? III. Analysis of FORS Configurations. *Chem. Phys.* **1982**, *71*, 65-78.
- (12) Roos, B. O. The Complete Active Space SCF Method in a Fock Matrix-Based Super-CI Formulation. *Int. J. Quantum Chem.* **1980**, *18 (S14)*, 175-189.
- (13) Roos, B. O.; Taylor, P. R.; Siegbahn, P. E. M. A Complete Active Space SCF Method (CASSCF) Using a Density Matrix Formulated Super-CI Approach. *Chem. Phys.* **1980**, *48*, 157-173.
- (14) Roos, B. O. The Complete Active Space Self-Consistent Field Method and Its Applications in Electronic Structure Calculations. *Adv. Chem. Phys.* **1987**, *69*, 399-444.
- (15) Olsen, J.; Roos, B. O.; Jørgensen, P.; Jensen, H. J. Aa. Determinant Based Configuration Interaction Algorithms for Complete and Restricted Configuration Interaction Spaces. *J. Chem. Phys.* **1988**, *89*, 2185-2192.
- (16) Malmqvist, P.-Å.; Rendell, A.; Roos, B. O. The Restricted Active Space Self-Consistent Field Method, Implemented with a Split Graph Unitary Group Approach. *J. Phys. Chem.* **1990**, *94*, 5477-5482.
- (17) Ivanic, J. Direct Configuration Interaction and Multiconfigurational Self-Consistent-Field Methods for Multiple Active Spaces with Variable Occupations. I. Method. *J. Chem. Phys.* **2003**, *119*, 9364-9375.
- (18) Ma, D.; Li Manni, G.; Gagliardi, L. The Generalized Active Space Concept in Multiconfigurational Self-Consistent Field Methods. *J. Chem. Phys.* **2011**, *135*, 044128.
- (19) Vogiatzis, K. D.; Manni, G. L.; Stoneburner, S. J.; Ma, D.; Gagliardi, L. Systematic Expansion of Active Spaces beyond the CASSCF Limit: A GASSCF/SplitGAS Benchmark Study. *J. Chem. Theory Comput.* **2015**, *11*, 3010-3021.
- (20) Levine, D. S.; Hait, D.; Tubman, N. M.; Lehtola, S.; Whaley, K. B.; Head-Gordon, M. CASSCF with Extremely Large Active Spaces Using the Adaptive Sampling Configuration Interaction Method. *J. Chem. Theory Comput.* **2020**, *16*, 2340-2354.



- (21) Xu, L. T.; Dunning, T. H., Jr. A Cautionary Tale: Problems in the Valence-CASSCF Description of the Ground State ( $X^1\Sigma^+$ ) of BF. *J. Chem. Phys.* **2020**, *153*, 114113.
- (22) West, A. C.; Schmidt, M. W.; Gordon, M. S.; Ruedenberg, K. A Comprehensive Analysis in Terms of Molecule-Intrinsic, Quasi-Atomic Orbitals. II. Strongly Correlated MCSCF Wave Functions. *J. Phys. Chem. A* **2015**, *119*, 10360-10367.
- (23) West, A. C.; Schmidt, M. W.; Gordon, M. S.; Ruedenberg, K. A Comprehensive Analysis in Terms of Molecule-Intrinsic, Quasi-Atomic Orbitals. III. The Covalent Bond Structure of Urea. *J. Phys. Chem. A* **2015**, *119*, 10368-10375.
- (24) West, A. C.; Schmidt, M. W.; Gordon, M. S.; Ruedenberg, K. A Comprehensive Analysis in Terms of Molecule-Intrinsic, Quasi-Atomic Orbitals. IV. Bond Breaking and Bond Forming along the Dissociative Reaction Path of Dioxetane. *J. Phys. Chem. A* **2015**, *119*, 10376-10389.
- (25) McDouall, J. J. W.; Robb, M. A. An Intrinsic Localization Procedure for Active CAS SCF Orbitals. *Chem. Phys. Lett.* **1986**, *132*, 319-324.
- (26) McDouall, J. J. W.; Robb, M. A. The Transformation of CAS SCF Wavefunctions to Valence Bond Space. *Chem. Phys. Lett.* **1987**, *142*, 131-135.
- (27) Blancafort, L.; Celani, P.; Bearpark, M. J.; Robb, M. A. A Valence-Bond-Based Complete-Active-Space-Self-Consistent-Field Method for the Evaluation of Bonding in Organic Molecules. *Theor. Chem. Acc.* **2003**, *110*, 92-99.
- (28) Thorsteinsson, T.; Cooper, D. L. Exact Transformations of CI spaces, VB Representations of CASSCF Wavefunctions and the Optimization of VB Wavefunctions. *Theor. Chim. Acta* **1996**, *94*, 233-245.
- (29) Thorsteinsson, T.; Cooper, D. L.; Gerratt, J.; Karadakov, P. B.; Raimondi, M. Modern Valence Bbond Representations of CASSCF Wwavefunctions. *Theor. Chim. Acta* **1996**, *93*, 343-366.
- (30) Hirao, K.; Nakano, H.; Nakayama, K.; Dupuis, M. A Complete Active Space Valence Bond (CASVB) Method. *J. Chem. Phys.* **1996**, *105*, 9227-9239.
- (31) Gerratt, J.; Lipscomb, W. N. Spin-Coupled Wave Functions for Atoms and Molecules. *Proc. Natl. Acad. Sci. USA* **1968**, *59*, 332-335.
- (32) Ladner, R. C.; Goddard, W. A., III. Improved Quantum Theory of Many-Electron Systems. V. Spin-Coupling Optimized GI Method. *J. Chem. Phys.* **1969**, *51*, 1073-1087.
- (33) Gerratt, J.; Cooper, D. L.; Karadakov, P. B.; Raimondi, M. Modern Valence Bond Theory. *Chem. Soc. Rev.* **1997**, 87-100.
- (34) Dunning, T. H., Jr.; Xu, L. T.; Takeshita, T. Y.; Lindquist, B. A. Insights into the Electronic Structure of Molecules from Generalized Valence Bond Theory. *J. Phys. Chem. A* **2016**, *120*, 1763-1778.
- (35) Dunning, T. H., Jr; Xu, L. T.; Takeshita, T. Y. Fundamental Aspects of Recoupled Pair Bonds. I. Recoupled Pair Bonds in Carbon and Sulfur Monofluoride. *J. Chem. Phys.* **2015**, *142*, 034113.
- (36) Dunning, T. H., Jr; Takeshita, T. Y.; Xu, L. T. Fundamental Aspects of Recoupled Pair Bonds. II. Recoupled Pair Bond Dyads in Carbon and Sulfur Difluoride. *J. Chem. Phys.* **2015**, *142*, 034114.
- (37) Sinanoğlu, O. Many-Electron Theory of Atoms, Molecules and Their Interactions. *Adv. Chem. Phys.* **1964**, *6*, 315-412.
- (38) Coulson, C. A. Present State of Molecular Structure Calculations. *Rev. Mod. Phys.* **1960**, *32*, 170-177.
- (39) Xu, L. T.; Dunning, T. H., Jr. Generalized Valence Bond Description of the Ground States ( $X^1\Sigma_g^+$ ) of Homonuclear Pnictogen Diatomic Molecules: N<sub>2</sub>, P<sub>2</sub>, and As<sub>2</sub>. *J. Chem. Theory Comput.* **2015**, *11*, 2496-2507.
- (40) Boys, S. F. Construction of Some Molecular Orbitals to Be Approximately Invariant for Changes from One Molecule to Another. *Rev. Mod. Phys.* **1960**, *32*, 296-299.
- (41) Foster, J. M.; Boys, S. F. Canonical Configuration Interaction Procedure. *Rev. Mod. Phys.* **1960**, *32*, 300-302.

**Spin-Coupled Generalized Valence Bond Theory:  
New Perspectives on the Electronic Structure of Molecules and Chemical Bonds**

- (42) Edmiston, C.; Ruedenberg, K. Localized Atomic and Molecular Orbitals. *Rev. Mod. Phys.* **1963**, *35*, 457-465.
- (43) Pipek, J.; Mezey, P. G. A Fast Localization Procedure Applicable for *Ab Initio* and Semiempirical Linear Combination of Atomic Orbital Wave Functions. *J. Chem. Phys.* **1989**, *90*, 4916-4926.
- (44) Høyvik, I.-M.; Kristensen, K.; Kjærgaard, T.; Jørgensen, P. A Perspective on the Localizability of Hartree-Fock Orbitals. *Theor. Chem. Acc.* **2014**, *133*, 1417.
- (45) Exceptions do occur, for example, in SCGVB descriptions of chemical reactions as the orbitals in the reactants evolve into the orbitals of the products along the reaction path.
- (46) Gillespie, R. J.; Popelier, P. L. *A. Chemical Bonding and Molecular Geometry. From Lewis to Electron Densities*; Oxford University Press, Oxford, England, **2001**; pp. 68-69.
- (47) Pauncz, R. *Spin Eigenfunctions, Construction and Use*; Springer US: Boston, 1979.
- (48) Rumer, G. Spin Valence Theory. *Göttinger Nachr.*, 1932, **3**, 337-341.
- (49) Kotani, M.; Amemiya, A.; Ishiguro, E.; Kimura, T. *Tables of Molecular Integrals*, Maruzen, Tokyo, 1963.
- (50) Serber, R. Extension of the Dirac Vector Model to Include Several Configurations. *Phys. Rev.* **1934**, *45*, 461-467.
- (51) Serber, R. The Solutions of Problems Involving Permutation Degeneracy. *J. Chem. Phys.* **1934**, *2*, 697-710.
- (52) Simonetta, M.; Gianinetti, E.; Vandoni, I. Valence Bond Theory for Simple Hydrocarbon Molecules, Radicals and Ions. *J. Chem. Phys.*, **1968**, *48*, 1579-1594.
- (53) Raos, G.; Gerratt, J.; Cooper, D. L.; Raimondi, M. On the Role of Different Spin Bases within Spin-Coupled Theory. *Mol. Phys.* **1993**, *79*, 197-216.
- (54) Chirgwin, B. H.; Coulson, C. A. The Electronic Structure of Conjugated Systems. VI. *Proc. R. Soc. Lond. A* **1950**, *201*, 196-209.
- (55) Gallup, G. A.; Norbeck, J. M. Population Analyses of Valence-Bond Wavefunctions and BeH<sub>2</sub>. *Chem. Phys. Lett.* **1973**, *21*, 495-500.
- (56) Karadakov, P. B.; Gerratt, J.; Cooper, D. L.; Raimondi, M. SPINS: A Collection of Algorithms for Symbolic Generation and Transformation of Many-Electron Spin Eigenfunctions. *Theor. Chim. Acta* **1995**, *90*, 51-73.
- (57) Karadakov, P. B.; Cooper, D. L.; Duke, B. J.; Li, J. Spin-Coupled Theory for 'N Electrons in M Orbitals' Active Spaces. *J. Phys. Chem. A* **2012**, *116*, 7238-7244.
- (58) Wu, W.; Su, P.; Shaik, S.; Hiberty, P. C. Classical Valence Bond Approach by Modern Methods. *Chem. Rev.* **2011**, *111*, 7557-7593.
- (59) Chen, Z.; Wu, W. Ab Initio Valence Bond Theory: A Brief History, Recent Developments, and Near Future. *J. Chem. Phys.* **2020**, *153*, 090902.
- (60) Coulson, C. A.; Fischer, I. XXXIV. Notes on the Molecular Orbital Treatment of the Hydrogen Molecule. *Philos. Mag.* **1949**, *40*, 386-393.
- (61) van Lenthe, J. H.; Balint-Kurti, G. G. The Valence-Bond SCF (VB SCF) Method. Synopsis of Theory and Test Calculations of OH Potential Energy Curve. *Chem. Phys. Lett.* **1980**, *76*, 138-142.
- (62) van Lenthe, J. H.; Balint-Kurti, G. G. The Valence-Bond Self-Consistent Field Method (VB-SCF) Theory and Test Calculations. *J. Chem. Phys.* **1983**, *78*, 5699-5713.
- (63) Shaik, S.; Danovich, D.; Hiberty, P. C. To Hybridize or Not to hybridize? This is the Dilemma. *Comput. Theoret. Chem.* **2017**, *1116*, 242-249.
- (64) Hiberty, P. C.; Flament, J. P.; Noizet, E. Compact and Accurate Valence Bond Functions with Different Orbitals for Different Configurations: Application to the Two Configuration Description of F<sub>2</sub>. *Chem. Phys. Lett.* **1992**, *189*, 259.

- (65) Hiberty, P. C.; Humbel, S.; Byrman, C. P.; van Lenthe, J. H. Compact Valence Bond Functions with Breathing Orbitals: Application to the Bond Dissociation Energies of F<sub>2</sub> and HF. *J. Chem. Phys.* **1994**, *101*, 5969.
- (66) Hiberty, P. C.; Shaik, S. Breathing-Orbital-Valence Bond Method – A Modern Valence Bond Method That Includes Dynamic Correlation. *Theor. Chem. Acc.* **2002**, *108*, 255-272.
- (67) Hiberty, P. C.; Shaik, S. BOVB – A Valence Bond Method Incorporating Static and Dynamic Correlation Effects. In *Valence Bond Theory*; Cooper, D. L., Ed.; Elsevier Science B.V.: 2002.
- (68) Fletcher, G. D. The Variational Subspace Valence Bond Method. *J. Chem. Phys.* **2015**, *142*, 134112.
- (69) Cooper, D. L.; Thorsteinsson, T.; Gerratt. Fully Variational Optimization of Modern VB Wave Functions Using the CASVB Strategy. *J. Int. J. Quant. Chem.* **1997**, *65*, 439-451.
- (70) Li, J.; Duke, B.; McWeeny, R. VB2000: An Ab Initio Valence Bond Program Bases in Product Function Method and the Algebrant Algorithm (SciNet Technologies, San Diego, CA, 2000).
- (71) Chen, Z.; Ying, F.; Chen, X.; Song, J.; Su, P.; Song, L.; Mo, Y.; Zhang, Q.; Wu, W. XMVB 2.0: A New Version of Xiamen Valence Bond Program. *Int. J. Quantum. Chem.* **2015**, *115*, 731-737.
- (72) Fletcher, G. D.; Bertoni, C.; Keçeli, M.; D'Mello, M. VALENCE: A Massively Parallel Implementation of the Variational Subspace Valence Bond Method. *J. Comput. Chem.* **2019**, *40*, 1664-1673.
- (73) Pyper, N. C.; Gerratt, J. Spin-Coupled Theory of Molecular Wavefunctions: Application to the Structure and Properties of LiH(X<sup>2</sup>Σ<sup>+</sup>), BH(X<sup>2</sup>Σ<sup>+</sup>), Li<sub>2</sub>(X<sup>1</sup>Σ<sub>g</sub><sup>+</sup>) and HF(X<sup>1</sup>Σ<sup>+</sup>). *Proc. R. Soc. Lond. A* **1977**, *355*, 407-439.
- (74) Gerratt, J.; Raimondi, M. The Spin-Coupled Valence Bond Theory of Molecular Electronic Structure. I. Basic theory and Application to the <sup>2</sup>Σ<sup>+</sup> state of BeH. *Proc. R. Soc. Lond. A* **1980**, *371*, 525-552.
- (75) Cooper, D. L.; Gerratt, J.; Raimondi, M. Modern Valence Bond Theory. *Adv. Chem. Phys.* **1987**, *69*, 319-397.
- (76) Clarke, N. J.; Raimondi, M.; Sironi, M.; Gerratt, J.; Cooper, D. L. Optimization of Virtual Orbitals in the Framework of a Multiconfiguration Spin-Coupled Wave function. *Theor. Chem. Acc.* **1998**, *99*, 8-17.
- (77) da Silva, E. C.; Gerratt, J.; Cooper, D. L.; Raimondi, M. Study of the Electronic States of the Benzene Molecule Using Spin-Coupled Valence Bond theory. *J. Chem. Phys.* **1994**, *101*, 3866-3887.
- (78) Wang, J. G.; Stancil, P. C.; Turner, A. R.; Cooper, D. L. Charge Transfer of O<sup>3+</sup> Ions with Atomic Hydrogen. *Phys. Rev. A* **2003**, *67*, 012710.
- (79) Olsen, J. Novel Methods for Configuration Interaction and Orbital optimization for Wave Functions Containing Non-orthogonal Orbitals with Applications to the Chromium Dimer and Trimer. *J. Chem. Phys.* **2015**, *143*, 114102.
- (80) Werner, H.-J.; Knowles, P. J.; Amos, R. D.; Bernhardsson, A.; Berning, A.; Celani, P.; Cooper, D. L.; Deegan, M. J. O.; Dobbyn, A. J.; Eckert, F.; et al., *Molpro, version 2010.1*, a package of ab initio programs, see <http://www.molpro.net>.
- (81) Werner, H.-J.; Knowles, P. J.; Knizia, G.; Manby, F. R.; Schütz, M. Molpro: A General-Purpose Quantum Chemistry Program Package. *WIREs Comput Mol Sci* **2011**, *2*, 242-253.
- (82) Werner, H.-J.; Knowles, P. J. An Efficient Internally Contracted Multiconfiguration-Reference Configuration Interaction Method. *J. Chem. Phys.* **1988**, *89*, 5803-5814.
- (83) Knowles, P. J.; Werner, H.-J. An Efficient Method for the Evaluation of Coupling Coefficients in Configuration Interaction Calculations. *Chem. Phys. Lett.* **1988**, *145*, 514-522.
- (84) Shamasundar, K. R.; Knizia, G.; Werner, H.-J. A New Internally Contracted Multi-Reference Configuration Interaction Method. *J. Chem. Phys.* **2011**, *135*, 054101.
- (85) Dunning, T. H., Jr. Gaussian Basis Sets for Use in Correlated Molecular Calculations. I. The Atoms Boron through Neon and Hydrogen. *J. Chem. Phys.* **1989**, *90*, 1007-1023.
- (86) Kendall, R. A.; Dunning, Jr., T. H.; Harrison, R. J. Electron Affinities of the First-Row Atoms Revisited. Systematic Basis Sets and Wave Functions. *J. Chem. Phys.* **1992**, *96*, 6796-6806.

**Spin-Coupled Generalized Valence Bond Theory:  
New Perspectives on the Electronic Structure of Molecules and Chemical Bonds**

- (87) Botch, B. H.; Dunning, Jr. T. H. Theoretical Characterization of Negative Ions. Calculation of the Electron Affinities of Carbon, Oxygen, and Fluorine. *J. Chem. Phys.* **1982**, *76*, 6046-6056.
- (88) Xu, L. T.; Dunning, T. H., Jr. Orbital Hybridization in Modern Valence Bond Wave Functions: Methane, Ethylene, and Acetylene. *J. Phys. Chem. A* **2020**, *124*, 204-214.
- (89) NIST Chemistry WebBook (Standard Reference Database Number 69), Constants of Diatomic Molecules, accessed on October 1, 2020.
- (90) Feller, D.; Dixon, D. A.; Peterson, K. A. Heats of Formation of Simple Boron Compounds. *J. Phys. Chem. A* **1998**, *102*, 7053-7059.
- (91) Di Lonardo, G.; Douglas, A. E. The Electronic Spectrum of HF. I. The  $B^1\Sigma^+-X^1\Sigma^+$  Band System. *Can. J. Phys.* **1973**, *51*, 434-445.
- (92) Bulewicz, E. M.; Phillips, L. F.; Sugden, T. M. Determination of Dissociation Constants and Heats of Formation of Simple Molecules by Flame Photometry. *Trans. Faraday Soc.* **1961**, *57*, 921-931.
- (93) Bader, R. F. W.; Henneker, W. H.; Cade, P. E. Molecular Charge Distributions and Chemical Binding. *J. Chem. Phys.* **1967**, *46*, 3341-3363.
- (94) Bodner, G.; Klobuchar, M.; Geelan, D. The Many Forms of Constructionism. *J. Chem. Educ.* **2001**, *78*, 1107-1121.
- (95) Xu, L. T.; Dunning, T. H., Jr. Variations in the Nature of Triple Bonds: The  $N_2$ , HCN, and  $HC_2H$  Series. *J. Phys. Chem. A* **2016**, *120*, 4526-4533.
- (96) Mulliken, R. S. Note on Electronic States of Diatomic Carbon, and the Carbon-Carbon Bond. *Phys. Rev.* **1939**, *56*, 778-781.
- (97) LePetit, M. B.; Malrieu, J. P. Interaction of  $s^2$  Pairs in  $Be_2$  and  $C_2$ : The UHF Instability, Symptom of an Atomic Promotion. *Chem. Phys. Lett.* **1990**, *169*, 285-291.
- (98) Xu, L. T.; Dunning, Jr., T. H. Insights into the Perplexing Nature of the Bonding in  $C_2$  from Generalized Valence Bond Calculations. *J. Chem. Theory Comput.* **2014**, *10*, 195-201.
- (99) Su, P.; Wu, J.; Gu, J.; Wu, W.; Shaik, S.; Hiberty, P. C. Bonding Conundrums in the  $C_2$  Molecule: A Valence Bond Study. *J. Chem. Theory Comput.* **2011**, *7*, 121-130.
- (100) Shaik, S. S.; Danovich, D.; Wu, W.; Su, P.; Rzepa, H. S.; Hiberty, P. C. Quadruple Bonding in  $C_2$  and Analogous Eight-Valence Electron Species. *Nat. Chem.* **2012**, *4*, 195-200.
- (101) Shaik, S.; Rzepa, H. S.; Hoffmann, R. One Molecule, Two Atoms, Three Views, Four Bonds. *Angew. Chem. Int. Ed.* **2013**, *52*, 3020-3033.
- (102) Cooper, D. L.; Penotti, F. E.; Ponec, R. Why Is the Bond Multiplicity in  $C_2$  So Elusive. *Comput. Theor. Chem.* **2015**, *1053*, 189-194.
- (103) Goddard, W. A., III; Dunning, T. H., Jr.; Hunt, W. J.; Hay, P. J. Generalized Valence Bond Description of Bonding in Low-Lying States of Molecules. *Acc. Chem. Res.* **1973**, *6*, 368-376.
- (104) Dupuis, M.; Liu, B. Theoretical Study of  $C_2$  and  $C_2^-$ . *J. Chem. Phys.* **1980**, *73*, 337-342.
- (105) Karadakov, P. B.; Kirsopp, J. Magnetic Shielding Studies of  $C_2$  and  $C_2H_2$  Support Higher than Triple Bond Multiplicity in  $C_2$ . *Chem. Eur. J.* **2017**, *23*, 12949-12954.
- (106) Cooper, D. L.; Ponec, R.; Kohout, M., New Insights from Domain-Averaged Fermi Holes and Bond Order Analysis into the Bonding Conundrum in  $C_2$ . *Mol. Phys.* **2016**, *114*, 1270-1284.
- (107) Zhao, L.; Pan, S.; Holzmann, N.; Schwerdtfeger, P.; Frenking, G. Chemical Bonding and Bonding Models of Main-Group Compounds. *Chem. Rev.* **2019**, *119*, 8781-8845.
- (108) Schmidt, M. W.; Ivanic, J.; Ruedenberg, K. Electronic Structure Analysis of the Ground-State Potential Energy Curve of  $Be_2$ . *J. Phys. Chem. A* **2010**, *114*, 8687-8696.

- (109) El-Khatib, M.; Bendazzoli, G.L.; Evangelisti, S.; Helal W.; Leininger, T.; Tenti, L.; Angeli, C. Beryllium Dimer: A Bond Based on Non-Dynamical Correlation. *J. Phys. Chem. A* **2014**, *118*, 6664-6673.
- (110) Xu, L. T.; Dunning, T. H., Jr. The Nature of the Chemical Bond and the Role of Non-dynamical and Dynamical Correlation in Be<sub>2</sub>. *J. Chem. Phys.* **2020**, *152*, 214111.
- (111) A. Krapp, F. M. Bickelhaupt, and G. Frenking, Orbital Overlap and Chemical Bonding. *Chem. Eur. J.* **2006**, *12*, 9196-9216.
- (112) L. Zhao, S. Pan, N. Holzmann, P. Schwerdtfeger, and G. Frenking, Chemical Bonding and Bonding Models of Main-Group Compounds. *Chem. Rev.* **2019**, *119*, 8781-8845.
- (113) Frenking, G.; Bickelhaupt, F. M. The EDA Perspective of Chemical Bonding. In *The Chemical Bond. Fundamental Aspects of Chemical Bonding*; Frenking, G.; Shaik, S., Eds.; Wiley VCH: 2014.
- (114) Cui, Z.; Yang, W.; Zhao, L.; Ding, Y.; Frenking, G. Unusually Short Be–Be Distances With and Without a Bond in Be<sub>2</sub>F<sub>2</sub> and in the Molecular Discs Be<sub>2</sub>B<sub>8</sub> and Be<sub>2</sub>B<sub>7</sub><sup>−</sup>. *Angew. Chem.* **2016**, *128*, 7972-7977.
- (115) Liu, X.; Zhong, R.; Zhang, M.; Wu, S.; Geng, Y.; Su, Z. Be≡Be triple bond in Be<sub>2</sub>X<sub>4</sub>Y<sub>2</sub> clusters (X = Li, Na and Y = Li, Na, K) and a perfect classical Be≡Be triple bond presented in Be<sub>2</sub>Na<sub>4</sub>K<sub>2</sub>. *Dalton Trans.* **2019**, *48*, 14590-14594.
- (116) Rohman, S. S.; Kashyap, C.; Ullah, S. S.; Guha, A. K.; Mazumder, L. J.; Sharma, P. K. Ultra-Weak Metal–Metal Bonding: Is There a Beryllium-Beryllium Triple Bond? *Chem. Phys. Chem* **2019**, *20*, 516-518.
- (117) Rohman, S. S.; Kashyap, C.; Ullah, S. S.; Mazumder, L. J.; Sahu, P. P.; Kalita, A.; Reza, S.; Hazarika, P. P.; Borah, B.; Guha, A. K. Revisiting Ultra-Weak Metal-Metal Bonding. *Chem. Phys. Lett.* **2019**, *730*, 411-415.
- (118) Liu, X.; Zhang, M.; Yu, S.; Geng, Y.; Zhang, X.; Ding, Y.; Su, Z. Beryllium–Beryllium Double- $\pi$  Bonds in the Octahedral Cluster of Be<sub>2</sub>( $\mu_2$ -X)<sub>4</sub> (X = Li, Cu, BeF). *Phys. Chem. Chem. Phys.* **2018**, *20*, 23898-23902.
- (119) Zhao, X.-F.; Yuan, C.; Li, S.-D.; Wu, Y.-B.; Wang, X. Simulating the Effect of a Triple Bond to Achieve the Shortest Main Group Metal–Metal Distance in Diberyllium Complexes: A Computational Study. *Dalton Trans.* **2018**, *47*, 14462-14467.
- (120) Penotti, F. E.; Cooper, D. L.; Karadakov, P. B.; Ponc, R. Nature of the Chemical Bonding in D<sub>3h</sub> [MH<sub>3</sub>M]<sup>+</sup> Cations (M = Be, Mg). *Int. J. Quantum Chem.* **120**, e26183 (2020).
- (121) Miessler, G. L.; Tarr, D.A. *Inorganic Chemistry, Third Edition*; Pearson Prentice Hall: Upper Saddle River, New Jersey, 2004.
- (122) Pauling, L. The Nature of the Chemical Bond. Application of Results Obtained from the Quantum Mechanics and from a Theory of Paramagnetic Susceptibility to the Structure of Molecules. *J. Am. Chem. Soc.* **1931**, *53*, 1367-1400.
- (123) Pauling, L. *The Nature of the Chemical Bond, 3rd Ed.*; Cornell University Press: Ithaca, NY, 1960.
- (124) Reed, A. E.; von Ragué Schleyer, P. Chemical Bonding in Hypervalent Molecules. The Dominance of Ionic Bonding and Negative Hyperconjugation over d-Orbital Participation. *J. Am. Chem. Soc.* **1990**, *112*, 1434-1445.
- (125) Magnusson, E. Hypercoordinate Molecules of Second Row Elements: d Functions of d Orbitals? *J. Am. Chem. Soc.* **1990**, *112*, 7940-7951.
- (126) Pacchioni, G.; Bagus, P. S. Metal-Phosphine Bonding Revisited. S-Basicity, p-Acidity, and the Role of Phosphorus d Orbitals in Zerovalent Metal-Phosphine Complexes. *Inorg. Chem.* **1992**, *31*, 4391-4398.
- (127) Pimentel, G. C. The Bonding in Trihalide and Bifluoride Ions by the Molecular Orbital Method. *J. Chem. Phys.* **1951**, *19*, 446-448.
- (128) Rundle, R. E. The Implications of Some Recent Structures for Chemical Valence Theory. *Surv. Prog. Chem.* **1963**, *1*, 81-130.
- (129) Pitzer, K. S. Bonding in Xenon Fluorides and Halogen Fluorides. *Science* **1963**, *139*, 414-415
- (130) Coulson, C. A. The Nature of the Bonding in Xenon Fluorides and Related Molecules. *J. Chem. Soc.* **1964**, *1964*, 1442-1454.

## Spin-Coupled Generalized Valence Bond Theory: New Perspectives on the Electronic Structure of Molecules and Chemical Bonds

- (131) Rundle, R. E. On the Probable Structure of XeF<sub>4</sub> and XeF<sub>2</sub>. *J. Am. Chem. Soc.* **1963**, 85, 112-113.
- (132) Cooper, D. L.; Cunningham, T. P.; Gerratt, J.; Karadakov, P. B.; Raimondi, M. Chemical Bonding to Hypercoordinate Second-Row Atoms: d Orbital Participation Versus Democracy. *J. Am. Chem. Soc.* **1994**, 116, 4414-4426.
- (133) Cunningham, T. P.; Cooper, D. L.; Gerratt, J.; Karadakov, P. B.; Raimondi, M. Chemical Bonding in Oxohalides of Hypercoordinate Nitrogen and Phosphorus. *Int. J. Quantum Chem.* **1996**, 60, 393-400.
- (134) Cunningham, T. P.; Cooper, D. L.; Gerratt, J.; Karadakov, P.; Raimondi, M. *J. Chem. Soc., Faraday Trans.* **1997**, 93, 2247-2254.
- (135) Cooper, D. L.; Gerratt, J.; Raimondi, M. Hypercoordinate Bonding to Main Group Elements: The Spin-Coupled Point of View. In *Pauling's Legacy: Modern Modelling of the Chemical Bond*; Maksic, Z. B.; Orville-Thomas, W. J., Eds.; Elsevier Science B. V.: 1999.
- (136) Cooper, D. L. Spin-Coupled Description of the Chemical Bonding in Hypercoordinate Chlorine. *Theor. Chem. Acc.* **2001**, 105, 323-327.
- (137) Woon, D. E.; Dunning, T. H., Jr. Theory of Hypervalency: Recoupled Pair Bonding in SF<sub>n</sub> (*n* = 1-6). *J. Phys. Chem. A* **2009**, 113, 7915-7926.
- (138) Goddard, W. A., III; Blint, R. J. The Generalized Valence Bond View of Molecules: The BH<sub>n</sub> Series. *Chem. Phys. Lett.* **1972**, 14, 616-622.
- (139) Kiang, T.; Zare, R. N. Stepwise Bond Dissociation Energies in Sulfur Hexafluoride. *J. Am. Chem. Soc.* **1980**, 102, 4024-4029.
- (140) Yang, X.; Boggs, J. E. Ground and Valence-Excited States of SF. A Multireference Configuration Interaction with Single and Double Excitations+Q Study. *J. Chem. Phys.* **2005**, 122, 194307.
- (141) Lindquist, B. A.; Woon, D. E.; Dunning, T. H., Jr. Effects of Ligand Electronegativity on Recoupled Pair Bonds with Application to Sulfurane Precursors. *J. Phys. Chem. A* **2014**, 118, 5709-5719.
- (142) Goddard, W. A., III; Harding, L. B. The Description of Chemical Bonding from Ab Initio Calculations. *Ann. Rev. Phys. Chem.* **1978**, 29, 363-396.
- (143) Leiding, J.; Woon, D. E.; Dunning, T. H., Jr. Bonding and Isomerization in SF<sub>n-1</sub>Cl (*n* = 1-6): A Quantum Chemical Study. *J. Phys. Chem. A* **2011**, 115, 329-341.
- (144) Leiding, J.; Woon, D. E.; Dunning, T. H., Jr. Bonding in SCl<sub>n</sub> (*n* = 1-6): A Quantum Chemical Study. *J. Phys. Chem. A* **2011**, 115, 4757-4764.
- (145) Woon, D. E.; Dunning, T. H., Jr. Recoupled Pair Bonding in PF<sub>n</sub> (*n* = 1-5). *J. Phys. Chem. A* **2010**, 114, 8845-8851.
- (146) Leiding, J.; Woon, D. E.; Dunning, T. H., Jr. Bonding in PF<sub>2</sub>Cl, PF<sub>3</sub>Cl, and PF<sub>4</sub>Cl: Insight into Isomerization and Apicophilicity from Ab Initio Calculations and the Recoupled Pair Bonding Model. *Theor. Chem. Acc.* **2014**, 133, 1428.
- (147) Lindquist, B. A.; Takeshita, T. Y.; Woon, D. E.; Dunning, T. H., Jr. Bonding in Sulfur-Oxygen Compounds—HSO/SOH and SOO/OSO: An Example of Recoupled Pair  $\pi$  Bonding. *J. Chem. Theory Comput.* **2013**, 9, 4444-4452.
- (148) Lindquist, B. A.; Dunning, T. H., Jr. Bonding in FSSF<sub>3</sub>: Breakdown in Bond Length-Bond Strength Correlations and Implications for SF<sub>2</sub> Dimerization. *J. Phys. Chem. Lett.* **2013**, 4, 3139-3143.
- (149) Lindquist, B. A.; Engdahl, A. L.; Woon, D. E.; Dunning, T. H., Jr. Insights into the Electronic Structure of Disulfur Tetrafluoride Isomers from Generalized Valence Bond Theory. *J. Phys. Chem. A* **2014**, 118, 10117-10126.
- (150) Takeshita, T. Y.; Lindquist, B. A.; Dunning, T. H., Jr. Insights into the Electronic Structure of Ozone and Sulfur Dioxide from Generalized Valence Bond Theory: Bonding in O<sub>3</sub> and SO<sub>2</sub>. *J. Phys. Chem. A* **2015**, 119, 7683-7694.

- (151) Lindquist, B. A.; Takeshita, T. Y.; Dunning, T. H., Jr. Insights into the Electronic Structure of Ozone and Sulfur Dioxide from Generalized Valence Bond Theory: Addition of Hydrogen Atoms. *J. Phys. Chem. A* **2016**, *120*, 2720-2726.
- (152) Lindquist, B. A.; Dunning, Jr. T. H. The Nature of the SO bond of Chlorinated Sulfur–Oxygen Compounds. *Theor. Chem. Acc.* **2014**, *133*, 1443.
- (153) Chen, L.; Woon, D. E.; Dunning, T. H., Jr. Bonding in  $\text{ClF}_n$  ( $n = 1-7$ ) Molecules: Further Insights into the Electronic Structure of Hypervalent Molecules and Recoupled Pair Bonds. *J. Phys. Chem. A* **2009**, *113*, 12645-12654.
- (154) Chen, L.; Woon, D. E.; Dunning, T. H., Jr. High Level Ab Initio Calculations for  $\text{ClF}_n^+$  ( $n = 1-6$ ) Ions: Refining the Recoupled Pair Bonding Model. *J. Phys. Chem. A* **2013**, *117*, 4251-4266.
- (155) Chen, L.; Woon, D. E.; Dunning, T. H., Jr. High Level Ab Initio Calculations on  $\text{ClF}_n^-$  ( $n = 1-6$ ): Recoupled Pair Bonding Involving a Closed-Shell Central Atom. *Comput. Theoret. Chem.* **2017**, *1116*, 73-85.
- (156) Woon, D. E.; Dunning, Jr. T. H., Jr. A Comparison Between Polar Covalent Bonding and Hypervalent Recoupled Pair Bonding in Diatomic Chalcogen Halide Species  $\{\text{O,S,Se}\} \times \{\text{F,Cl,Br}\}$ . *Mol. Phys.* **2009**, *107*, 991-998.
- (157) Woon, D. E.; Dunning, T. H., Jr. Hypervalency and Recoupled Pair Bonding in the p-Block Elements. *Comput. Theor. Chem.* **2011**, *963*, 7-12.
- (158) Dunning, T. H., Jr.; Woon, D. E.; Leiding, J.; Chen, L. The First Row Anomaly and Recoupled Pair Bonding in the Halides of the Late p-Block Elements. *Acc. Chem. Res.* **2013**, *46*, 359-368.
- (159) Takeshita, T. Y.; Dunning, T. H., Jr. Generalized Valence Bond Description of Chalcogen-Nitrogen Compounds. I. NS, F(NS), and H(NS). *J. Phys. Chem. A* **2015**, *119*, 1446-1455.
- (160) Takeshita, T. Y.; Dunning, T. H., Jr. Generalized Valence Bond Description of Chalcogen-Nitrogen Compounds. II. NO, F(NO), and H(NO). *J. Phys. Chem. A* **2015**, *119*, 1456-1463.
- (161) Dixon, D. A.; Arduengo, A. J., III; Fukunaga, T. A New Inversion Process at Group V (Group 15) Elements. Edge Inversion Through a Planar T-Shaped Structure. *J. Am. Chem. Soc.* **1986**, *108*, 2461-2462.
- (162) Xu, L. T.; Takeshita, T. Y.; Dunning, T. H., Jr. Why Edge Inversion? Theoretical Characterization of the Bonding in the Transition States for Inversion in  $\text{F}_n\text{NH}_{(3-n)}$  and  $\text{F}_n\text{PH}_{(3-n)}$  ( $n = 0-3$ ). *Theor. Chem. Acc.* **2014**, *133*, 1493.
- (163) Xu, L. T.; Thompson, J. V. K.; Dunning, T. H., Jr. Spin-Coupled Generalized Valence Bond Description of Group 14 Species: The Carbon, Silicon and Germanium Hydrides,  $\text{XH}_n$  ( $n = 1-4$ ). *J. Phys. Chem. A* **2019**, *123*, 2401-2419.
- (164) Cooper, D. L.; Gerratt, J.; Raimondi, M. The Electronic Structure of the Benzene Molecule. *Nature* **1986**, *323*, 699-701.
- (165) Cooper, D. L.; Wright, S. C.; Gerratt, J.; Raimondi, M. The Electronic Structure of Heteroaromatic Molecules. Part 1. Six-Membered Rings. *J. Chem. Soc., Perkin Trans. 2* **1989**, 255-261.
- (166) Cooper, D. L.; Wright, S. C.; Gerratt, J.; Raimondi, M. The Electronic Structure of Heteroaromatic Molecules. Part 2. Five-Membered Rings. *J. Chem. Soc., Perkin Trans. 2* **1989**, 263-267.
- (167) Cooper, D. L.; Gerratt, J.; Raimondi, M. The Spin-Coupled Valence Bond Description of Benzenoid Aromatic Molecules. In *Topics in Current Chemistry 1990, Vol. 153*; Springer-Verlag Berlin Heidelberg, 1990.
- (168) Karadakov, P. B.; Ellis, M.; Gerratt, J.; Cooper, D. L.; Raimondi, M. The Electronic Structure of Borabenzene: Combination of an Aromatic  $\pi$ -Sextet and a Reactive  $\sigma$ -Framework. *Int. J. Quantum Chem.* **1997**, *63*, 441-449.
- (169) Cooper, D. L.; Gerratt, J.; Raimondi, M. The Spin-Coupled Description of Aromatic, Antiaromatic and Nonaromatic Systems. *Theoret. Comput. Chem.* **1999**, *6*, 503-518.
- (170) Grant Hill, J.; Karadakov, P. B.; Cooper, D. L. The Spin-Coupled Picture of Clamped Benzenes. *Mol. Phys.* **2006**, *104*, 677-680.

**Spin-Coupled Generalized Valence Bond Theory:  
New Perspectives on the Electronic Structure of Molecules and Chemical Bonds**

- (171) Xu, L. T.; Cooper, D. L.; Dunning, T. H., Jr. Resolving a Puzzling Anomaly in the Spin-Coupled Generalized Valence Bond Description of Benzene. *J. Comput. Chem.* **2020**, *41*, 1421-1426.
- (172) Small, D. W.; Head-Gordon, M. Post-modern Valence Bond Theory for Strongly Correlated Electron Spins. *Phys. Chem. Chem. Phys.* **2011**, *13*, 19285-19297
- (173) Wright, S. C.; Cooper, D. L.; Gerratt, J.; Raimondi, M. Spin-Coupled Description of Cyclobutadiene and 2,4-Dimethylenecyclobutane-1,3-diyl: Antipairs. *J. Phys. Chem.* **1992**, *96*, 7943-7952.
- (174) Karadakov, P. B.; Gerratt, J.; Cooper, D. L.; Raimondi, M. The Electronic Structure of Cyclooctatetraene and the Modern Valence-Bond Understanding of Antiaromaticity. *J. Phys. Chem.* **1995**, *99*, 10186-10195.
- (175) Karadakov, P. B.; Hill, J. G.; Cooper, D. L. The Unusual Electronic Mechanism of the [1,5] Hydrogen Shift in (Z)-1,3-Pentadiene Predicted by Modern Valence Bond Theory. *Faraday Discuss.* **2007**, *135*, 285-297.
- (176) Karadakov, P. B.; Cooper, D. L. Modern Valence-Bond Description of Aromatic Annulene Ions. *Theor. Chem. Acc.* **2013**, *133*, 1421.
- (177) Karadakov, P. B.; Cooper, D. L. Modern Valence-Bond Description of Homoaromaticity. *J. Phys. Chem. A* **2016**, *120*, 8769-8779.
- (178) Karadakov, P. B.; Cooper, D. L. Does the Electronic Structure of Möbius Annulenes Follow Heilbronner's Ideas? *ChemPhysChem* **2018**, *19*, 3186-3190.
- (179) Karadakov, P. B.; Di, M.; Cooper, D. L. Excited-state Aromaticity Reversals in Möbius Annulenes. *J. Phys. Chem. A* **2020**, *124*, 9611-9616.
- (180) Karadakov, P. B.; Cooper, D. L. Modern Valence-Bond Descriptions of Polycyclic Fused Aromatic Compounds Involving Cyclopropenyl Rings. *Comput. Theor. Chem.* **2017**, *1116*, 32-39.
- (181) Ogliaro, F.; Cooper, D. L.; Karadakov, P. B. Bent-Bond Versus Separated-Bond Models: A Spin-Coupled Survey for a Few Organic and Inorganic Systems. *Int. J. Quantum Chem.* **1999**, *74*, 223-229.
- (182) Karadakov, P. B.; Gerratt, J.; Cooper, D. L.; Raimondi, M. The Nature of the Carbon-Carbon Bonds in Cyclopropane and Cyclobutane: A Comparison Based on Spin-Coupled Theory. *J. Am. Chem. Soc.* **1994**, *116*, 7714-7721.
- (183) Karadakov, P. B.; Gerratt, J.; Cooper, D. L.; Raimondi, M. Modern Valence-Bond Description of Bonding in Strained Three-Membered Rings: Cyclopropane, Aziridine, Ethene Oxide, Phosphirane and Thiirane. *J. Mol. Struct. (THEOCHEM)* **1995**, *341*, 13-24.
- (184) Cooper, D. L.; Karadakov, P. B. Spin-coupled Descriptions of Organic Reactivity *Int. Rev. Phys. Chem.* **2009**, *28*, 169-206.
- (185) Karadakov, P. B.; Cooper, D. L.; Gerratt, J. Modern Valence-Bond Description of Chemical Reaction Mechanisms: Diels-Alder Reaction. *J. Am. Chem. Soc.* **1998**, *120*, 3975-3981.
- (186) Blavins, J. J.; Cooper, D. L.; Karadakov, P. B. Spin-Coupled Study of the Electronic Mechanism of the Hetero-Diels-Alder Reaction of Acrolein and Ethene. *J. Phys. Chem. A* **2005**, *109*, 231-235.
- (187) Hill, J. G.; Cooper, D. L.; Karadakov, P. B. Spin-Coupled Description of Aromaticity in the Retro Diels-Alder Reaction of Norbornene. *J. Phys. Chem. A* **2008**, *112*, 12823-12828.
- (188) Blavins, J. J.; Karadakov, P. B.; Cooper, D. L. Modern Valence-Bond Description of Chemical Reaction Mechanisms: The 1,3-Dipolar Addition of Methyl Azide to Ethene. *J. Phys. Chem. A* **2003**, *107*, 2548-2559.
- (189) Karadakov, P. B.; Cooper, D. L.; Gerratt, J. Modern Valence-Bond Description of Chemical Reaction Mechanisms: The 1,3-Dipolar Addition of Fulminic Acid to Ethyne. *Theor. Chem. Acc.* **1998**, *100*, 222-229.
- (190) Blavins, J. J.; Karadakov, P. B.; Cooper, D. L. Modern Valence-Bond Description of Chemical Reaction Mechanisms: The 1,3-Dipolar Addition of Diazomethane to Ethene. *J. Org. Chem.* **2001**, *66*, 4285-4292.



- (191) Karadakov, P. B.; Cooper, D. L.; Uhe, A. Modern Valence Bond Description of the Electronic Mechanism of a [1,3] Sigmatropic Rearrangement Linking Bicyclo[3.2.0]hept-2-ene and Bicyclo[2.2.1]hept-2-ene (Norbornene). *Int. J. Quantum Chem.* **2009**, *109*, 1807-1811.
- (192) Bingel, W. A.; Luttke, W. Hybrid Orbitals and Their Applications in Structural Chemistry. *Angew. Chem., Int. Ed.* **1981**, *20*, 899-990.
- (193) Alabugin, I. V.; Bresch, S.; Gomes, G. d. P. Orbital Hybridization: A Key Electronic Factor in the Control of Structure and Reactivity. *J. Phys. Org. Chem.* **2015**, *28*, 147-162.
- (194) Pauling, L. The Nature of the Chemical Bond. Application of Results Obtained from the Quantum Mechanics and from a Theory of Paramagnetic Susceptibility to the Structure of Molecules. *J. Am. Chem. Soc.* **1931**, *53*, 1367-1400.
- (195) Slater, J. C. Directed Valence in Polyatomic Molecules. *Phys. Rev.* **1931**, *37*, 481-489.
- (196) Van Vleck, J. H.; Sherman, A. The Quantum Theory of Valence. *Rev. Mod. Phys.* **1935**, *7*, 167-228.
- (197) Grushow, A. Is It Time to Retire the Hybrid Atomic Orbital? *J. Chem. Educ.* **2011**, *88*, 860-862.
- (198) Tro, N. J. Retire the Hybrid Atomic Orbital? Not So Fast. *J. Chem. Educ.* **2012**, *89*, 567-568.
- (199) DeKock, R. L.; Strikwerda, J. R. Retire Hybrid Atomic Orbitals? *J. Chem. Educ.* **2012**, *89*, 569-569.
- (200) Landis, C. R.; Weinhold, F. Comment on "Is It Time to Retire the Hybrid Atomic Orbital?" *J. Chem. Educ.* **2012**, *89*, 570-572.
- (201) Truhlar, D. G. Are Molecular Orbitals Delocalized? *J. Chem. Educ.* **2012**, *89*, 573-574.
- (202) Hiberty, P. C.; Volatron, F.; Shaik, S. In Defense of Hybrid Atomic Orbitals. *J. Chem. Educ.* **2012**, *89*, 575-577.
- (203) Grushow, A. In Response to Those Who Wish to Retain Hybrid Atomic Orbitals in the Curriculum. *J. Chem. Educ.* **2012**, *89*, 578-579.
- (204) Lamoureux, G.; Ogilvie, J. F. Hybrid Atomic Orbitals in Organic Chemistry. Part 1: Critique of Formal Aspects. *Quim. Nova* **2019**, *42*, 812-816.
- (205) Lamoureux, G.; Ogilvie, J. F. Hybrid Atomic Orbitals in Organic Chemistry. Part 2: Critique of Practical Aspects. *Quim. Nova* **2019**, *42*, 817-822.
- (206) NIST Atomic Spectra Database. [https://physics.nist.gov/PhysRefData/ASD/levels\\_form.html](https://physics.nist.gov/PhysRefData/ASD/levels_form.html).
- (207) Lie, G. C.; Clementi, E. Study of the Electronic structure of Molecules. XXII. Correlation Energy Corrections as a Functional of the Hartree-Fock Type Density and Its Application to the Homonuclear Diatomic Molecules of the Second Row Atoms. *J. Chem. Phys.* **1974**, *60*, 1288-1296.
- (208) Takeshita, T. Y.; Dunning, T. H., Jr. Fundamental Aspects of Recoupled Pair Bonds. III. The Frustrated Recoupled Pair Bond in Oxygen Monofluoride. *J. Phys. Chem. A* **2016**, *120*, 9607-9611.
- (209) Pauling, L. The Nature of the Chemical Bond. II. The One-Electron Bond and the Three-Electron Bond. *J. Am. Chem. Soc.* **1931**, *53*, 3225-3237.
- (210) Palke, W. E.; Goddard, W. A., III. Electronic Structure of LiH According to a Generalization of the Valence-Bond Method. *J. Chem. Phys.* **1969**, *50*, 4524-4532.